2016-07-14

# The Physiological Effects of the Guanylin Peptides in the Intestine of the Gulf Toadfish (Opsanus beta)

Ilan M. Ruhr
*University of Miami*, ilanruhr@gmail.com

UNIVERSITY OF MIAMI

# THE PHYSIOLOGICAL EFFECTS OF THE GUANYLIN PEPTIDES IN THE INTESTINE OF THE GULF TOADFISH (*OPSANUS BETA*)

By

Ilan M. Ruhr

A DISSERTATION

Submitted to the Faculty
of the University of Miami
in partial fulfillment of the requirements for
the degree of Doctor of Philosophy

Coral Gables, Florida

August 2016

UNIVERSITY OF MIAMI

A dissertation submitted in partial fulfillment of
The requirements for the degree of
Doctor of Philosophy

# THE PHYSIOLOGICAL EFFECTS OF THE GUANYLIN PEPTIDES IN THE INTESTINE OF THE GULF TOADFISH (*OPSANUS BETA*)

Ilan M. Ruhr

Approved:

| | |
|---|---|
| _____<br>Martin Grosell, Ph.D.<br>Professor of Marine Biology and Ecology | _____<br>Marjorie F. Oleksiak, Ph.D.<br>Associate Professor of Marine Biology and Ecology |
| _____<br>M. Danielle McDonald, Ph.D.<br>Associate Professor of Marine Biology and Ecology | _____<br>Lynne L. Fieber, Ph.D.<br>Associate Professor of Marine Biology and Ecology |
| _____<br>Martin Tresguerres, Ph.D.<br>Assistant Professor of Marine Biology<br>University of California, San Diego | _____<br>Guillermo Prado, Ph.D.<br>Dean of the Graduate School |

RUHR, ILAN M. (Ph.D., Marine Biology and Ecology)
The Physiological Effects of the Guanylin Peptides in the Intestine of the Gulf Toadfish (*Opsanus beta*) (August 2016)

Abstract of a dissertation at the University of Miami.

Dissertation supervised by Professor Martin Grosell.
No. of pages in text: (152)

The findings in the present dissertation describe the regulatory role the guanylin peptides play in seawater teleost intestinal physiology through the use of the model organism, the Gulf toadfish (*Opsanus beta*). For the majority of the findings, renoguanylin (a guanylin peptide exclusive to teleost fish) is used as an experimental tool and elicits responses in the posterior intestine and rectum of the Gulf toadfish, but does not affect the anterior intestine. Both the posterior intestine and rectum display secretory short-circuit currents, reversed transepithelial potentials, and increased conductance in response to renoguanylin stimulation. These changes are driven primarily by $Cl^-$ secretion via activation of an apical cystic fibrosis transmembrane conductance regulator (CFTR) $Cl^-$ channel, and inhibition of the apical absorptive ion transporters, SLC26a6 (a $HCO_3^-$/$Cl^-$ antiporter) and NKCC2 (SLC12a1). The combined effects of renoguanylin stimulation on the posterior intestine and rectum are inhibited transepithelial salt and water absorption. This is an unexpected response by the intestine of a seawater teleost, given that these fish must continually drink water and absorb it by the intestine to counteract pervasive branchial water loss to their hypertonic environment. Furthermore, the response to renoguanylin is elevated when Gulf toadfish are acclimated to

hypersalinity, a situation that increases the formation of carbonate precipitates in the intestine, as part of normal osmoregulatory processes. The tissue response in hypersalinity also coincides with increased gene expression of CFTR and NKCC1 (SLC12a2), which constitute a $Cl^-$-secretory pathway that is stimulated by renoguanylin. The above observations suggest that the renoguanylin-stimulated secretory response is, at the very least, important when teleosts encounter hypertonic environments. It is proposed that the secretory response facilitates the removal of solids, such as carbonate precipitates, from the intestinal tract. A secretory response would ensure the availability of fluid in the intestinal lumen for the purposes of increasing the efficiency of peristaltic movement of solids.

## DEDICATION

To my mom and dad, who left behind friends and family in Peru for the cold, northern frontier that is Canada, in search of something better for us. We lived the characteristic immigrant life of little means and struggles. But in typical immigrant fashion, my parents placed the value of a good education for their children above all else. While my sister excelled at school from an early age, I – in classic, stubborn fashion – hated school and performed poorly for a long time. Despite my scholarly struggles, my parents always told me that they believed in me and that I could do great things if I tried. Today, I hope I have made them proud. This dissertation is for you. Thank you for all your love.

I can't imagine what my life would be like today without the friends I've made here in Miami. I don't want to imagine it, actually. You know you've got a special group of friends when they organize a memorial service for your dead dog. To Tara, Kim, Pete, Teddy, Marlena, Cristina, Bree-Anna, Monica, Ford, Rivah, Justin, Jay, Luke, the Slidin' into Third and 69ers crews (in particular Chad, Royce, Tony, and Rory), Ryan, Rudolf, and Eleanor, and so many other Miami and RSMAS people: thank you from the very bottom of my heart. I have had so many laughs and made so many fond memories with you all.

Lastly, I also dedicate this dissertation to my companion of ten years who traveled with me across the Atlantic (twice). You left this world before we could embark on our next adventure. You kept me grounded, showed me unconditional love, and made me smile all day, every day. That adorable family who also wanted to take you home that summer day should've fought harder for you. You were worth everything. Thank you.

## ACKNOWLEDGMENTS

I'd like to extend my deep appreciation and thanks to my advisor, Martin Grosell, for having been a fantastic mentor and leader throughout my 5 years here in Miami. Thank you for allowing me to carve my own research path, providing me the unforgettable opportunities to travel the world, being there when I needed words of wisdom, and telling me to keep fit.

I'd also like to thank my committee members: Danielle "Super Mentor" McDonald for being plain awesome and always welcoming me into your office to chat; Martin Tresguerres for your invaluable contributions to my research and being a pal at conferences; Margie Oleksiak for your kindness and for dogsitting my little man; and Lynne Fieber for always being there when I needed advice about so many random things. You've all been incredibly amazing.

None of my achievements could have been possible without the additional support I've received here at RSMAS. My labmates, Rachael (work wife), Ed, Christina, Charlotte, the two Kevins, Andrew, Lela, Georgie, Madeline, Dan, John, Emil, and Yadong, have been the best support system I could've ever asked for. Molly and Maria: you two have added much needed levity when I've felt cranky. Doug Crawford: a ray of caffeinated sunshine in the mornings. To the RSMAS community: a family away from home.

Thank you all so very much.

## TABLE OF CONTENTS

**LIST OF FIGURES**

**LIST OF TABLES**

# Chapter 1

## Introduction

The ability to regulate salt and water across membranes is essential to all life. Indeed, organisms, from bacteria to mammals, have evolved unique ionoregulatory mechanisms to maintain necessary ion and water levels, in their intra- and extracellular spaces (Bradley, 2009). Seawater teleost fish, for example, maintain an extracellular osmolality of 300-330 mOsm $kg^{-1}$, despite the fact that they live in a hypertonic environment (roughly 1000 mOsm $kg^{-1}$). This situation leads to continual passive water loss and ion gain, via the gills, and is compensated by constant ingestion of water and absorption of fluid by the intestine (Marshall and Grosell, 2006). For intestinal water absorption to occur, the ingested seawater must be desalinated in order to decrease the large outward osmotic gradient that exists between ingested seawater and extracellular fluids. Esophageal desalination is the first step in this important process, whereby the majority of the $Na^+$ and $Cl^-$ contained in the ingested seawater is removed, resulting in a fluid that is isotonic to extracellular fluids (Grosell, 2010; Marshall and Grosell, 2006) once it reaches the anterior intestine. In the intestine, ion transporters allow for solute-coupled water absorption, which compensates for branchial water loss (Skadhauge, 1969; Skadhauge, 1974).

One of the major intestinal salt transporters is the apical $Na^+/K^+/2Cl^-$-cotransporter type two, NKCC2 (SLC12a1), that transports salts down their electrochemical gradient from the intestinal lumen into the blood (Frizzell *et al.*, 1979; Halm *et al.*, 1985; Musch *et al.*, 1982). Interestingly, the regulation of blood acid-base

balance is associated with salt and fluid absorption. Another $Cl^-$ transporter, SLC26a6 (an apical $Cl^-/HCO_3^-$ exchanger), found on the apical membrane (Kurita *et al.*, 2008), can be responsible for up to 70% of luminal $Cl^-$ uptake in exchange with intracellular $HCO_3^-$. (Grosell, 2006). Indeed, there appears to be excess $Cl^-$ absorption in the anterior intestine relative to $Na^+$ uptake, in addition a high rate of $HCO_3^-$ secretion (Grosell and Genz, 2006). Titration of $HCO_3^-$ (into $CO_2$ and $H_2O$) by protons ($H^+$) extruded from an apical v-type $H^+$-ATPase (VHA) and precipitation of $HCO_3^-$ by intestinal $Ca^{2+}$ and $Mg^{2+}$ (to form $CaCO_3$ and $MgCO_3$ precipitates) facilitates fluid absorption by lowering intestinal osmolality further (Grosell *et al.*, 2009a; Grosell *et al.*, 2005; Wilson and Grosell, 2003; Wilson *et al.*, 2002). Overall, absorption of salts, coupled to base secretion and carbonate precipitation, decreases the osmolality of the intestinal fluid and allows for net fluid absorption.

An area of seawater teleost physiology that has been largely neglected is the study of secretory mechanisms present in the intestine. Although counterintuitive, secretory mechanisms might be beneficial for normal intestinal function. For example, in order to reduce harmful blockages, carbonate precipitates are readily removed from the intestinal tract by peristalsis. The efficiency of peristalsis is improved if the solid (e.g. carbonate precipitates) being moved is more aqueous (Schulze, 2015), which could be achieved by water secretion or inhibited water uptake. This would require that intestinal absorptive mechanisms, vital to hydration, be inhibited. Indeed, a few studies have revealed the presence of secretory-type ion transporters in the marine teleost intestine (Cutler and Cramb, 2002; Hiroi *et al.*, 2008; Li *et al.*, 2014; Singer *et al.*, 1998) that would be required for fluid secretion, which are similar to those found in the marine teleost gill

(Evans *et al.*, 2005; Marshall and Grosell, 2006). Furthermore, studies conducted on the winter flounder (*Pseudopleuronectes americanus*) reveal that vasoactive intestinal peptide decreases intestinal absorption through the downstream effects of cyclic adenosine monophosphate (cAMP) and causes net $Cl^-$ secretion (O'Grady and Wolters, 1990; Rao *et al.*, 1984). Additionally, atrial natriuretic factor inhibits NKCC2 transport activity via cyclic guanosine monophosphate (cGMP) in the winter flounder intestine (O'Grady *et al.*, 1985). These studies demonstrate that the components for ion secretion and, thus, inhibited water absorption, exists and can be activated by hormones produced by teleost fish (Takei, 2008).

More recently, the homologous guanylin family of peptides has been studied for its role in regulating teleost intestinal physiology. These peptides, comprising of guanylin and uroguanylin, were first discovered in mammalian intestinal and renal fluids (Currie *et al.*, 1992; Greenberg *et al.*, 1997; Hamra *et al.*, 1993) and have been shown to regulate body electrolyte and fluid homeostasis by modulating the activity of various ion transporters (Arshad and Visweswariah, 2012; Forte, 1999; Forte and Hamra, 1996). The guanylin peptides have also been sequenced in the European and Japanese eels (*Anguilla anguilla* and *A. japonica,* respectively), including renoguanylin (a new member exclusively expressed in fish), and are believed to play an important role in seawater survival (Comrie *et al.*, 2001a; Cramb *et al.*, 2005; Yuge *et al.*, 2003). Indeed, their expression, as well as that of their apical receptor – guanylyl cyclase-C (GC-C), which has intrinsic GC activity – increases up to six-fold in both eel species when they are acclimated from freshwater to seawater (Cramb *et al.*, 2005; Kalujnaia *et al.*, 2009; Yuge *et al.*, 2003; Yuge *et al.*, 2006). The higher gene expression levels in seawater-acclimated

teleosts suggests that there is the potential for reversing the normal absorptive osmoregulatory processes of the seawater teleost intestine, despite the fact fluid absorption is necessary for seawater survival, and that this response might somehow be essential for a seawater existence.

In mammals, the guanylin peptides reverse intestinal osmoregulatory processes from net absorption to net secretion by activating GC-C, leading to increased cGMP formation with many downstream effects (Chao *et al.*, 1994; Currie *et al.*, 1992; Schulz *et al.*, 1990). Among these effects is the opening of apical cystic fibrosis transmembrane conductance regulator (CFTR) $Cl^-$ channels and the subsequent $Cl^-$ and $HCO_3^-$ secretion into the intestinal lumen that leads to fluid secretion as well as inhibited NKCC2 transport and $Na^+/H^+$ (NHE) exchange activity (Chao *et al.*, 1994; Cuthbert *et al.*, 1994; Greenberg *et al.*, 1997; Guba *et al.*, 1996; Toriano *et al.*, 2011). These effects occur along the entire intestine; are only observed when guanylin or uroguanylin are applied to the mucosal (luminal) side of the tissue; and seem to be initiated under two separate conditions (Joo *et al.*, 1998). In the first instance, salt loading of rat intestinal tissues leads to increases in guanylin and uroguanylin gene expression, protein production, and peptide secretion into the lumen (Carrithers *et al.*, 2002; Kita *et al.*, 1999; Li *et al.*, 1996). As stated above, electrolyte secretion causes fluid secretion, which is thought to dilute the brush border of the intestine and allow for normal osmoregulatory processes to continue. In the second instance, the guanylin peptides seem to be involved in defending the pH of the intestinal lumen. Indeed, it has been shown that uroguanylin is more potent at low pH, suggesting that this peptide is biologically active when acidic chyme enters the intestine from the stomach (Hamra *et al.*, 1997; Joo *et al.*, 1998).

In seawater teleosts, however, the purpose of guanylin peptide stimulation is unknown. In addition to digestion, the marine teleost intestine serves a vital function in water balance to a greater extent than in other vertebrates. At the onset of this dissertation, only one study had investigated the physiological effects of the guanylin peptides in seawater teleosts. Said study demonstrated that the effects of guanylin, uroguanylin, and renoguanylin were restricted to the mid and posterior intestine of the Japanese eel by reversing the absorptive short-circuit current ($I_{SC}$) and reducing tissue resistance (i.e. increasing conductance) (Yuge and Takei, 2007), in contrast to the stimulatory effects of guanylin and uroguanylin along the entire length of the mammalian intestine. Accordingly, the first objective (Chapter 2) of this dissertation was to further elucidate the mechanisms by which the guanylin peptides modulate ion transport in seawater teleosts. Specifically, Chapter 2 confirms region-specific responses of the seawater teleost intestine to the guanylin peptides, identifies ion transporters that might mediate the guanylin peptide response, and reveals changes in $Na^+$, $Cl^-$, fluid, and $HCO_3^-$ fluxes.

The findings described in Chapter 2 formed the basis for the subsequent chapters of this dissertation. It describes mechanisms initiated by the guanylin peptides in the Gulf toadfish (*Opsanus beta*) intestine, whereby an apical CFTR and basolateral NKCC1 conduit for $Cl^-$ is activated, $Na^+$ absorption is inhibited, $HCO_3^-$ secretion is decreased, and fluid secretion occurs. These effects largely agree with a later study on the Japanese eel, which revealed that guanylin stimulation of intestinal tissues reversed net ion absorption, which led to inhibited water absorption (Ando *et al.*, 2014). Moreover, the findings described in Chapter 2 corroborate what is known in mammals: that activation of

GC-C by the guanylin peptides stimulates secretion of fluid and $Cl^-$ and inhibits $Na^+$ absorption (Forte and Hamra, 1996). However, the regulation of $HCO_3^-$ secretion by the guanylin peptides differs considerably between seawater teleosts and mammals. $HCO_3^-$ secretion is further stimulated in rat intestinal tissues by guanylin and uroguanylin, (Bengtsson *et al.*, 2007; Guba *et al.*, 1996), whereas it is reduced in the Gulf toadfish. **The hypothesis proposed by Chapter 2** is that the guanylin peptides will stimulate secretory mechanisms in the Gulf toadfish intestine and that its purpose is to facilitate the removal of solids, such as carbonate precipitates, from the intestine. Thus, inhibiting $HCO_3^-$ secretion during a guanylin peptide stimulatory response might lead to lower water absorption, due to the possibility of decreased carbonate precipitate formation. Chapter 3 builds upon these findings with the objective of investigating the effects of renoguanylin stimulation in the posterior intestine from Gulf toadfish exposed to normal (35 ppt) and hypersaline (60 ppt) seawater. Acclimating Gulf toadfish from 35 to 50 ppt seawater more than doubles carbonate precipitate formation (Genz *et al.*, 2008). The findings in Chapter 2 reveal that fluid secretion is initiated in the Gulf toadfish posterior intestine as a result of renoguanylin stimulation that could facilitate solid removal. Thus, **the objective for Chapter 3** was to gather more support for the above hypothesis, by acclimating Gulf toadfish to conditions demanding greater excretion of precipitated carbonates.

Accordingly, if the hypothesis proposed in this dissertation is correct, then some of the components of the guanylin peptide response, made up of guanylin, uroguanylin, GC-C, NKCC1, and CFTR, would be expected to be expressed more highly at 60 ppt. At the physiological level, this would be characterized by a greater response by the posterior

intestine to renoguanylin, driven by greater $Cl^-$ and fluid secretion (due to greater CFTR and NKCC1 gene expression), and less $HCO_3^-$ secretion at 60 ppt than at 35 ppt. However, the findings described in Chapter 3 show that, despite there being a greater decrease in fluid absorption by the posterior intestine from the 60 ppt fish in response to renoguanylin, $HCO_3^-$ secretion increased, rather than decreased. Recall that in mammals, guanylin and uroguanylin elevate $HCO_3^-$ secretion (Bengtsson *et al.*, 2007; Guba *et al.*, 1996; Joo *et al.*, 1998), similarly to what is seen in the posterior intestine of Gulf toadfish acclimated to 60 ppt. These observed increases in $HCO_3^-$ secretion in posterior intestine of the 60 ppt fish are not due to increased gene expression of either apical SLC26a6 or basolateral NBCe1 and are likely are post-translational (Grosell *et al.*, 2009b; Taylor *et al.*, 2010). Thus, in Chapter 3, the role of SLC26a6 was also investigated and describes the possibility that the activity of this transporter is regulated by the downstream effects of renoguanylin. **Chapter 4 builds upon these findings and tests the hypothesis** that the downstream effects of renoguanylin stimulation likely act on SLC26a6.

In addition, Chapter 4 investigated the physiology of the Gulf toadfish rectum. To my knowledge, only three other studies have tested the physiology of the seawater teleost rectum (Carvalho *et al.*, 2012; Gregorio *et al.*, 2013; Kim *et al.*, 2008). Moreover, it is still unclear what initiates the guanylin peptide response, the enzymes that cleave the guanylin pro-peptides into their biologically active compounds, and the length of the stimulatory response (Forte, 1999). Accordingly, the fate of the fluid that is not fully absorbed by the posterior intestine and, therefore, moves into the rectum after stimulation by renoguanylin remained unknown. **Chapter 4 investigates whether the rectum could be involved in absorbing this fluid or if it also responds to renoguanylin** by

comparing the response to renoguanylin by the posterior intestine and rectum. The findings in Chapter 4 describe differences in osmoregulatory physiology between the posterior intestine and rectum. It reveals stark differences in the major $Cl^-$-uptake pathway, whereby the dependence on the apical SLC26a6 and NKCC2 ion transporters are investigated. It was thought that NKCC2 was the major ion-uptake pathway in seawater teleosts [(Ando, 1980; Musch *et al.*, 1982), for review (Takei *et al.*, 2014)]. More recently, however, SLC26a6 was implicated in $Cl^-$ transport and could be responsible for up 70% of intestinal $Cl^-$ absorption in many seawater teleost species, including the Gulf toadfish [for review (Grosell, 2006)]. Thus, Chapter 4 also describes differences in ion transporter selectivity between two gastrointestinal tissues within the same species.

Overall, this dissertation describes the effects of guanylin peptide stimulation on the Gulf toadfish intestine. It details the effects renoguanylin stimulation has on ion transporters important to water absorption and on ion-secretory pathways that are activated. Moreover, this dissertation reveals heterogeneity in intestinal function among the anterior intestine, posterior intestine, and rectum of the Gulf toadfish. Although the second portion of the above hypothesis (that a secretory response facilitates removal of solids from the intestine) is not fully validated by this dissertation, its findings provide some support of this overarching hypothesis.

Chapters 2-4 are all published in the peer-reviewed literature in the *Am J Physiol - Reg, Int, Comp Physiol*: **(2)** Ruhr, I.M., *et al*. 2014. R1167-R1179. **(3)** Ruhr, I.M., *et al.* 2015. 309(4): R399-R409. **(4)** Ruhr, I.M., *et al.* 2016. DOI: 10.1152/ajpregu.00033.2016.

## Chapter 2

## Guanylin peptides regulate electrolyte and fluid transport in the Gulf toadfish (*Opsanus beta*) posterior intestine


### Summary

The physiological effects of guanylin and uroguanylin on fluid and electrolyte transport in the teleost fish intestine have yet to be thoroughly investigated. In the present study, the effects of guanylin, uroguanylin, and renoguanylin (RGN; a guanylin and uroguanylin homolog) on short-circuit current ($I_{SC}$) and the transport of $Cl^-$, $Na^+$, bicarbonate ($HCO_3^-$), and fluid in the Gulf toadfish (*Opsanus beta*) intestine was determined using Ussing chambers, pH-stat titration, and intestinal sac experiments. guanylin, uroguanylin, and RGN reversed the $I_{SC}$ of the posterior intestine (absorptive-to-secretory), but not of the anterior intestine. RGN decreased baseline $HCO_3^-$ secretion, but increased $Cl^-$ and fluid secretion in the posterior intestine. The secretory response of the posterior intestine coincides with the presence of basolateral NKCC1 and apical CFTR, the latter of which is lacking in the anterior intestine and is not permeable to $HCO_3^-$ in the posterior intestine. However, the response to RGN by the posterior intestine is counterintuitive given the known role of the marine teleost intestine as a salt- and water-absorbing organ. These data demonstrate that marine teleosts possess a tissue-specific secretory response, apparently associated with seawater adaptation, whose exact role remains to be determined.

## Background

Regulation of salt, water, and acid-base balance by the osmoregulatory organs of teleost fish are vital processes for maintaining homeostasis in a diverse range of habitats and are accomplished through various compensatory responses. To combat diffusive fluid loss, marine teleosts drink seawater (SW) and absorb both salts and water in the intestine (Smith, 1930). It is well established that the absorptive-type $Na^+/K^+/2Cl^-$-cotransporter, NKCC2 (SLC12a1), transports salts down their electrochemical gradient from the intestinal lumen across the apical membrane into the enterocytes (Frizzell *et al.*, 1979; Halm *et al.*, 1985; Tresguerres *et al.*, 2010). More recently, an additional pathway for $Cl^-$ absorption, by SLC26a6 (an apical $Cl^-/HCO_3^-$ antiporter), was identified to exchange intestinal $Cl^-$ for intracellular $HCO_3^-$, and can be responsible for up to 70% of $Cl^-$ uptake (Grosell, 2006). Fluid absorption follows absorption of osmolytes via these two ion uptake pathways. In addition, titration of $HCO_3^-$ (to form $CO_2$ and $H_2O$) by protons ($H^+$) extruded by an apical v-type $H^+$-ATPase (VHA) and precipitation of $HCO_3^-$ with intestinal $Ca^{2+}$ and $Mg^{2+}$ (to form Ca- and $MgCO_3$ precipitates) facilitates fluid absorption by lowering intestinal fluid osmolality (Grosell, 2006; Grosell, 2010; Grosell *et al.*, 2009a; Grosell *et al.*, 2005; Wilson *et al.*, 2009; Wilson and Grosell, 2003; Wilson *et al.*, 2002). Ultimately, absorption of salts, coupled to base secretion, allows for solute-coupled and osmotic fluid absorption.

Although the marine teleost intestine is vital to salt and fluid absorption, it also exhibits secretory characteristics with respect to $Cl^-$ and fluid. Studies have revealed possible pathways for both $Cl^-$ secretion, via an apical cystic fibrosis transmembrane conductance regulator (CFTR) channel, and fluid secretion into the intestinal lumen by

marine teleosts (Marshall *et al.*, 2002; Takei *et al.*, 2006; Yuge and Takei, 2007), both of which are common in terrestrial animals (Diaz *et al.*, 1988; Hallback *et al.*, 1991). It has been proposed that the function of apical CFTR is to facilitate $Cl^-$ and fluid secretion for the elimination of toxins from the intestine (Marshall *et al.*, 2002; Singer *et al.*, 1998). However, neither the exact function nor the regulatory pathways responsible for switching intestinal ion and fluid absorption to secretion are known.

Guanylin and uroguanylin are upstream regulators of apical CFTR, and modulate intestinal $Na^+$, $Cl^-$, fluid, and $HCO_3^-$ fluxes in mammals (Arshad and Visweswariah, 2013; Müller and Dieplinger, 2012; Toriano *et al.*, 2011). Guanylin and uroguanylin bind to guanylyl cyclase-C (GC-C), a transmembrane receptor on the apical membrane of intestinal tissues a receptor that possesses GC activity (Müller and Dieplinger, 2012; Schulz *et al.*, 1992; Schulz *et al.*, 1990), causing an intracellular transduction cascade that increases the formation of cyclic guanosine monophosphate (cGMP). cGMP can either stimulate cGMP-dependent protein kinase (PKG) or lead to increases in cyclic adenosine monophosphate (cAMP) levels that stimulate cAMP-dependent protein kinase (PKA); both PKG and PKA activate CFTR (Arshad and Visweswariah, 2012; Arshad and Visweswariah, 2013; Chao *et al.*, 1994; Currie *et al.*, 1992; Hamra *et al.*, 1997; Kuhn *et al.*, 1994). In mammals, this leads to $Cl^-$, fluid, and $HCO_3^-$ secretion into the intestinal lumen to help neutralize the effects of acidic chyme (Allen and Flemström, 2005; Bengtsson *et al.*, 2007; Guba *et al.*, 1996; Seidler *et al.*, 1997). This process is especially important after the ingestion of food, where guanylin and uroguanylin are secreted into the intestine, bind to GC-C and activate its GC subunits that elevate the levels of intracellular cGMP in enterocytes (Arshad and Visweswariah, 2013).

Guanylin, uroguanylin, and renoguanylin (RGN) are also present in teleost fish; intestinal tissues express guanylin and uroguanylin, while renal tissue express uroguanylin and RGN (Comrie *et al.*, 2001a; Cramb *et al.*, 2005; Kalujnaia *et al.*, 2009; Yuge *et al.*, 2003). Although the physiological function of the guanylin peptides in teleosts is still uncertain, studies have shown that they may play a role in long-term salinity adaptation. Both guanylin and uroguanylin mRNA expression increases following a 24-h transfer from freshwater (FW) to SW by at least twofold in the Japanese eel (*Anguilla japonica)* (Cramb *et al.*, 2005; Kalujnaia *et al.*, 2009; Yuge *et al.*, 2003), a pattern also observed in the rat after salt loading of intestinal tissues (Carrithers *et al.*, 2002; Kita *et al.*, 1999; Li *et al.*, 1996). In mammalian tissues, guanylin and uroguanylin either increase the secretory short-circuit current ($I_{SC}$) of the intestine or reverse an absorptive $I_{SC}$, while in teleosts, these peptides have no effect on the anterior intestine of the Japanese eel, but do reverse the $I_{SC}$ of the mid and posterior intestine, resulting in a net serosa-to-mucosa flux of, presumably, $Cl^-$ ions (Joo *et al.*, 1998; Seidler *et al.*, 1997; Yuge and Takei, 2007).

However, considering that the intestine of marine teleosts must absorb water to avoid dehydration and that the guanylin peptides cause fluid secretion in mammalian intestinal cells, would marine teleosts respond to these peptides in a similar manner? Evidence from the Japanese eel supports the view of net fluid secretion into the intestinal lumen, due to the reversal of the $I_{SC}$ in the mid and posterior intestine by guanylin, uroguanylin, and RGN (Yuge and Takei, 2007). These observations would suggest that marine teleosts secrete fluid into the intestinal lumen via the guanylin peptide-induced activation of the intracellular cascade that occurs in mammals. However, it remains to be

confirmed that the secretory current is conducted by $Cl^-$ and whether this current promotes fluid secretion. Moreover, the molecular components of the secretory ion transport pathway have yet to be firmly established.

The purpose of this study was to further characterize the physiological effects of the guanylin peptides in marine teleost fish by investigating their effects on Gulf toadfish (*Opsanus beta*) intestinal epithelium. A secretory short-circuit current response to luminal application of the guanylin peptides was anticipated and hypothesized to (i) be most pronounced in the posterior instestine, (ii) be driven by net secretion of $Cl^-$, and (iii) be associated with net fluid secretion and enhanced $HCO_3^-$ secretion. Furthermore, it was hypothesized that (iv) a secretory pathway would be present in the guanylin-responsive segments of the intestine.

## Materials and Methods

### *Experimental Animals*

Gulf toadfish (*Opsanus beta*) were caught as bycatch from a local shrimp fisherman in Biscayne Bay, FL. Immediately upon arrival in the laboratory, the Gulf toadfish were briefly placed in a freshwater bath (3 min) and then treated with malachite green to remove ectoparasites following the protocol from McDonald et al. (McDonald *et al.*, 2003). Gulf toadfish were separated by size and 8-10 fish were placed in 62-litre tanks, with a continuous flow-through of sand-filtered seawater from Biscayne Bay (30-34 ppt salinity, 26-29°C). Gulf toadfish were fed to satiation weekly, but food was withheld for 72 h prior to experimentation. Fish husbandry and experimental procedures were performed according to an approved University of Miami Animal Care Protocol

(IACUC no. 10-293, renewal 02). All Gulf toadfish used for experimentation were sacrificed using 0.2 g $l^{-1}$ MS-222 (Argent) solution buffered with 0.3 g $l^{-1}$ $NaHCO_3^-$, followed by severing of the spinal cord at the cervical vertebra.

*cDNA Cloning*

Cloning was performed using cDNA constructed from homogenized Gulf toadfish intestinal tissues (Taylor *et al.*, 2010). Partial cDNAs of a guanylin -like and a uroguanylin -like peptide were cloned by 3'- and 5'-rapid amplification of cDNA ends (RACE) using a universal primer and designed-sense primers (Table 2.1). PCR amplifications were performed according to a modified protocol from Yuge et al. (Yuge *et al.*, 2003) using Taq DNA polymerase and buffer (Invitrogen). After 3'- and 5'-RACE procedures were performed, gene specific primers (Table 2.1) were used in PCR reactions to determine the full sequence of the guanylin and uroguanylin prohormones.

Table 2.1. Sequences of primers for cDNA cloning

| Name | Sequence |
|---|---|
| GN-F* | 5'-ATCTGCGCTAATGCTGCCTGCAC-3' |
| GN-R* | 5'-GTGCAGGCAGCATTAGCGCAGAT-3' |
| tfGN-F | 5'-AGCAAAGGGCAGCATCTGCA-3' |
| tfGN-R | 5'-TGGCAAGATGTTTGTGGCTTTGC-3' |
| tfUGN-F** | 5'-CCGACCCTCTCATGCCGCAGG-3' |
| tgUGN-R** | 5'-TGCACGGAGGCATCGAGCTG-3' |
| Universal Primer† | 5'-CTAATACGACTCACTATAGGGCAAGCGTGGTATCAACGCAGAGT-3'<br>5'-CTAATACGACTCACTATAGGGC-3' |

*Designed sense primers taken and/or modified from Yuge et al. 2003
**Gene-specific primers designed from annotated Gulf toadfish transcriptome
†Universal primer (Clontech SMARTer™ RACE cDNA Amplification Kit) consists of both a long and short sequence

*Composition of salines, hormones, and inhibitors*

Japanese eel guanylin, uroguanylin, and RGN peptides were resuspended into $10^{-3}$ mol $l^{-1}$ stock solutions in nano-pure water. The final concentrations for the guanylin peptides in the luminal saline were $10^{-9}$-$10^{-5}$ mol $l^{-1}$. Luminal (pH=7.0) and serosal (pH=7.8) salines were prepared as per Table 2.2. When using the pH-stat titration system, luminal pH was maintained at 7.8 by titration using a 0.005N HCl solution. Bafilomycin (Enzo Life Sciences) was used to inhibit the apical VHA, and prepared in DMSO at 1.0 mmol $l^{-1}$ for application in a final concentration of 2 μmol $l^{-1}$ and 0.1% DMSO, which has been previously used in the Gulf toadfish (Grosell *et al.*, 2009b; Guffey *et al.*, 2011). CFTRinh-172 (Sigma) was used to inhibit a putative apical CFTR channel (Akiba *et al.*, 2005; Bodinier *et al.*, 2009a; Bodinier *et al.*, 2009b; Marshall *et al.*, 2002), and prepared in DMSO at 1.0 mmol $l^{-1}$ for application in a final concentration of 10 μmol $l^{-1}$ and 0.1% DMSO, which is in the mid-range solubility limit for this blocker (Akiba *et al.*, 2005).

*In vitro short-circuit current, transepithelial potential, and $HCO_3^-$ secretion experiments on isolated intestinal tissue: effects of Japanese Eel guanylin peptides*

In order to measure the effects of Japanese eel guanylin peptides (guanylin, uroguanylin, and RGN) on $I_{SC}$, transepithelial potential (TEP), and transepithelial conductance ($G_{TE}$), Ussing chambers (Physiological Instruments) were employed. Segments of anterior and posterior intestine from each experimental Gulf toadfish (ranging from 20 to 30 g) were excised, cut open, and mounted onto tissue holders (model P2413, Physiological Instruments), which exposed 0.71 $cm^2$ of excised tissue, and

were positioned between two half-chambers (model 2400, Physiological Instruments). Each half-chamber contained 2 ml of appropriately gassed mucosal or serosal saline (Table 2.2). Salines in each half-chamber were continually mixed by airlift gassing with either 100% $O_2$ (mucosal) or 0.3% $CO_2$ in $O_2$ (serosal) (Table 2.2), as described in Genz and Grosell (Genz and Grosell, 2011). The temperatures of the salines in the chambers were maintained at 25°C. Current and voltage electrodes were connected to amplifiers (model VCC600, Physiological Instruments) and, depending on the experiment, recorded either differences in $I_{SC}$ under voltage-clamp conditions at 0.0 mV, with 3s of 1 mV pulses (mucosal-to-serosal) at 60s intervals, or differences in TEP under current-clamp conditions at 0.0 μA, with 3s of 10 μA pulses (mucosal-to-serosal), also at 60s intervals. Epithelial conductance ($G_{TE}$) was determined from inflections in $I_{SC}$ and TEP during pulsing using Ohms law. $I_{SC}$ and TEP measurements were recorded on a computer using BIOPAC systems Acqknowledge software (v. 3.8.1).

In order to simultaneously measure electrophysiological parameters (TEP) and $HCO_3^-$ secretion on the isolated intestinal tissues, Ussing chambers were set up in tandem with a pH-stat titration system (TIM 854 or 856 Titration Managers, Radiometer), as outlined previously (Grosell and Genz, 2006). A pH electrode (model PHC4000.8, Radiometer) and a microburette tip (from which acid was delivered) were submersed in the luminal half-chamber to allow for pH readings and pH-stat titrations. Mucosal salines (injected into the luminal half-chamber) were maintained at a physiological pH of 7.8 throughout all experiments, to allow for symmetrical pH conditions on either side of the epithelium. The pH values and rate of acid titrant (0.005 mol $l^{-1}$ HCl) additions were recorded onto personal computers using the Titramaster software (v. 5.1.0). Epithelial

$HCO_3^-$ secretion rates were calculated from the rate of titrant addition and its concentration, as described in Grosell and Genz (Grosell and Genz, 2006).

To determine the dose response and effective concentrations of the three eel peptides, guanylin, uoguanylin and RGN were added to the luminal half-chamber in a dose-dependent manner ($10^{-9}$–$10^{-5}$ mol $l^{-1}$), as described in Yuge et al. (Takei and Yuge, 2007), while $I_{SC}$ was recorded. Luminal peptide concentrations were increased once stable $I_{SC}$ readings were reached. The length of time to reach a stable reading varied according to individual preparations, resulting in a range of time courses for the peptide and intestinal segment studied (guanylin: AI 189-452 min, PI 180-369 min; uroguanylin: AI 243-399 min, PI 155-440 min; and RGN: AI 176-372 min, PI 254-449 min). All subsequent experiments were performed using only RGN due to limited supplies of guanylin and uroguanylin.

To determine if the secretory anion flux observed following peptide addition was due to the activation of apical CFTR, the CFTR inhibitor CFTRinh-172 was added to the luminal half-chamber prior to the addition of RGN, while TEP and $HCO_3^-$ secretion were recorded. To determine if observed, and unexpected, reductions in $HCO_3^-$ secretion following peptide addition were due to stimulation of apical $H^+$-secretion, the VHA inhibitor, bafilomycin, was added to the luminal half-chamber simultaneously with RGN. Because the effects of bafilomycin can be transient (Grosell *et al.*, 2009b; Guffey *et al.*, 2011), bafilomycin and RGN were added concurrently, rather than in sequence, to capture the immediate effects of this inhibitor on the tissues.

Vehicle controls using 0.1% DMSO (n=5) showed no impact of DMSO on the tissue response to RGN for either $I_{SC}$ or $HCO_3^-$ secretion (data not shown).

*Dependence of $HCO_3^-$ secretion on mucosal $Cl^-$ concentration*

Considering the unexpected reduction in $HCO_3^-$ secretion following peptide addition, the dependence of $HCO_3^-$ secretion on mucosal $Cl^-$ concentrations was examined. Low $Cl^-$ levels were achieved by replacing $Cl^-$ salts with corresponding gluconate salts, while higher levels were achieved by partially replacing $MgSO_4$ with $MgCl_2$. The pH-stat titration experiments were limited in time (~1 hour per flux period) as serosal-to-mucosal $Cl^-$ flux, as well as $Cl^-$ leaking from the pH electrode, contributed to altered $Cl^-$ concentrations during the flux period, especially during low $Cl^-$ conditions. $HNO_3$, rather than HCl, was used as titrant in these experiments in an attempt to reduce $Cl^-$ contamination. All experiments were initiated with a control flux (standard mucosal saline, Table 2.2, $[Cl^-]$ = 129 mmol $l^{-1}$), and then a subsequent flux with $Cl^-$-manipulated saline. Subsamples of the mucosal saline during the second flux were obtained at the beginning and end of each flux to verify actual luminal $Cl^-$ concentrations. Secretion rates of $HCO_3^-$ from the second flux period are expressed as a fraction of the initial control secretion rates.

*Intestinal Sac Preparations*

Intestinal sac preparations were used to examine the net flux of water, $HCO_3^-$, $Cl^-$, and $Na^+$ across the anterior and posterior intestinal epithelia, and followed a modified protocol from Genz and Grosell (Genz and Grosell, 2011). The entire length of the

intestine was excised from an adult Gulf toadfish and cut distally to the pyloric sphincter and proximally to the rectal sphincter. A PE50 catheter was inserted into the anterior end of the excised intestine and tied off with a silk suture. The appropriate mucosal saline (Table 2.2) was then injected into the catheter to rinse the intestine of any debris, precipitates, and intestinal fluids. The anterior portion of the intestine was then tied off with a silk suture and cut to make the anterior sac preparation. The mid intestine was discarded, while a new PE50 catheter was inserted into the posterior portion and the distal end was tied off to make the posterior sac. Two mucosal salines were used for this experiment (Table 2.2): control mucosal saline and treatment mucosal saline containing $5x10^{-8}$ mol $l^{-1}$ RGN. The volume of injected mucosal saline was determined by weighing a 5-ml syringe before and after filling (Table 2.2). After filling an intestinal preparation with appropriate mucosal saline, the intestinal sac was blot-dried and weighed; it was then placed in a scintillation vial filled with 15 ml of serosal saline gassed with 0.3% $CO_2$. The preparations were left for a 2-hr flux period, after which each intestinal sac was blot-dried, weighed, and its mucosal saline collected. The sac tissue itself was then cut down its midline, spread onto tracing paper, and traced to measure its surface area. Subsamples of mucosal saline were collected at the beginning and end of the 2-hr flux period.

Water, $HCO_3^-$, $Cl^-$, and $Na^+$ from the mucosal samples were analyzed using the following methods. $HCO_3^-$ equivalents were calculated by the Henderson-Hasselbalch equation, using mucosal pH values, total $CO_2$ (measured by a Corning 965 carbon dioxide analyzer) readings from individual intestinal sac preparations, and a pK of 9.46 (Grosell *et al.*, 2005). Concentrations of $Na^+$ were measured using flame spectrometry

(Varian 220FS), while $Cl^-$ concentrations were measured using anion chromatography (DIONEX 120). The fluxes for these ions were calculated from the differences between the initial and final amounts of each ion, taking into account the flux period and tissue surface area. Water flux was calculated by taking the difference between the initial and final volume (mass) of each intestinal sac, also taking into account the flux period and tissue surface area.

Table 2.2. Composition of salines for short-circuit current and pH-stat titration experiments

| Compound | Mucosal* | Serosal |
|---|---|---|
| NaCl (mmol $l^{-1}$) | 69.0 | 151.0 |
| KCl (mmol $l^{-1}$) | 5.0 | 3.0 |
| $MgSO_4$ (mmol $l^{-1}$) | 77.5 | 0.88 |
| $MgCl_2$ (mmol $l^{-1}$) | 22.5 | |
| $Na_2HPO_4$ (mmol $l^{-1}$) | | 0.5 |
| $KH_2PO_4$ (mmol $l^{-1}$) | | 0.5 |
| $CaCl_2$ (mmol $l^{-1}$) | 5.0 | 1.0 |
| HEPES, free acid (mmol $l^{-1}$) | | 3.0 |
| HEPES salt (mmol $l^{-1}$) | | 3.0 |
| Urea (mmol $l^{-1}$) | | 4.5 |
| Glucose (mmol $l^{-1}$) | | 5.0 |
| Osmolality (mOsm $l^{-1}$)** | 310 | 310 |
| pH | 7.8† | 7.8 |
| Gas¥ | 100% $O_2$ | 0.3% $CO_2$ in $O_2$ |

*Mucosal application of guanylin, uroguanylin, or renoguanylin, ($10^{-9}$-$10^{-5}$ mol $l^{-1}$).
**Adjusted with mannitol to ensure transepithelial isosmotic conditions in all experiments.
†pH 7.80 was maintained by pH-stat titration.
¥Salines gassed for at least 1 h prior to experimentation.

*Immunohistochemistry*

The anterior and posterior intestinal segments were excised from adult Gulf toadfish, from which CFTR, NKCC (for both NKCC1 and -2), and NKA were immunolocalized following a modified protocol from Bodinier et al. (Bodinier *et al.*,

2009a; Bodinier *et al.*, 2009b). After dissection, intestinal tissues were fixed in Z-fix (Anatech Ltd.) for 48 h, followed by a 1-week immersion in 70% ethanol. Tissues were then dehydrated in ascending grades of ethanol (three washes in 95%, followed by three washes in 100%). Following dehydration, tissues were prepared for wax imbedding by immersing them in two washes of butanol, followed by two washes with Histochoice (Amresco). Tissues were finally immersed in four washes of paraplast (McCormick Scientific) and imbedded. Serial sections (4 μm) were cut from the tissues using a Leitz microtome (model 1512). Sections were transferred and mounted onto Poly-L-lysin-coated slides and dried for 24 h at 37°C. Slides were then prepared for antibody treatment by immersing them into 2 washes of Histochoice (Amresco), 5 washes of decreasing alcohol (100→50% ethanol), and 1 wash in PBS. Subsequently, slides were incubated in 10 mmol $l^{-1}$ citric acid solution and placed in a microwave for two 5-min incubations to reveal antigenic sites. Slides were then immersed in 0.01% Tween-20 in PBS, followed by immersion in a 5% skim milk solution, and three washes in PBS. Primary antibody (10 μg $ml^{-1}$) was dissolved in 0.5% skim milk in PBS, added to each slide, and incubated for 1 h at 37°C. The primary antibodies consisted of monoclonal mouse CFTR (R&D Systems), polyclonal goat NKCC1, and polyclonal rabbit NKA (Santa Cruz Biotechnology). After the 1-h incubation, slides were immersed in three PBS washes. The secondary antibodies consisted of anti-mouse IgG, anti-goat IgG, and anti-rabbit IgG (Alexa Fluor 488, 350, and 568, respectively, from Invitrogen). Slides were once again incubated in 37°C for 1 h, followed by three successive washes in PBS. Coverslips were placed on the slides using ProLong Gold Antifade Reagent (Molecular Probes). Control slides were treated with the same conditions, but without primary antibody. Slides were

observed with an Olympus fluorescent microscope (u-tvo.5xc-2), with attached QImaging camera (Retiga EXi, Fast 1394); iVision and Fiji software were used to analyze images.

*Statistical analyses*

Data are presented as absolute means ± SEM. Means were compared for significant differences using Student's or paired t-tests, Mann-Whitney rank sum tests, and one-way repeated measures analysis of variance (ANOVA) tests as appropriate. The Holm-Sidak test was used, when appropriate, for all multisample comparison tests. All t-tests are two-tailed unless stated otherwise. One-tailed tests were used to analyze changes in $Na^+$, $Cl^-$, and fluid absorption, which have been shown to be inhibited after guanylin peptide stimulation in the mammals (Forte, 1999; Forte and Hamra, 1996). SigmaStat 3.5 and SigmaPlot 11.0 were used for statistical analyses and to calculate EC50 values. Means were considered significantly different when $p<0.05$.

## Results

*cDNA Cloning*

Two distinct guanylin-like peptides and their prepropeptides were cloned from Gulf toadfish intestinal cDNA, revealing peptides of 108 and 109 amino acids (Fig. 2.1). The two cloned peptide variants differ at six amino acid positions at residues 1, 3, 9-11, and 13 (Fig. 2.1). They were sufficiently different from one another to identify them as Gulf toadfish guanylin (tf guanylin) and Gulf toadfish uroguanylin (tf guanylin), after comparing them to the sequences of birds, mammals, reptiles, and teleosts (Fig. 2.2). In

addition, these putative tf guanylin and tf uroguanylin peptides were verified by comparing their nucleotide sequences (Fig. 2.1) to identical sequences found in the intestinal transcriptome of the Gulf toadfish.

Moreover, tf guanylin differed from Japanese eel guanylin and renoguanylin (RGN) at residues 1, 3, and 8, and at residues 1 and 3, respectively. tf uroguanylin exhibited greater variation than guanylin and differed from Japanese eel uroguanylin and RGN at residues 1, 3, 10, 11, and 13, and at residues 1, 9-11, and 13, respectively (Fig. 2.2).

Fig. 2.1. cDNA sequences of guanylin and uroguanylin prohormones from the intestine of the Gulf toadfish. 3'- and 5'-RACE reactions were performed to acquire overlapping portions of each transcript using degenerate primers, based on the nucleotide sequences of mature peptides (boxed) from several teleost species. Subsequently, full prohormone sequences were obtained using gene-specific primers, resulting in peptides of 108 (guanylin) and 109 (uroguanylin) amino acids in length.

Fig. 1

Guanylin

```
 M  K  A  T  F  T  A  I  V  L  L  V  F  A  L  A  S  A  S  E  A  V  Q  V  H  E
ATGAAGGCCACGTTCACCGCCATTGTGCTCCTCGTCTTTGCTCTCGCTTCGGCTTCAGAGGCGGTGCAAGTCCACGAG    78
 G  G  L  S  F  S  L  E  A  V  K  K  L  Q  E  L  T  E  S  G  D  A  V  Q  A  Q
GGCGGATTGTCATTCTCACTGGAAGCCGTGAAGAAGCTCCAGGAGCTGACAGAGAGCGGCGATGCGGTGCAAGCACAA   156
 S  P  R  L  L  V  R  N  N  A  V  C  D  N  P  E  L  P  E  E  L  L  P  L  C  K
AGTCCTCGCCTCCTGGTGCGCAACAACGCCGTCTGTGACAACCCCGAACTCCCAGAGGAGCTCCTGCCCCTCTGCAAG   234
 Q  R  A  A  S  A  S  F  A  R  L  A  M  V  P  M  D  V  C  E  I  C  A  F  A  A
CAAAGGGCAGCATCTGCATCGTTCGCCAGACTAGCGATGGTTCCCATGGACGTGTGTGAGATCTGCGCTTTTGCTGCC   312
 C  T  G  C
TGCACTGGATGC                                                                      324
```

Uroguanylin

```
 M  K  L  L  T  V  A  V  A  L  T  L  C  L  C  S  V  A  A  D  V  H  V  K  V  G
ATGAAGCTGCTGACTGTTGCCGTGGCTCTGACCTTGTGTTTGTGCAGCGTGGCTGCAGACGTGCACGTGAAGGTTGGA    78
 E  K  S  F  P  L  E  A  V  K  R  L  K  E  L  T  D  L  D  G  H  V  S  P  H  L
GAAAAGAGCTTCCCCTTGGAGGCAGTCAAGCGGCTGAAGGAGCTGACGGATCTGGACGGCCACGTCAGCCCTCATCTC   156
 T  A  A  N  V  A  A  V  C  A  D  P  L  M  P  Q  V  F  Q  A  A  C  Q  E  N  A
ACCGCGGCGAATGTTGCAGCTGTTTGTGCCGACCCTCTCATGCCGCAGGTCTTTCAGGCGGCGTGCCAAGAGAACGCA   234
 A  A  I  V  F  S  K  L  V  Y  I  I  T  P  L  D  L  C  E  I  C  A  N  P  S  C
GCAGCCATTGTTTTCTCCAAATTAGTGTATATTATCACGCCTTTGGATCTCTGTGAAATTTGTGCCAATCCCTCCTGC   312
 Y  G  C  L  N
TATGGATGTCTGAAC                                                                   327
```

Fig. 2.2. Sequence comparisons of mature guanylin (GN), uroguanylin (UGN), and renoguanylin (RGN) from various bird, mammalian, reptilian, and teleost species. Gulf toadfish amino acid residues from guanylin and uroguanylin that are identical to those of other species are colour-coded and in bold. Amino acid residues in red are conserved across most species and illustrate the close sequence homology of the guanylin peptides. NCBI accession numbers are in order from top to bottom. **Guanylin**: AB080640.1, FM173262.1, BX866654, CA045042, CK402502, KJ549666, CD759824, BJ877267, M95174, M93005, Z73607, XM_004406665.1, XM_002189797.2, XM_005014992.1, EMP42088.1, and XM_006278378.1; **RGN**: AB080641.1; **Uroguanylin**: BX3093850, CA041361, BJ512940, KJ549667, FM173261.1, AB080642.1, CK401577, CD283474, U34279, Z83746, U14322, and XP_004406740.1.

| | |
|---|---|
| Japanese Eel GN | YDECEICMFAACTGC |
| European Eel GN | YDECEICMFAACTGC |
| Trout GN | MDICEICAFAACTGC |
| Salmon GN | MDICEICAFAACTGC |
| Catfish GN | MDVCEICAFAACTGC |
| **Toadfish GN** | **MDVCEICAFAACTGC** |
| Zebrafish GN | VDVCEICAFAACTGC |
| Medaka GN | RDLCEICAFAACTGC |
| Human GN | PGTCEICAYAACTGC |
| Rat GN | PNTCEICAYAACTGC |
| Pig GN | PSTCEICAYAACAGC |
| Walrus GN | PRSCEICAFAACAGC |
| Zebra Finch GN | DDLCEICANAACAGCF |
| Mallard GN | ADLCEICANAACSGCF |
| Green Sea Turtle GN | PELCEICAFAACAGC |
| American Alligator GN | MELCEICVNAACAGC |
| | |
| Japanese EEL RGN | ADLCEICAFAACTGCL |
| | |
| Trout UGN | PDLCEICAHPACFGCLP |
| SaLmon UGN | PDLCEICAHPACFGCLP |
| Medaka UGN | SDPCEICANPSCFGCLK |
| **Toadfish UGN** | **LDLCEICANPSCYGCLN** |
| European Eel UGN | PDPCEICANAACTGCL |
| Japanese Eel UGN | PDPCEICANAACTGCL |
| Catfish UGN | PDPCEICANAACTGCVFNKI |
| Zebrafish UGN | IDPCEICANVGCTGC |
| Human UGN | NDDCELCVNVACTGCL |
| Pig UGN | GDDCELCVNVACTGCS |
| Rat UGN | TDECELCINVACTGC |
| Walrus UGN | KDNCELCVNVACTGCL |
| Soft-shelled Turtle UGN | IDICEICANAACAGCL |

*Effects of eel guanylin peptides on $I_{SC}$*

The effects of eel guanylin, uroguanylin, and RGN on dissected Gulf toadfish tissues mounted in Ussing chambers are clear. A one-way, repeated measures ANOVA revealed that the $I_{SC}$ of the anterior intestine (n=6 for all treatments) remained unchanged (Fig. 2.3A, B, C), while in the posterior intestine, there was a significant reversal of the $I_{SC}$ (from mucosa-to-serosa to serosa-to-mucosa), due to the eel guanylin peptides, in a dose-dependent manner (**Table 2.3**). The maximal $\Delta I_{SC}$ in the posterior intestine due to eel guanylin, uroguanylin, and RGN (n=5, 6, 6, respectively) occurred at concentrations of $\geq 10^{-7}$, $10^{-7}$, and $2x10^{-7}$ mol $l^{-1}$ (Fig. 2.3D, E, F), respectively, with EC50 values of $5.82x10^{-8}$ (guanylin), $4.90x10^{-8}$ (uroguanylin), and $1.16x10^{-8}$ mol $l^{-1}$ (RGN). The differences observed in response to the eel peptides in the posterior intestine are in agreement with those from a previous report (Yuge and Takei, 2007). Differences in $G_{TE}$ values between the anterior and posterior intestinal segments, independent of the dose of the three eel guanylin peptides, were significant (Table 2.4). No differences in $G_{TE}$ across doses in the anterior intestine were observed, but $G_{TE}$ increased in the posterior intestine in a dose dependent manner for all three eel guanylin peptides, matching the changes in observed $I_{SC}$ (Table 2.4).

*Effects of eel RGN on $HCO_3^-$ Secretion*

Surprisingly, mucosal application of eel RGN to posterior intestinal tissue, mounted in an Ussing chamber-pH-stat titration system, significantly reduced $HCO_3^-$ secretion, depressing the mean secretion rate between 13.3-21.2% (Fig. 2.4A). Additionally, the TEP of the posterior tissues significantly decreased 30 min after

exposure to RGN (Fig. 2.4B). However, $G_{TE}$ remained unaffected after mucosal application of RGN, with a mean value of 5.6±0.1 mS $cm^{-2}$.

To examine if the observed inhibition of $HCO_3^-$ secretion in the posterior intestine due to RGN may have been caused by a downstream effect of RGN acting on the apical VHA, both bafilomycin and RGN were applied to the mucosal saline in an Ussing chamber-pH-stat titration system. Following the results of the previous experiment, a one-way, repeated measures ANOVA revealed that this treatment reduced the mean $HCO_3^-$ secretion rate by 12.9-34.5% after mucosal application (Fig. 2.5A). The TEP also decreased significantly 30 min after treatment with RGN and bafilomycin (Fig. 2.5B). Similarly to the previous experiment, $G_{TE}$ remained unaffected after treatment (4.68±0.12 mS $cm^{-2}$). Mean $HCO_3^-$ secretion rates in Fig. 2.4A and Fig. 2.5A, in the pre-RGN-treated (control) tissues, fall within the range previously reported for the Gulf toadfish posterior intestine (Grosell, 2006; Guffey *et al.*, 2011).

*Intestinal sac preparations: $Na^+$, $Cl^-$, Water, and $HCO_3^-$ fluxes*

As hypothesized, a one-tailed test revealed that eel RGN resulted in a significant stimulation of a secretory $Cl^-$ flux in the posterior intestine (Fig. 2.6B), while no effect was present in either the control tissues or in the eel RGN-treated anterior intestinal tissues. However, in both the anterior and posterior intestinal sac preparations, there were no differences in $Na^+$ flux between control and eel RGN-treated tissues (Fig. 2.6A). As for water, a one-tailed test revealed that eel RGN stimulation resulted in significant net fluid secretion in the posterior intestinal sacs (Fig. 2.6D), while no effects were present in control tissues or eel RGN-stimulated anterior intestinal sacs. Contradictory to our

hypothesis, however, a one-tailed test revealed that eel RGN significantly decreased $HCO_3^-$ secretion (similarly to the pH-stat titration experiment) by roughly 34% in the posterior intestinal sacs (Fig. 2.6C) compared to controls or eel RGN-treated anterior intestinal sacs.

*Intestinal sac preparations: $Na^+$, $Cl^-$, Water, and $HCO_3^-$ fluxes*

As hypothesized, a one-tailed test revealed that eel RGN resulted in a significant stimulation of a secretory $Cl^-$ flux in the posterior intestine (Fig. 2.6B), while no effect was present in either the control tissues or in the eel RGN-treated anterior intestinal tissues. However, in both the anterior and posterior intestinal sac preparations, there were no differences in $Na^+$ flux between control and eel RGN-treated tissues (Fig. 2.6A). As for water, a one-tailed test revealed that eel RGN stimulation resulted in significant net fluid secretion in the posterior intestinal sacs (Fig. 2.6D), while no effects were present in control tissues or eel RGN-stimulated anterior intestinal sacs. Contradictory to our hypothesis, however, a one-tailed test revealed that eel RGN significantly decreased $HCO_3^-$ secretion (similarly to the pH-stat titration experiment) by roughly 34% in the posterior intestinal sacs (Fig. 2.6C) compared to controls or eel RGN-treated anterior intestinal sacs.

*Effects of CFTRinh-172 and RGN on ion transport across the posterior intestine*

Neither treatment with CFTRinh-172 nor with subsequent treatment of RGN in the mucosal half-chamber of an Ussing chamber affected the $HCO_3^-$ secretion rate in the posterior intestine (Fig. 2.7A). CFTRinh-172 did not affect posterior intestinal TEP,

however, as with previous experiments, RGN did cause a significant decrease in TEP despite being applied after CFTRinh-172 (Fig. 2.7B). The typical stimulation of $I_{SC}$ by RGN was prevented by pre-treatment with CFTRinh-172 (Fig. 2.7C). Similarly to the previous experiments, $G_{TE}$ remained unaffected across all treatments with a mean value of 6.08±1.00 mS $cm^{-2}$. It is worth mentioning that 5-nitro-2-(3-phenylpropylamino) benzoic acid (NPPB), a known CFTR blocker used in the Japanese eel (Yuge and Takei, 2007), was initially tested. However, application of NPPB alone resulted in a net secretory $I_{SC}$, similarly to that produced by the eel peptides (possibly acting as a general $Cl^-$ transporter blocker). Thus, CFTRinh-172 was used in the present study.

*Immunohistochemistry: tissue-specific differences in histology*

Differences between the anterior and posterior intestine (n=3) concerning the presence of apical CFTR, apical NKCC2, basolateral NKA, and basolateral NKCC1 were observed. In the anterior intestine, NKCC1-like, NKCC2-like, and NKA-like immunoreactivity was observed in the enterocytes (Fig. 2.9A). These same transporters were also observed in the posterior intestine, along with CFTR-like immunoreactivity in the apical membrane (Fig. 2.9B, C). These results indicate distinct differences in apical CFTR localization between the anterior and posterior intestine and are in agreement with previous reports of other marine teleost species (Bodinier *et al.*, 2009a; Li *et al.*, 2014; Marshall *et al.*, 2002).

Fig 2.3. Dose-dependent effects of mucosal application of (A, D) guanylin (GN), (B, E) uroguanylin (UGN), and (C, F) renoguanylin (RGN) on the short circuit current ($I_{SC}$) of anterior and posterior intestinal epithelia. Values are represented as the difference in short circuit current ($\Delta I_{SC}$) from control (no dose) conditions as a function of peptide concentration. Anterior intestinal (A-C) tissues were dosed with $10^{-9}$-$10^{-6}$ M of the peptides, while posterior intestinal (d-f) tissues were dosed with $10^{-9}$-$10^{-5}$ M of the peptides. Values are means ± SEM (n=5-6). † indicates significant differences ($p<0.05$) between anterior and posterior intestine, while * indicates significant effects of increasing dose within a tissue.

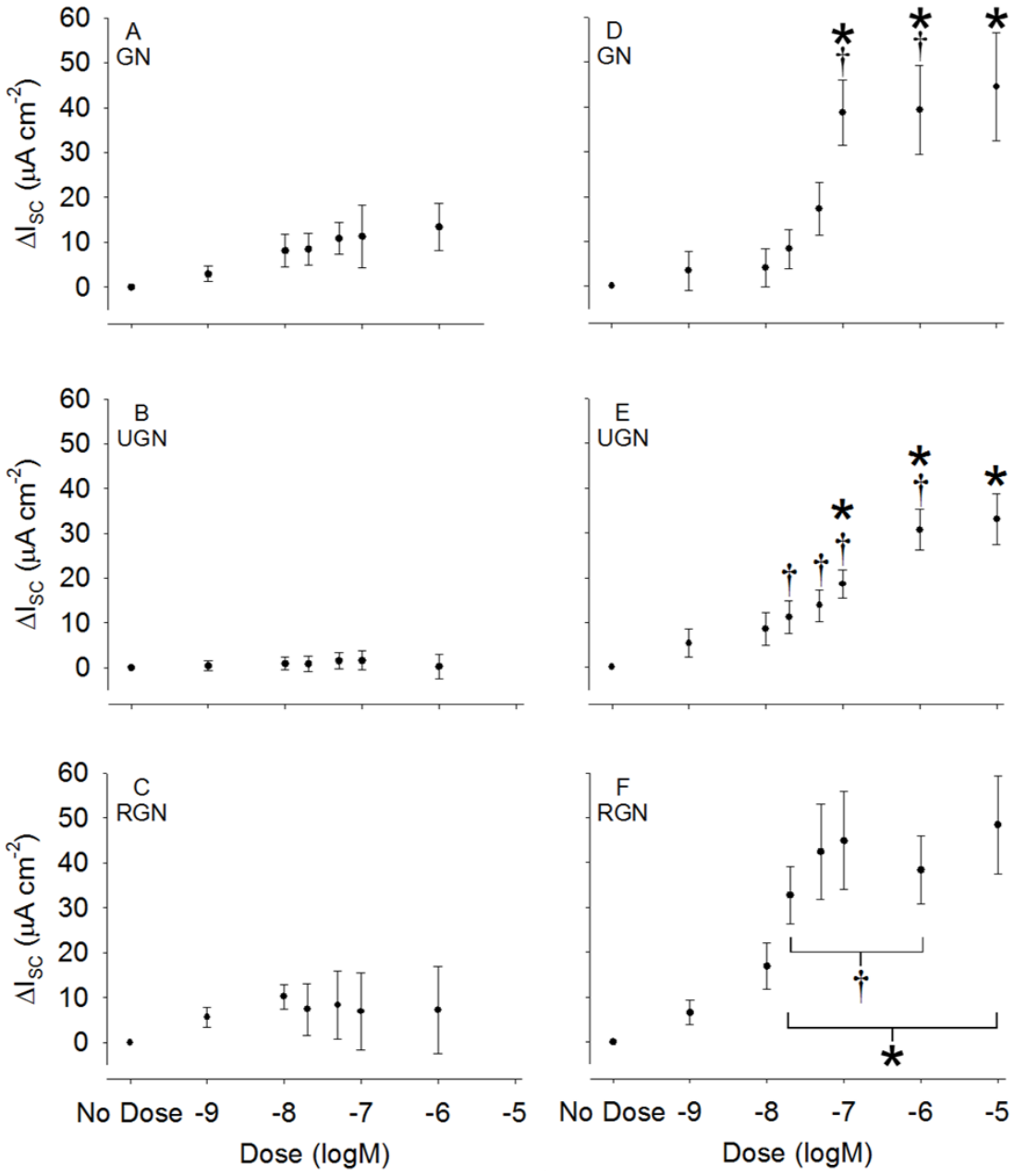

Table 2.3. Short-circuit current ($I_{SC}$) of the anterior (AI) and posterior intestine (PI) in response to guanylin (GN), uroguanylin (UGN), and renoguanylin (RGN).

| | | $I_{SC}$ ($\mu A\ cm^{-2}$) | | | | | | | |
|---|---|---|---|---|---|---|---|---|---|
| Dose (mol $l^{-1}$) | | Control | $10^{-9}$ | $10^{-8}$ | $2x10^{-8}$ | $5x10^{-8}$ | $10^{-7}$ | $10^{-6}$ | $10^{-5}$ |
| GN | AI | -25.4±16.6 | -7.5±2.6 | -5.5±2.9 | -20.3±17.9 | -18.3±18.4 | -25.5±23.2 | -28.0±26.2 | |
| | PI | -22.3±15.4 | -18.8±18.8 | -18.1±18.2 | -14.0±17.9 | -5.0±18.67 | 14.5±24.9* | 17.0±20.0* | 22.2±20.8* |
| UGN | AI | -8.8±6.8 | -8.4±7.3 | -7.9±8.0 | -8.0±8.1 | -7.3±8.4 | -4.0±8.8 | -5.4±9.4 | |
| | PI | -25.9±4.6 | -21.0±4.0 | -17.7±3.9 | -7.0±8.7 | -5.0±8.1 | -1.5±6.7* | 9.5±5.3* | 12.5±6.4* |
| RGN | AI | -7.3±2.5 | -1.7±3.7 | 1.4±3.0 | -4.5±5.9 | -6.1±5.2 | -8.6±5.4 | -9.3±5.5 | |
| | PI | -30.2±3.07 | -23.6±3.9 | -13.3±5.8 | 2.6±8.4* | 12.3±12.5* | 14.7±12.8* | 6.2±8.0* | 18.3±12.9* |

Values are means ± SEM; n = 5-6 for the responses of each anterior and posterior intestinal segment to guanylin, uroguanylin, and RGN, respectively. Peptides were applied to the mucosal half-chamber (2 mL volume) of an Ussing chamber in a cumulative manner. Negative mean values denote net absorption, while positive mean values denote net secretion. The time course for each experiment varied among individuals (see text for details). *indicates significant effects of increasing dose within a tissue from the control.

Table 2.4. Transepithelial conductance ($G_{TE}$) of the anterior (AI) and posterior intestine (PI) in response to guanylin (GN), uroguanylin (UGN), and renoguanylin (RGN).

| | | $G_{TE}$ (mS $cm^{-2}$) | | | | | | | |
|---|---|---|---|---|---|---|---|---|---|
| Doses (mol $l^{-1}$) | | Control | $10^{-9}$ | $10^{-8}$ | $2x10^{-8}$ | $5x10^{-8}$ | $10^{-7}$ | $10^{-6}$ | $10^{-5}$ |
| GN | AI† | 8.86±1.06 | 8.69±1.22 | 8.41±2.42 | 8.41±1.68 | 8.97±1.50 | 8.46±2.69 | 9.38±1.89 | |
| | PI | 6.62±1.44 | 7.00±1.25 | 6.97±1.22 | 7.37±1.04 | 7.22±1.16 | 7.16±1.22 | 7.34±1.37 | 8±1.12 * |
| UGN | AI† | 11.03±0.36 | 11.33±0.54 | 11.30±0.57 | 10.98±0.35 | 11.37±0.43 | 11.51±0.53 | 11.59±0.52 | |
| | PI | 6.29±0.50 | 6.10±0.50 | 6.20±0.54 | 6.22±0.55 | 6.28±0.63 | 6.17±0.59 | 6.41±0.55 | 7.32±0.64* |
| RGN | AI† | 10.44±0.33 | 10.29±0.31 | 10.56±0.28 | 10.63±0.36 | 11.08±0.26 | 11.27±0.22 | 11.43±0.39 | |
| | PI | 5.94±0.53 | 5.89±0.53 | 5.89±0.55 | 6.42±0.74 | 6.65±0.92 | 6.96±0.88 | 6.63±1.09 | 7.09±1.04* |

Values are means ± SEM; n = 5-6 for the responses of each anterior and posterior intestinal segment to guanylin, uroguanylin, and RGN, respectively. Peptides were applied to the mucosal half-chamber (2 mL volume) of an Ussing chamber in a cumulative manner. † indicates that the $G_{TE}$ value of the anterior intestine at any given dose is significantly greater than its counterpart value in the posterior intestine ($p<0.05$), while * indicates differences from the control within a tissue.

Fig. 2.4. (A) $HCO_3^-$ secretion and (B) transepithelial potential (TEP) of isolated posterior intestinal tissue following mucosal application of renoguanylin (RGN; $5x10^{-8}$ M; indicated by the arrow) in Ussing chambers. Values are means ± SEM (n=6-7). *Indicates significant differences ($p<0.05$) in $HCO_3^-$ secretion and in TEP from the control period (0-30 min).

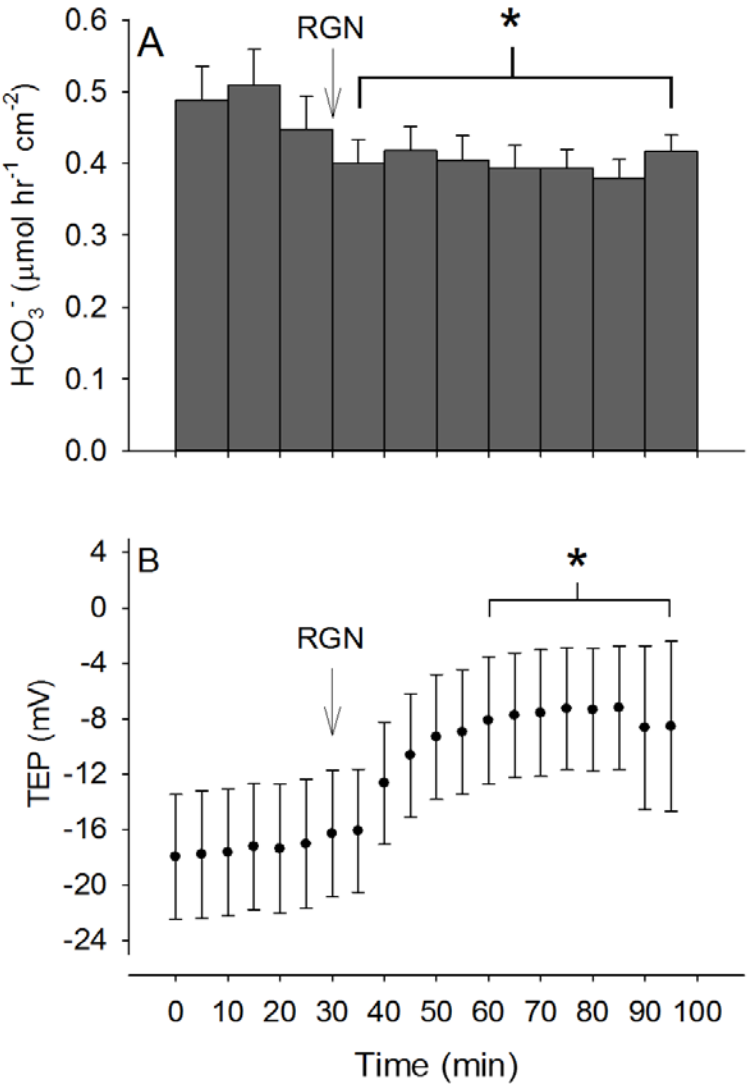

Fig. 2.5. (A) $HCO_3^-$ secretion and (B) transepithelial potential (TEP) of isolated posterior intestinal tissue exposed to mucosal doses of bafilomycin (baf; 2 µM) and renoguanylin (RGN; $5x10^{-8}$ M), indicated by an arrow. Values are means ± SEM (n=5-6). *Indicates significant differences ($p<0.05$) from the control period (0-30 min).

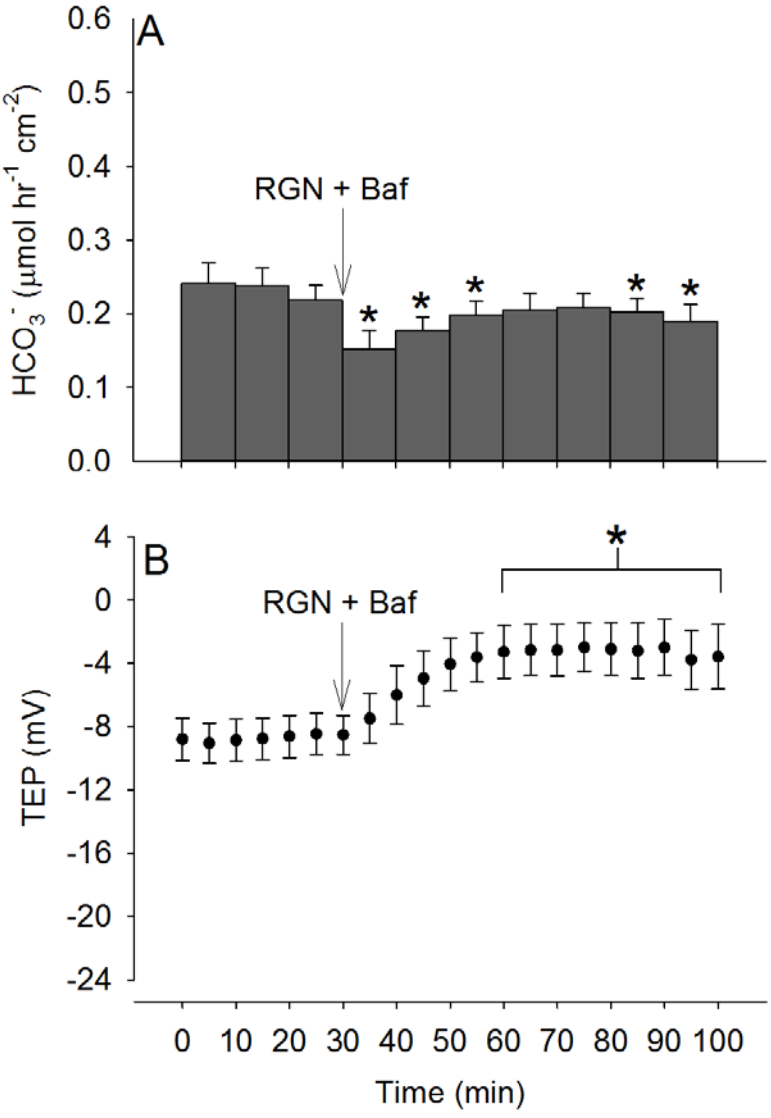

Fig. 2.6. (A) $Na^+$, (B) $Cl^-$, (C) water, and (D) $HCO_3^-$ fluxes obtained from Gulf toadfish anterior and posterior intestinal sac preparations with and without luminal addition of renoguanylin (RGN). Negative and positive values indicate secretion and absorption, respectively. Values are means ± SEM (n=5-15). *Indicates significant differences ($p<0.05$) within a tissue (i.e. the control (CTRL) and treatment (RGN) groups).

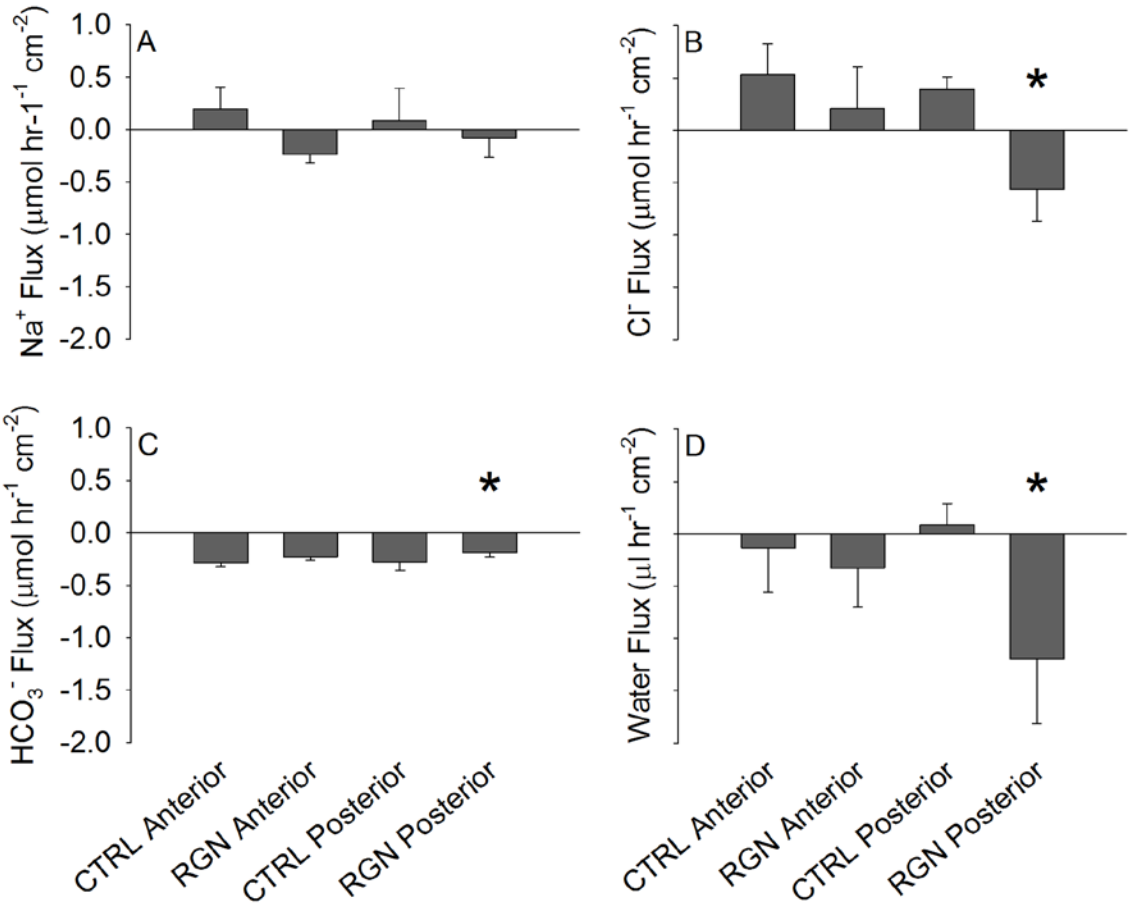

Fig. 2.7. (A) $HCO_3^-$ secretion, (B) transepithelial potential (TEP), and (C) short-circuit current ($I_{SC}$) of isolated posterior intestinal tissue exposed to mucosal application of CFTRinh-172 (10 µM) and renoguanylin (RGN; $5x10^{-8}$ M), indicated by arrows. Values are means ± SEM (n=5-6). *Indicates significant differences ($p<0.05$) from the control period (0-30 min).

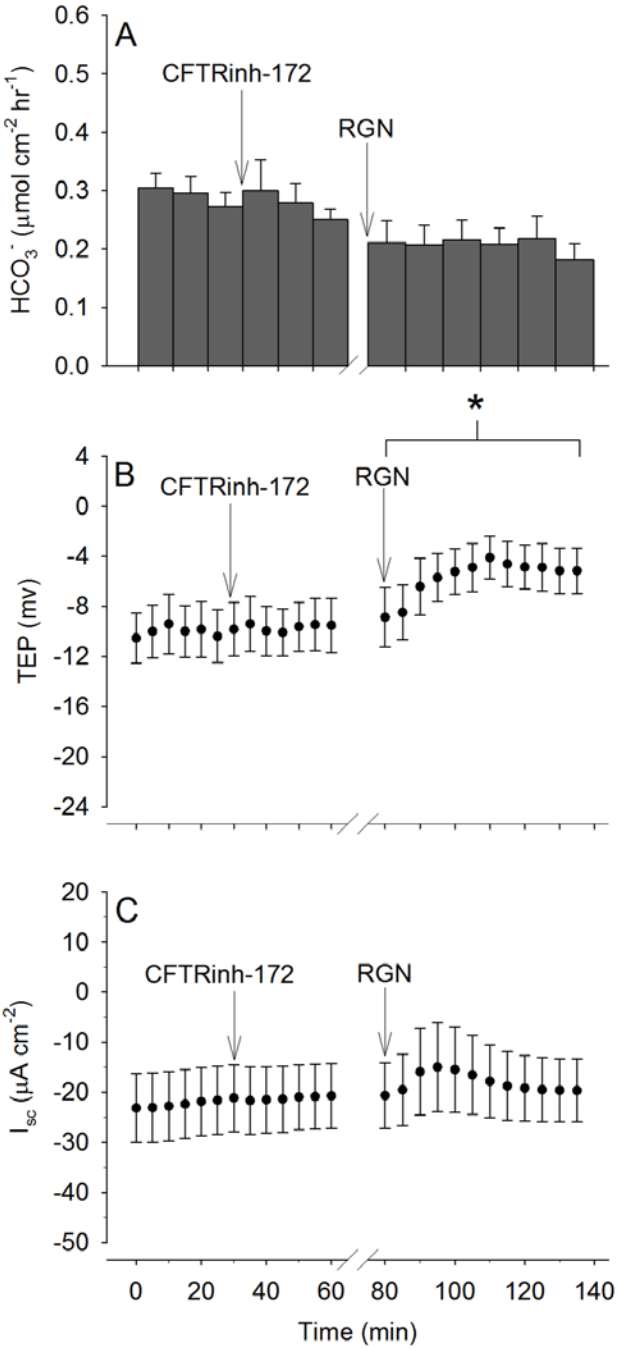

*Dependence of $HCO_3^-$ secretion on mucosal $Cl^-$ concentration*

Contrary to expectations, intestinal $HCO_3^-$ secretion rates were unaffected by luminal $Cl^-$ concentrations (Fig 2.8) within the range tested (3.8-154.8 mmol $l^{-1}$).

Fig. 2.8. $HCO_3^-$ secretion rates by anterior intestinal epithelia as a function of mucosal $Cl^-$ concentrations of the Gulf toadfish. Values are means ± SEM. An initial control flux was measured using salines described in Table 1 prior to replacing luminal salines with different $Cl^-$ levels. Data is presented as normalized to the $HCO_3^-$ secretion rates during the initial 1-h control period. Horizontal error lines indicate the change in [$Cl^-$] over time during the second flux period while vertical error bars indicate variation in $HCO_3^-$ secretion rate over time during the second flux period.

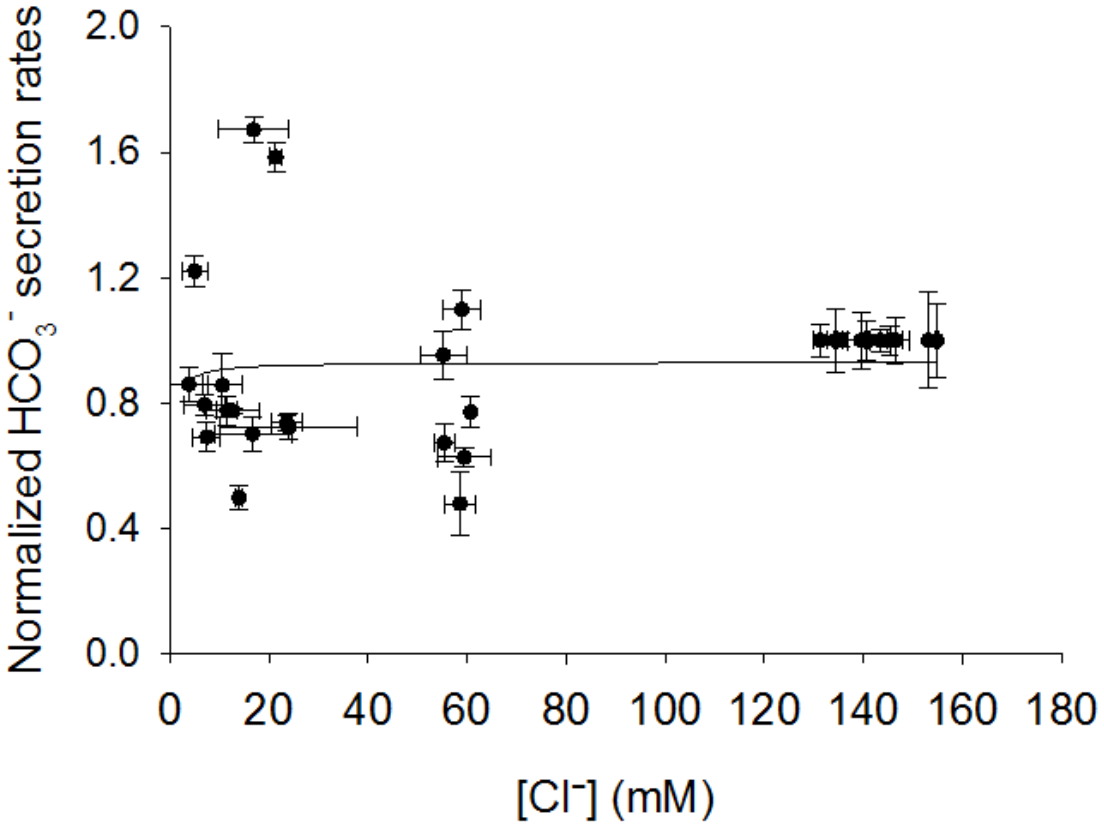

Fig. 2.9. Overlaid fluorescence image (40x magnification) of NKA-like (red, basolateral), CFTR-like (green, apical), NKCC1-like (blue, basolateral), and NKCC2-like (blue apical) immunoreactivity in adult Gulf toadfish (a) anterior and (b) posterior intestine. (c) A higher magnification image (100x) of the posterior intestine (showing presumed fluorescence for the three above-mentioned ion transporters), in which individual nuclei (N) can be clearly distinguished. AM: apical membrane; BM: basolateral membrane; L: lumen

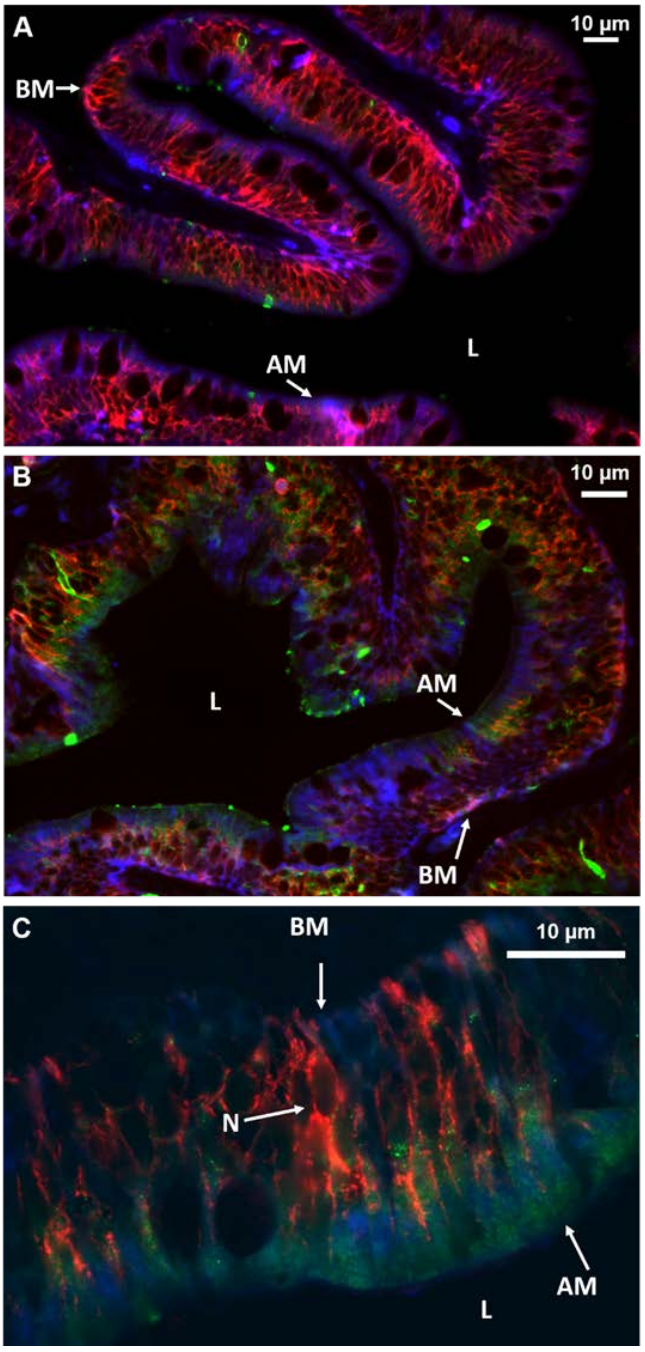

## Conclusion

*Tissue-specific responses to eel* guanylin*, uro*guanylin*, and RGN*

Despite the evolutionary distances between the selected animal classes listed in Fig. 2, the amino acid sequences of guanylin and uroguanylin are remarkably well conserved. In the majority of sequences across species and animal classes, the amino acid residues 4-8 (CEICA), 10-12 (AAC), and 14-15 (GC) do not differ. Eel RGN produced effects in the intestine of both the Gulf toadfish and Japanese eel, presumably because of its high degree of similarity to guanylin from both these species. Thus, despite these minor differences, our initial analyses gave us confidence that the Japanese guanylin peptides could be used to stimulate physiological responses in the Gulf toadfish tissue. Indeed, all eel guanylin peptides elicited robust responses from the Gulf toadfish posterior intestine, similarly to those observed in the Japanese eel and, in some cases, to mammalian intestinal epithelia as well. Moreover, the similarities in the amino acid sequences between eel RGN and tf guanylin may also explain the greater than fourfold difference in the EC50 value of eel RGN when compared to eel guanylin and uroguanylin. Thus, eel guanylin and eel uroguanylin might not bind to the Gulf toadfish guanylin receptors as readily as eel RGN.

The present study reveals that only the posterior portion of the Gulf toadfish intestine responds to mucosal application of eel guanylin, uroguanylin, and RGN by reversing $I_{SC}$, causing net $Cl^-$ and fluid secretion, and inhibiting $HCO_3^-$ secretion. Changes in $I_{SC}$, due to guanylin peptide stimulation, have also been observed in the Japanese eel (66) and may be common to marine teleosts. The Gulf toadfish and Japanese eel responses are in contrast to the effects of guanylin and uroguanylin in mammals,

where both peptides act on the entire mammalian intestinal tract (5, 14, 15, 31, 38, 42). A parsimonious explanation for the region-specific responses in the Gulf toadfish intestine to the guanylin peptides may be the distribution of possibly distinct GC-C subtypes and their different affinities for the guanylin peptides. Indeed, GC-C1 and GC-C2 are two GC-C subtypes so far characterized in the European (*Anguilla anguilla)* and Japanese eels (Comrie *et al.*, 2001b; Kalujnaia *et al.*, 2009; Yuge *et al.*, 2006). Two subtypes, OlGC6 and OlGC9, are also expressed in medaka (*Oryzias latipes*) (Iio *et al.*, 2005), while only one GC-C type has been found in mammals and it is the predominant GC in the intestine (Arshad and Visweswariah, 2012). Nonetheless, stimulation of fish and mammalian GC-Cs expressed in cell culture lines by guanylin or uroguanylin leads to significant guanylyl cyclase activity and increases in cGMP (Comrie *et al.*, 2001a; Currie *et al.*, 1992; de Sauvage *et al.*, 1992; Iio *et al.*, 2005; Schulz *et al.*, 1990; Yuge *et al.*, 2006), yet, in the anterior intestine of marine teleosts, these increases may not be occurring in significant amounts (if at all) to produce the downstream effects observed in the posterior intestine.

An equally parsimonious alternative/additional explanation to describe the regional response of the Gulf toadfish intestine to the guanylin peptides may be the observation of both basolateral NKCC1-like and apical CFTR-like immunoreactivity in the posterior intestine. Expression of basolateral NKCC1 and apical CFTR is not uncommon in the posterior intestine of marine and SW-adapted euryhaline teleost species (Bodinier *et al.*, 2009a; Cutler and Cramb, 2002; Hiroi *et al.*, 2008; Li *et al.*, 2014; Marshall *et al.*, 2002), which could form a secretory pathway for $Cl^-$.

Eel uroguanylin elicited a weaker response from the Gulf toadfish posterior intestine than did eel guanylin and RGN (despite a lower EC50 value than eel guanylin), and this difference appears to be more pronounced than that observed in the Japanese eel (Yuge and Takei, 2007). In the Japanese eel, it seems that the extracellular receptor making up GC-C1 binds preferentially to uroguanylin, while extracellular receptor making up GC-C2 is the predominant GN receptor (Yuge *et al.*, 2006). Although it is unknown if Gulf toadfish possess multiple GC-C receptors, it is possible that the presence of multiple Gulf toadfish GC-Cs bind eel uroguanylin and uroguanylin differentially, and it is conceivable that the posterior intestine of the Gulf toadfish expresses more of a GC-C subtype that binds favourably to eel guanylin and RGN over eel uroguanylin. In addition, it cannot be ruled out that the experimental conditions applied in the present study affected peptide-receptor interactions. In rat intestinal tissues and in T84 cells expressing rat GC-C, for example, tissues were most sensitive to uroguanylin in salines of pH 5.5, with guanylin being more effective between pH 7.4-8.0 (Hamra *et al.*, 1997; Joo *et al.*, 1998). It is plausible that uroguanylin elicited a weaker $I_{SC}$ reversal at the posterior intestine due to the pH of the mucosal saline used in this study (pH 7.8), which would interfere with its binding ability. However, the low pH hypothesis may not apply to teleost guanylin peptides as Yuge and collaborators (Yuge *et al.*, 2006) performed their experiments by applying eel guanylin peptides to a mucosal saline of pH 7.2, resulting in increases in intracellular cGMP levels in the Japanese eel.

*Eel guanylin, uroguanylin, and RGN reverse electrolyte and fluid transport in the posterior intestine*

In the present study, the eel guanylin peptides reversed the $I_{SC}$ of the Gulf toadfish posterior intestine from net absorptive to net secretory. This secretory response is in accordance to those observed in the Japanese eel mid and posterior intestine (Yuge and Takei, 2007), throughout the rat intestine (Joo *et al.*, 1998), and in T84 cells (Hamra *et al.*, 1997). Conversely, the $I_{SC}$ of the Gulf toadfish anterior intestine, as with the Japanese eel (Yuge and Takei, 2007), was unaffected by either of the eel guanylin peptides. The reversal of the posterior intestine's $I_{SC}$ by eel RGN coincides with a reversal of $Cl^-$ flux, which results in net $Cl^-$ and fluid secretion into the intestinal sac preparations. This response is similar to those observed in mammalian tissues and in T84 cells, in which mucosal application of guanylin has been shown to significantly alter the $I_{SC}$, activate apical CFTR, and cause $Cl^-$ and fluid secretion [for review in Forte (Forte, 1999)], and agrees with a guanylin-induced reversal of the $I_{SC}$ of the Japanese eel mid and posterior intestine (Yuge and Takei, 2007). Furthermore, in all Ussing chamber experiments performed in this study, mucosal application of eel RGN significantly decreased the serosa negative TEP of the posterior intestine, consistent with anion secretion. Moreover, eel RGN increased $G_{TE}$ modestly, but significantly, in the $I_{SC}$ studies on the posterior intestine; however, such increases were not observed in the subsequent studies and may be due to the dose of RGN to which we exposed tissues. In the $I_{SC}$ experiments, only posterior intestinal tissues exposed to $10^{-5}$ mol $l^{-1}$ guanylin, uroguanylin, or RGN demonstrated significant increases in $G_{TE}$. Curiously, while it

appears that $5x10^{-8}$ mol $l^{-1}$ RGN was sufficient to inhibit $HCO_3^-$ secretion and reverse $I_{SC}$, it was insufficient to cause changes in $G_{TE}$.

To determine if apical CFTR mediates the reversal of the $I_{SC}$ at the posterior intestine, via net $Cl^-$ secretion, we used CFTRinh-172, a known mammalian CFTR blocker (Kopeikin *et al.*, 2010). Yuge and Takei (Yuge and Takei, 2007) demonstrated that simultaneously exposing Japanese eel intestinal tissues to NPPB, another CFTR inhibitor, and guanylin did not affect the absorptive $I_{SC}$, suggesting that $Cl^-$ is secreted by apical CFTR. In the present study, exposing the Gulf toadfish posterior intestine to CFTRinh-172 prevented the RGN-stimulated change in $I_{SC}$. These results suggest that, as in mammals and in the Japanese eel, apical CFTR plays a primary role in $Cl^-$ secretion by the intestine and is activated by the downstream effects of GC-C activation. Consistent with these observations is evidence of apical CFTR-like immunoreactivity in the posterior intestine, but not in the anterior intestine, of the Gulf toadfish.

Apical expression of CFTR in the intestine of marine and SW-adapted teleosts has been documented previously (Bodinier *et al.*, 2009a; Gregorio *et al.*, 2013; Marshall *et al.*, 2002), and it has been revealed that apical CFTR expression may be important in SW adaptation (Bodinier *et al.*, 2009b). Moreover, the intestine of SW-adapted teleosts also expresses basolateral NKCC1 and apical NKCC2 (Cutler and Cramb, 2002; Gregorio *et al.*, 2013; Hiroi *et al.*, 2008). Immunohistochemisty in the present study also reveals apical expression of CFTR-like and NKCC2-like immunoreactivity, consistent with a previous report on the Gulf toadfish (Tresguerres *et al.*, 2010), and basolateral NKCC1-like immunoreactivity in the Gulf toadfish intestine. However, the distribution of these transporters is not uniform and the discontinuity of transporter types coincides with the

present report's physiological findings of $Cl^-$ secretion. In the anterior intestine, there is clear NKCC1-like and NKCC2-like immunoreactivity in the basolateral and apical membranes, respectively. Conversely, while NKCC1-like and NKCC2-like immunoreactivity is also found in the posterior intestine, apical CFTR-like immunoreactivity is present within this tissue as well. These regional differences in transporter immunoreactivity correlate well with the region-specific differences in $Cl^-$ and fluid secretion observed in this study. Although under normal conditions, NKCC2 acts as an important pathway for net $Cl^-$ absorption by the marine teleost intestine, the effects of eel RGN in this study and that of guanylin and uroguanylin in a previous report (Yuge and Takei, 2007) lead to a reversal of the $I_{SC}$ and result in net $Cl^-$ secretion. Staining for NKCC1 and apical CFTR in the Gulf toadfish posterior intestine and the aforementioned eel RGN-induced $Cl^-$ secretion suggests that NKCC1 and apical CFTR are stimulated, while NKCC2 may be inhibited, as suggested in the Japanese eel (Yuge and Takei, 2007), in order to provide a conduit for $Cl^-$ to travel from the blood, via the enterocytes, into the intestinal lumen (Fig. 2.10). Although the intracellular processes that lead to the activation of NKCC1 and apical CFTR, and possible inhibition of NKCC2, are unclear in fish, it is apparent that the guanylin peptides modify intracellular mechanisms to facilitate $Cl^-$ and fluid secretion.

The present study also revealed an unexpected inhibition of $HCO_3^-$ secretion, as opposed to the stimulatory effect observed in mammals. It has been shown that in mammalian intestinal tissues, using $Cl^-$-free saline inhibits $HCO_3^-$ secretion even in the presence of cAMP agonists (Spiegel *et al.*, 2003), suggesting apical anion exchange. Terrestrial mammals are generally $Cl^-$-limited, thus, an apical $Cl^-$-secreting CFTR

channel would fuel apical $Cl^-/HCO_3^-$ by recycling $Cl^-$ across the apical membrane (Spiegel *et al.*, 2003), which does not seem to be the case for the Gulf toadfish. Accordingly, in mammals, $HCO_3^-$ can be secreted into the intestine either through apical CFTR directly or by an apical anion exchanger that is secondary to $Cl^-$ secretion via CFTR. To examine if a similar increase in $HCO_3^-$ secretion in the Gulf toadfish was masked by an increase in VHA activity, bafilomycin was applied to inhibit this ATPase and revealed no effect of peptides on apical VHA. Consequently, in response to the guanylin peptides, it seems that mammals and marine teleosts modify $HCO_3^-$ secretion oppositely from one another, yet, similarly, increase both $Cl^-$ and fluid secretion.

The failure of the three eel guanylin peptides to increase $HCO_3^-$ secretion in the Gulf toadfish intestine is perhaps in part explained by the lack of $Cl^-$ limitation of the apical anion exchanger as demonstrated by the unaltered $HCO_3^-$ secretion rates even at luminal $Cl^-$ concentrations in the low mmol $l^{-1}$ range. It appears that the SLC26a6 anion exchanger, responsible for intestinal $HCO_3^-$ secretion in the gulf toadfish (Grosell *et al.*, 2009b), displays high $Cl^-$ affinity. Furthermore, our observations provide evidence that Gulf toadfish apical CFTR does not transport $HCO_3^-$ (as has been suggested in mammalian and fish tissues (Ishiguro *et al.*, 2009; Takei and Yuge, 2007)), since mucosal application of CFTRinh-172 alone had no effect on the $HCO_3^-$ secretion rate of the posterior intestine and since stimulation of $Cl^-$ secretion results in an inhibition, rather than stimulation, of $HCO_3^-$ secretion. The mechanisms for the eel RGN-induced inhibition of $HCO_3^-$ secretion in the Gulf toadfish intestine are unknown and require further investigation.

Fig. 2.10. Proposed effects of guanylin peptides in the posterior intestinal epithelia of Gulf toadfish (*Opsanus beta*). (A) Guanylin (GN), uroguanylin (UGN), or renoguanylin (RGN) bind to an apical guanylin cyclase-C (GC-C) receptor which activates guanylyl cyclase, which initiates an intracellular transduction cascade. (B) A downstream effect of GC-C activation is the opening of a putative apical cystic fibrosis transmembrane conductance regulator (CFTR) $Cl^-$ channel and presumably activation of NKCC1, allowing $Cl^-$ to cross the intestinal epithelia and enter the intestinal lumen. Water secretion is coupled to the induced secretory $Cl^-$ flux. (C) A yet-to-be investigated mechanism either decreases the activity of the apical SLC26a6 anion exchanger or inhibits the transport of intracellular $HCO_3^-$. This decrease in $HCO_3^-$ secretion is not a result of increased VHA activity/$H^+$ excretion. Symbols: (+) indicates direct or indirect stimulatory effects, (-) indicates direct or indirect inhibitory effects. TJ: tight junctions. Refs: (Cutler and Cramb, 2002; Grosell, 2010; Grosell, 2011; Kusakabe and Suzuki, 2000; Marshall *et al.*, 2002).

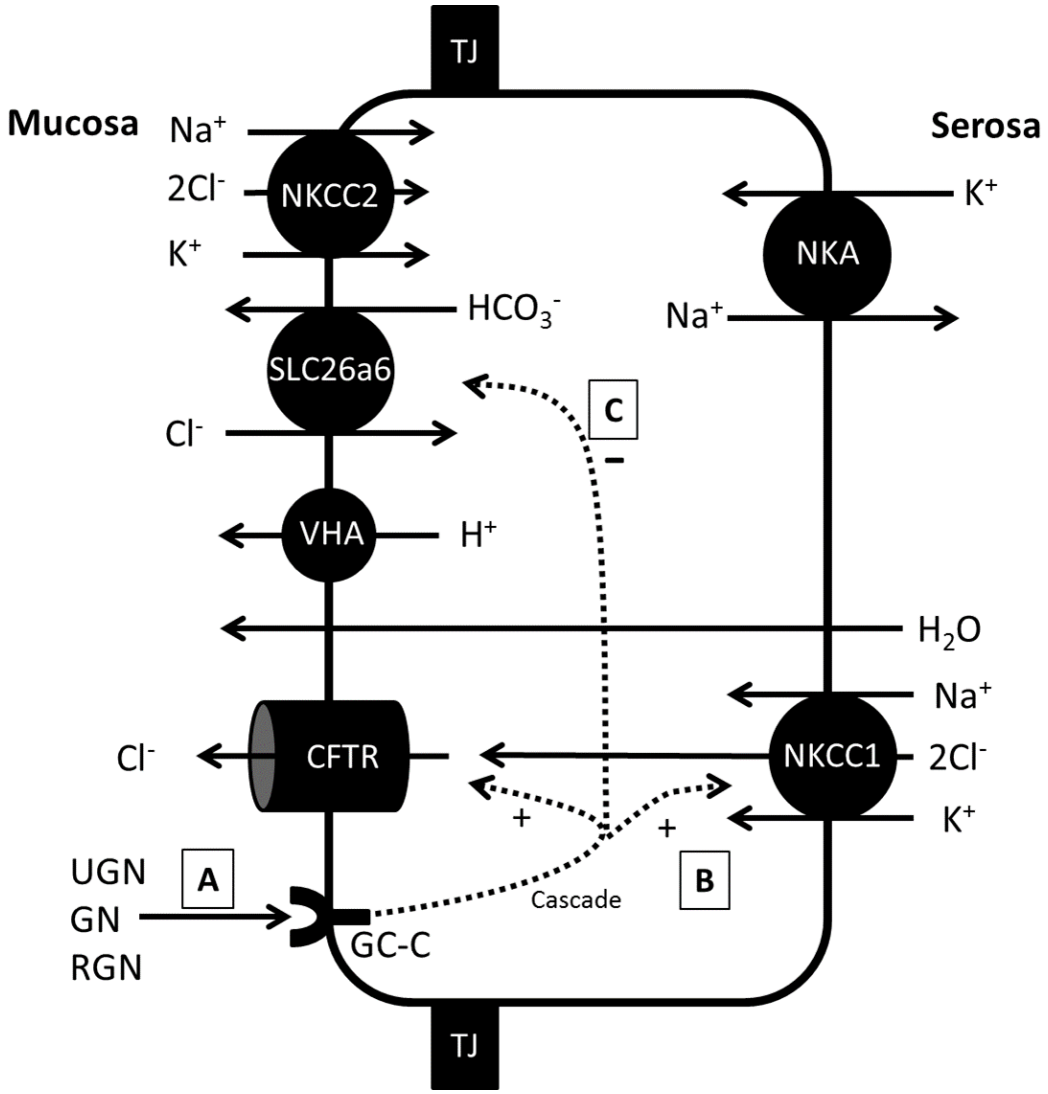

*Could inhibition of $HCO_3^-$ enhance fluid secretion?*

While the inhibition of $HCO_3^-$ secretion may be unexpected, it may serve to enhance fluid secretion into the intestinal lumen *in vivo*. The majority of $HCO_3^-$ secretion and NaCl absorption takes place in the anterior intestine, leading to a hypertonic absorbate of 650 mOsm within the lateral interspace (*lis*) that drives fluid absorption (Grosell, 2010; Grosell and Taylor, 2007). Under normal conditions, intestinal tissues can produce luminal $HCO_3^-$ concentrations as high as 100 mmol $l^{-1}$, and precipitation of $HCO_3^-$ by $Ca^{2+}$ (and to a lesser extent $Mg^{2+}$) can lead to luminal osmolalities being reduced by 70-100 mOsm (Marshall and Grosell, 2006; Wilson *et al.*, 2009; Wilson and Grosell, 2003; Wilson *et al.*, 2002). Furthermore, luminal titration of $HCO_3^-$ by $H^+$ secretion across the apical membrane by VHA further decreases the osmolality of the intestinal lumen by 20-30 mOsm (Grosell *et al.*, 2009a). Both these processes rely on luminal $HCO_3^-$ and promote water absorption (Marshall and Grosell, 2006). The present study reveals that eel RGN inhibits $HCO_3^-$ secretion, which *in vivo,* would act to elevate luminal osmolality due to reduced precipitate formation and limited $HCO_3^-$ titration. Thus, by inhibiting $HCO_3^-$ secretion in the posterior intestine, the increased osmotic pressure generated by unbound $Ca^{2+}$ and $Mg^{2+}$, untitrated $H^+$, and secreted $Cl^-$ (due to apical CFTR activation) would draw fluid from the blood.

*Perspectives and significance*

In both the Gulf toadfish and Japanese eel, guanylin peptide stimulation leads to a reversal of the absorptive $I_{SC}$ of the posterior intestine, but not the anterior intestine. In

contrast, the entire length of the mammalian intestine responds to the guanylin and uroguanylin. The present study clearly demonstrates that guanylin peptide stimulation in the Gulf toadfish drives net $Cl^-$ and fluid secretion in the posterior intestine, but, in contrast to mammals, results in the inhibition of $HCO_3^-$ secretion. The present study demonstrates inhibited $HCO_3^-$ secretion during CFTR-stimulated $Cl^-$ secretion and also reveals a lack of inhibition of $HCO_3^-$ secretion following mucosal application of CFTRinh-172. These results indicate that apical CFTR is not permeable to $HCO_3^-$, at least in the Gulf toadfish intestine. Additionally, the present study also provides immunohistological evidence for a potential $Cl^-$-secretory pathway via apical CFTR and basolateral NKCC1, present only in the posterior intestine, which could drive the observed $Cl^-$ and fluid secretion. Nevertheless, the contribution of the seemingly counterproductive fluid secretion by the distal intestine in osmoregulation remains to be investigated.

The traditional view of the marine teleost intestine is that of a net absorbing epithelium, for the purposes of rehydration. However, the present and previous studies (Yuge and Takei, 2007) demonstrate a robust secretory response in the distal intestinal segments following application of guanylin peptides. Furthermore, it is demonstrated that multiple plasma membrane transporters, such as SLC26a6 and NBCe1 (a basolateral $Na^+/HCO_3^-$-contransporter), in addition to apical CFTR or NKCC1, may be acted on by the guanylin peptides, based on the observed inhibition of $HCO_3^-$ secretion. Indeed, a recent study revealed that uroguanylin injected into mice resulted in decreased mRNA and protein expression of renal pendrin/SLC26a4, another $Na^+/HCO_3^-$ cotransporter

(Rozenfeld *et al.*, 2012). Future studies should examine if the guanylin peptides affect the activity of SLC26a6 and NBCe1.

The secretory response of the distal intestinal segments to the guanylin peptides may play a role in SW osmoregulation, as suggested by stimulated peptide gene expression in eels, following their transfer from FW to SW (Comrie *et al.*, 2001a; Comrie *et al.*, 2001b; Cramb *et al.*, 2005; Kalujnaia *et al.*, 2009; Yuge *et al.*, 2003; Yuge *et al.*, 2006). While the secretory response seems counterintuitive to the normal osmoregulatory function of the marine teleost intestine, it might facilitate the elimination/flushing of solid objects remaining after digestion and/or $CaCO_3$ precipitates that are formed in the marine teleost intestine. Clearly, the integrative function of the guanylin peptides in marine teleosts demands further study. Such studies should investigate the effect of salinity and other environmental factors on guanylin and uroguanylin peptide expression and release into the intestinal lumen (where they act in an auto- and paracrine fashion) to shed light on the overall whole animal function of these potent peptides.

*Acknowledgements*

We thank Drs. M. Danielle McDonald, Douglas L. Crawford, Marjorie F. Oleksiak, and Michael C. Schmale from the Rosenstiel School of Marine and Atmospheric Science at the University of Miami for the generous use of their equipment. MG is Maytag Professor of Ichthyology and is supported by NSF (IOS 1146695).

## Chapter 3

## The differential role of renoguanylin in osmoregulation and apical $Cl^-/HCO_3^-$ exchange activity in the posterior intestine of the Gulf toadfish (*Opsanus beta*)


### Summary

The guanylin family of peptides are effective regulators of intestinal physiology in marine teleosts. In the distal intestinal segments, they inhibit or reverse fluid absorption by inhibiting the absorptive short-circuit current ($I_{SC}$). The present findings demonstrate that mRNA from guanylin and uroguanylin, as well as at least one isoform of the guanylin peptide receptor, apical guanylyl cyclase-C (GC-C), was highly expressed in the intestine and rectum of the Gulf toadfish (*Opsanus beta*). In the posterior intestine, gene expression of GC-C, as well as the cystic fibrosis transmembrane conductance regulator (CFTR) and basolateral $Na^+/K^+/2Cl^-$-cotransporter (NKCC1), which comprise a $Cl^-$-secretory pathway, was greater in 60 ppt. The present study also shows that, in intestinal tissues from Gulf toadfish held in 35 ppt, renoguanylin (RGN) expectedly causes net $Cl^-$ secretion, inhibits both the absorptive $I_{SC}$ and fluid absorption, and decreases $HCO_3^-$ secretion, and this occurs to an even greater extent in 60 ppt, corresponding with the mRNA expression data. In contrast, RGN does not alter $Cl^-$ flux and, instead, elevates $HCO_3^-$ secretion in the 60 ppt group, suggesting increased apical $Cl^-/HCO_3^-$ exchange activity by SLC26a6. Overall, these findings reinforce the hypotheses that the guanylin peptide system is important for salinity acclimatization and that the secretory response could facilitate the removal of solids, such as $CaCO_3$ precipitates, from the intestine.

## Background

The vertebrate intestine is a multifunctional organ whose role and function is controlled by various hormones. Among these is the guanylin family of peptides, whose members modify the intestinal physiology of terrestrial mammals and teleost fish. In mammals, the intestinal guanylin family consists of guanylin and uroguanylin, which are upstream regulators of the apical guanylyl cyclase-C (GC-C), a receptor with intrinsic GC activity), in the intestine (Arshad and Visweswariah, 2012; Seidler *et al.*, 1997; Singer *et al.*, 1998). Activation of GC-C results in direct cyclic guanosine monophosphate (cGMP) and indirect cyclic adenosine monophosphate (cAMP) production, and activation of cAMP- and cGMP-dependent protein kinases (PKA and PKG, respectively), by phosphorylation, as well as phosphodiesterases (PDEs), all of which regulate the activities of a variety of cellular proteins and ion transporters [for review in Arshad and Visweswariah (Arshad and Visweswariah, 2012; Arshad and Visweswariah, 2013)].

Accordingly, this control over cellular processes distinguishes guanylin and uroguanylin as potent modulators of ion flux in the mammalian intestine. Through GC-C activation, guanylin and uroguanylin activate an apical cystic fibrosis transmembrane conductance regulator (CFTR) $Cl^-$ channel and stimulate $Cl^-$ secretion, which drives fluid secretion into the intestinal lumen (Cuthbert *et al.*, 1994; Joo *et al.*, 1998; Kuhn *et al.*, 1994). In addition, they modulate transepithelial absorption of $Na^+$ and secretion of $HCO_3^-$ in the intestine (Arshad and Visweswariah, 2013; Bengtsson *et al.*, 2007; Chao *et al.*, 1994; Toriano *et al.*, 2011). $HCO_3^-$ secretion is upregulated to maintain a stable intestinal pH when acidic chyme enters the intestine from the stomach (Bengtsson *et al.*,

2007; Guba *et al.*, 1996), while fluid and net $Cl^-$ secretion has been proposed to maintain osmotic homeostasis after the ingestion of a meal (Kita *et al.*, 1999). Indeed, salt loading of rat intestinal tissues leads to increases in guanylin mRNA abundance and peptide secretion, leading to fluid secretion that seems to compensate for any increases in intestinal osmolality (Carrithers *et al.*, 2002; Kita *et al.*, 1999; Li *et al.*, 1996).

Teleost fish also express guanylin and uroguanylin, as well as a third homologue, renoguanylin (RGN), in both the intestine and kidneys [for review (Takei, 2008; Takei and Yuge, 2007)]. Although their physiological role is still uncertain, these peptides most likely play a part in salinity acclimatization, since guanylin and uroguanylin are transcriptionally upregulated in both the European eel (*Anguilla anguilla*) and Japanese eel (*A. japonica*), following transfer from freshwater (FW) to seawater (SW) (Comrie *et al.*, 2001a; Cramb *et al.*, 2005; Kalujnaia *et al.*, 2009; Yuge *et al.*, 2003). This response seems counterintuitive because marine teleosts must continually absorb water across the intestinal epithelium in order to combat dehydration in the marine environment [for review in Grosell (Grosell, 2010)]. Yet, the guanylin peptides stimulate fluid secretion in the posterior intestine of the Gulf toadfish (*Opsanus beta*) (Ruhr *et al.*, 2014) and, consequently, must serve an important function.

Interestingly, while guanylin and uroguanylin have a physiological effect over the entire length of the mammalian intestinal tract (Bengtsson *et al.*, 2007; Currie *et al.*, 1992; Guba *et al.*, 1996; Kuhn *et al.*, 1994), their effects in the Japanese eel and Gulf toadfish are apparently restricted to the mid and posterior intestine, where they reverse the absorptive short-circuit current ($I_{SC}$) (Ando *et al.*, 2014; Ruhr *et al.*, 2014; Yuge and Takei, 2007). It has been demonstrated that, similarly to mammals, a switch from net $Cl^-$

absorption to net $Cl^-$ secretion, associated with the reversal of the $I_{SC}$ (from mucosa-to-serosa to serosa-to-mucosa), drives net fluid secretion in the Gulf toadfish posterior intestine (Ruhr *et al.*, 2014), and coincides with the inhibition of fluid absorption in the Japanese eel mid and posterior intestine (Ando and Takei, 2015; Ando *et al.*, 2014). Surprisingly, unlike in mammals (Bengtsson *et al.*, 2007; Guba *et al.*, 1996), $HCO_3^-$ secretion is partially inhibited by RGN in the Gulf toadfish posterior intestine (Ruhr *et al.*, 2014). Although unexpected, the inhibition of $HCO_3^-$ secretion in the Gulf toadfish might promote increased fluid secretion into the intestinal luminal by decreasing $Cl^-$ absorption and $CaCO_3$ precipitation, which would normally reduce luminal osmolality by up 100 mOsm [for review in Grosell (Grosell, 2010)]. Moreover, the absorption of $Cl^-$ and secretion of $HCO_3^-$ are intimately associated, in the marine teleost, by SLC26a6, an electrogenic apical $Cl^-/HCO_3^-$ antiporter (Kurita *et al.*, 2008), that might exchange up to 70% of intestinal $Cl^-$ uptake for intracellular $nHCO_3^-$ molecules (Grosell, 2006). Conversely, there is also evidence for a $Cl^-$-secretory pathway in the distal segments of the marine teleost intestine, comprised of apical CFTR and a basolateral $Na^+/K^+/2Cl^-$-cotransporter, NKCC1 (SLC12a2) (Ando *et al.*, 2014; Marshall *et al.*, 2002; Ruhr *et al.*, 2014; Singer *et al.*, 1998), and whose transport rates might be elevated by the guanylin peptides. Moreover, contrary to what might occur in mammals (Seidler *et al.*, 1997), there is no evidence that CFTR secretes $HCO_3^-$ in the Gulf toadfish posterior intestine (Ruhr *et al.*, 2014). Considering these effects, since one of the major $Cl^-$ uptake pathways in marine teleosts is through SLC26a6 and the guanylin peptides stimulate net $Cl^-$ secretion, it is likely that these peptides inhibit the exchange activity of SLC26a6, leading to the observed decreases in $HCO_3^-$ secretion in the Gulf toadfish posterior intestine.

Overall, the guanylin peptides either promote fluid secretion or hinder fluid absorption in the mid and posterior intestine of marine teleosts by possibly inhibiting NKCC2 (SLC12a1) and SLC26a6, and stimulating NKCC1 and apical CFTR, resulting in net $Cl^-$ secretion.

However, it is still unclear what physiological role the guanylin peptides play in marine teleosts. It has been hypothesized that the guanylin peptides only affect $Cl^-$ flux in the mid and posterior portions of the marine teleost intestine in order to fuel apical NKCC2 ion uptake and maintain fluid uptake (Ando *et al.*, 2014; Yuge and Takei, 2007). In the marine teleost intestine, the concentration of $Cl^-$ in the intestine decreases towards the rectum, while the concentration of divalent cations ($Ca^{2+}$, $Mg^{2+}$, and $SO_4^{2-}$) increases, making fluid absorption increasingly difficult [for review (Grosell, 2010; Marshall and Grosell, 2006)]. However, this hypothesis may not apply universally, since some marine teleost species, including the Gulf toadfish, rely extensively on SLC26a6 as a major transporter of intestinal $Cl^-$ uptake. Conversely, an alternative hypothesis proposes that the secretory response, initiated by the guanylin peptides, facilitates the removal of solids, such as undigested food or $CaCO_3$ precipitates, from the intestine (Ruhr *et al.*, 2014). It is possible that, due to the narrower diameter of the posterior intestine relative to the anterior portion, a secretory response would be needed to promote solids to move more easily into the rectum.

In order to test the latter hypothesis, the present study examined Gulf toadfish in control (35 ppt) and hypersaline (60 ppt) SW, since hypersalinity leads to increased intestinal $CaCO_3$ precipitation (Genz *et al.*, 2008). We hypothesized that acclimation to 60 ppt will lead to transcriptional upregulation of the components of the guanylin peptide

system, made up of guanylin, uroguanylin, GC-C, NKCC1, and CFTR, in the Gulf toadfish intestine. Greater expression of guanylin, uroguanylin, and GC-C could lead to altered intracellular signalling (i.e. by stimulating or inhibiting ion-transporting mechanisms) with which to enhance the secretory response and, thus, elimination of $CaCO_3$ by increasing tissue responsiveness to RGN.

## Material and Methods

*Experimental animals*

Gulf toadfish (*Opsanus beta*) were caught as bycatch from Biscayne Bay, FL, by shrimp fishermen. Upon arrival to the laboratory, Gulf toadfish were briefly placed in a freshwater bath (3 min) and then treated with malachite green to remove ectoparasites. Individuals were separated by size and 8-10 were placed in aerated 62-litre tanks, with continuous flow-through of sand-filtered SW from Biscayne Bay (34-36 ppt, 20-24°C). Gulf toadfish used for the present study were fed 5% of their body mass of squid seven days prior to experimentation. Gulf toadfish held in experimental tanks were placed in groups of 6-8 and acclimated over seven days to 35 ppt (control) or 60 ppt (hypersalinity), adjusted with Instant Ocean (SpectrumBrands, Inc). Each experimental tank was fitted with two recirculating pumps containing biological filters and a water heater maintained temperature at 25.5 ± 0.2°C. Tanks were monitored daily for temperature and salinity. Fish husbandry and experimental procedures followed an approved University of Miami Animal Care Protocol (IACUC no. 13-225, renewal 02). All Gulf toadfish used for experimentation were sacrificed using 0.2 g $l^{-1}$ MS-222

(Argent) solution, buffered with 0.3 g $1^{-1}$ $NaHCO_3^-$ (Sigma-Aldrich), followed by severing of the spinal cord at the cervical vertebra.

*Composition of salines, hormones, and inhibitors*

Japanese eel RGN was resuspended into $10^{-5}$ mol $l^{-1}$ stock solutions in nano-pure water and stored in -20°C. Only eel RGN was used in the present study, since it elicits the strongest response from the Gulf toadfish posterior intestine comparted to eel guanylin and uroguanylin (Ruhr *et al.*, 2014). Moreover, the amino acid sequence for eel RGN, ADLCEICAFAACTGCL (GenBank accession number: BAC76010.1), is nearly identical to Gulf toadfish (tf) guanylin, MDVCEICAFAACTGC (accession number: AIA09902.1) (Ruhr *et al.*, 2014). Mucosal (pH=7.8) and serosal (pH=7.8) salines were prepared as described in Table 3.1. These salines were used for intestinal tissues from Gulf toadfish exposed to both 35 and 60 ppt, since plasma and intestinal fluid osmolalities of Gulf toadfish at these two salinities are not significantly different (Genz *et al.*, 2011; McDonald and Grosell, 2006).

Table 3.1. Composition of salines for short-circuit current, pH-stat titration, and intestinal sac preparation experiments

| Compound | Mucosal* | Serosal | $HCO_3^-/CO_2$-free |
|---|---|---|---|
| NaCl (mmol $l^{-1}$) | 69.0 | 151.0 | 151.0 |
| KCl (mmol $l^{-1}$) | 5.0 | 3.0 | 3.0 |
| $MgSO_4$ (mmol $l^{-1}$) | 77.5 | 0.88 | 0.88 |
| $MgCl_2$ (mmol $l^{-1}$) | 22.5 | | |
| $Na_2HPO_4$ (mmol $l^{-1}$) | | 0.5 | 0.5 |
| $KH_2PO_4$ (mmol $l^{-1}$) | | 0.5 | 0.5 |
| $CaCl_2$ (mmol $l^{-1}$) | 5.0 | 1.0 | 1.0 |
| $NaHCO_3$ (mmol $l^{-1}$) | | 5.0 | |
| HEPES, free acid (mmol $l^{-1}$) | | 11.0 | 11.0 |
| HEPES salt (mmol $l^{-1}$) | | 11.0 | 11.0 |
| Urea (mmol $l^{-1}$) | | 4.5 | 4.5 |
| Glucose (mmol $l^{-1}$) | | 5.0 | 5.0 |
| Osmolality (mOsm $l^{-1}$)[§] | 325 | 325 | 325 |
| pH | 7.8[†] | 7.8 | 7.8 |
| Gas[¥] | 100% $O_2$ | 0.3% $CO_2$ in $O_2$ | 100% $O_2$ |

*Mucosal application of renoguanylin: $10^{-9}$-$10^{-6}$ mol $l^{-1}$ for short-circuit current and pH-stat experiments, $5x10^{-7}$ mol $l^{-1}$ for intestinal sac preparations

[§]Adjusted with mannitol to ensure transepithelial isosmotic conditions in all experiments.

[†]pH 7.80 was maintained by pH-stat titration.

[¥]Salines gassed for at least 1 h prior to experimentation.

*RNA isolation and molecular cloning*

Total RNA from Gulf toadfish tissues (50-100 mg $ml^{-1}$) was extracted using RNA STAT-60 (Tel-Test) and an Ultra-Turrax T8 tissue homogenizer (Ika-Werke). Traces of genomic DNA were removed from each isolate (10 μg per sample) with DNase I (Turbo DNA-free kit, Ambion). Total RNA was then quantified using a spectrophotometer (NanoDrop 1000 Spectrophotometer, Thermo Scientific) at 260 nm. A spot check of samples underwent gel electrophoresis to confirm RNA integrity. Isolated RNA (1 μg) from each sample was reverse transcribed into cDNA using random hexamers and the SuperScript First-Strand Synthesis System (Invitrogen) according to the manufacturer's protocol.

Genes were amplified by polymerase chain reaction (PCR) using taq polymerase (Invitrogen). The partial cDNA sequence for GC-C was cloned by 3'- or 5'-RACE using GC-C-F and -R, and a universal primer (Table 3.2). Full-length sequences were then cloned using designed sense primers, tfGC-C-F and -R [tf guanylin and tf uroguanylin were clone previously (Ruhr *et al.*, 2014)]. The following cycling parameters were used: 94°C for 3 min, followed by 40 cycles of 94°C for 30 s, 64°C for 30 s, 72°C for 3 min. Gene-specific primers for tf guanylin and tf uroguanylin were designed from their respective full-length sequences, as described in Ruhr et al. (Ruhr *et al.*, 2014), and those for tfCFTR and tfNKCC1 were designed from their respective partial sequences found in the Gulf toadfish transcriptome (C.M.R LeMoine, N. Corradi, P.J. Walsh, unpublished data).

Table 3.2. Sequences of primers for cDNA cloning and qPCR

| Name | Sequence |
|---|---|
| tfGN-F | 5’- AGCAAAGGGCAGCATCTGCA-3’ |
| tfGN-R | 5’- TGGCAAGATGTTTGTGGCTTTGC-3’ |
| tfUGN-F* | 5’-CCGACCCTCTCATGCCGCAGG-3’ |
| tfUGN-R* | 5’-TGCACGGAGGCATCGAGCTG-3’ |
| GC-C-F** | 5’ CACCACCTGTTGGCGTACCACC-3’ |
| GC-C-R** | 5’-GTCCAGCGCCATGCGGCAGATG-3’ |
| tfGC-C-F | 5’-CAGAGGCCACCATGCGGCGTCACCTA-3’ |
| tfGC-C-R | 5’-TTCACCAAGCGCTGCTCCGACCAA-3’ |
| tfNKCC-F* | 5’-TCCTGCAGCAGCTCGTTGAG-3’ |
| tfNKCC-R* | 5’-GAGCACGTGGCGGCCTTCGAGGAT-3’ |
| tfCFTR-F* | 5’-GTTTCATCACCGGCATGAACG-3’ |
| tfCFTR-R* | 5’-GTGCCTTTCTGTAGATGGCTCCAA-3’ |
| EF1α-F | 5’-AGGTCATCATCCTGAACCAC-3’ |
| EF1α-R | 5’-GTTGTCCTCAAGCTTCTTGC-3’ |
| Universal Primer† | 5’-CTAATACGACTCACTATAGGGCAAGCGTGGTATCAACGCAGAGT-3’ |
| | 5’-CTAATACGACTCACTATAGGGC-3’ |

*Gene-specific primers designed from the Gulf toadfish (tf) annotated genome
**Designed sense primers
†Universal primer (Clontech SMARTer RACE cDNA Amplification Kit) consists of both a long and short sequence.
GN (guanylin). UGN (uroguanylin). GC-C (guanylyl cyclase-C-associated receptor).

*Real-time PCR: hypersalinity*

To test the effects of 60 ppt on the expression of tf guanylin, tf uroguanylin, tfGC-C, tfNKCC1, and tfCFTR mRNA, the following procedure was used. First, the tissue distribution of tf guanylin, tf uroguanylin, and tfGC-C was quantified by real-time, quantitative PCR (qPCR). An acute salinity transfer (to 60 ppt) was then used to determine if tf guanylin, tf uroguanylin, tfGC-C, tfNKCC1, and tfCFTR transcription changed over time (0, 6, 12, 24, and 96 h), following the protocol by Taylor et al. (Taylor *et al.*, 2010). Gulf toadfish were held in SW aquaria as described above and were given a lethal dose of MS-222 anaesthetic, followed by spinal cord severing at the cervical vertebrae. Tissues were collected by dissection and immediately snap frozen in liquid nitrogen. As described above, tissues were collected, RNA isolated, and cDNA synthesized. qPCR (Mx4000, Stratagene) was used to measure tfNKCC1, tfCFTR, tfGC-C, tf guanylin, and tf uroguanylin expression using gene-specific primers (Table 3.2). Power SYBR Green (Applied BioSystems) was used as the reporter dye. Cycling parameters were as follows: 95°C for 10 min, 40-50 cycles of 95°C for 30 s, 55-60°C for 30 s, and 72°C for 30 s. The specificity for all PCR products was confirmed by observing a distinct, corresponding melting peak for each product following each qPCR run using a melting curve analysis (guanylin: 79-85, uroguanylin: 81-86, GC-C: 80-86, NKCC1: 81-86, and CFTR: 80-85 in °C). Calculations were performed based on the approach described by Pfaffl (Pfaffl, 2001). Gene expression was normalized to EF1α and scaled relative to the tissue with the lowest gene expression for the tissue distribution study and to the 0-h control for the salinity challenge study.

*Determining the effects of hypersalinity on short-circuit current and $HCO_3^-$ secretion*

Ussing chambers (model 2400, Physiologic Instruments) were used to determine differences in short-circuit current ($I_{SC}$), transepithelial potential (TEP), and transepithelial conductance ($G_{TE}$) in the posterior intestine of 35 and 60 ppt-exposed Gulf toadfish treated with RGN. The posterior intestine of each individual Gulf toadfish (ranging from 15-30 g) was excised, cut open, and mounted onto tissues holders (model P2413, Physiologic Instruments). The tissue holders exposed 0.71 $cm^2$ of excised tissue and were placed between the two half-chambers of the Ussing apparatus.

Measurements of $I_{SC}$ were performed under symmetrical conditions; both the mucosal (apical membrane/luminal side) and serosal (basolateral membrane/blood side) half-chambers of the Ussing apparatus were bathed in serosal saline (2 ml) and continually mixed by airlift gassing using 0.3% $CO_2$ in $O_2$ (Table 3.1) and maintained at 25 °C by a recirculating bath (model 1160S, VWR), following a similar procedure by Grosell and Genz (Grosell and Genz, 2006). To measure $I_{SC}$ and TEP, current and voltage electrodes were connected to amplifiers (model VCC600, Physiologic Instruments). Current electrodes recorded differences in $I_{SC}$ under voltage-clamp conditions at 0.0 mV, with 3 s of 2-mV pulses (mucosal-to-serosal) at 60-s intervals. Voltage electrodes recorded differences in TEP under current-clamp conditions at 0.0 μA with 3 s of 10-μA pulses (mucosal-to-serosal) at 60-s intervals. Ohms law was used to calculate $G_{TE}$, determined from the deflections in $I_{SC}$ and TEP during pulsing. $I_{SC}$ and TEP data were recorded by Acqknowledge software (v. 3.8.1, BIOPAC Systems) onto a computer.

To determine the dose response and effective concentration (EC) of RGN on the Gulf toadfish posterior intestine, RGN was added in increasing doses to the mucosal half-chamber, when $I_{SC}$ values became stable ($10^{-9}$-$10^{-6}$ mol $l^{-1}$), as described in Ruhr et al. (Ruhr *et al.*, 2014). $I_{SC}$ values were recorded as described above. For the data presented, negative and positive $I_{SC}$ values refer to absorptive and secretory currents, respectively.

A pH-stat titration system (TIM 854 or 856 Titration Managers, Radiometer) set up in tandem with an Ussing chamber was used to measure $HCO_3^-$ secretion on isolated posterior intestinal tissues from 35 and 60 ppt-exposed Gulf toadfish, as described in Grosell and Genz (Grosell and Genz, 2006). Luminal-side tissues were bathed in mucosal saline (2 ml) and blood-side tissues were bathed in an equal volume of serosal saline (Table 3.1). The salines in each half-chamber were continually mixed by airlift gassing using 100% $O_2$ (mucosal half-chamber) or 0.3% $CO_2$ in $O_2$ (serosal half-chamber) (Table 3.1). In the mucosal half-chamber, a pH electrode (model PHC4000.8, Radiometer) and microburrette tip (which secreted acid into the half-chamber) were submersed in order to maintain a constant pH of 7.8, which allowed for symmetrical pH conditions on either side of the intestinal epithelium. The amount of acid titrant (0.005 mol $l^{-1}$ HCl) and pH values were recorded on computers using the Titramaster software (v. 5.1.0). Epithelial $HCO_3^-$ secretion rates were calculated from both the rate of titrant secreted and its concentration, as described in Grosell and Genz (Grosell and Genz, 2006).

To assess whether the increased $HCO_3^-$ secretion in the posterior intestine of 60 ppt-acclimated Gulf toadfish after RGN treatment was derived from endogenous $CO_2$ production or was dependent on serosal $HCO_3^-/CO_2$ absorption, a $HCO_3^-/CO_2$-free

serosal saline (Table 3.1) was used to compare secretion rates with the rates obtained using serosal saline containing 5 mmol $l^{-1}$ $HCO_3^-$ (Table 3.1). Similarly to a study by Ruhr et al. (Ruhr *et al.*, 2014), posterior intestinal sections from both control and 60 ppt-acclimated Gulf toadfish were exposed to 100 min in the presence of serosal $HCO_3^-$ (including a 30-min control, followed by a 70-min flux in which the mucosal saline had been spiked with $10^{-7}$ mol $l^{-1}$ RGN). Immediately after this 100-min flux, the serosal saline was replaced with a serosal saline devoid of $HCO_3^-$ and gassed with $O_2$ for an additional 70 min. A reverse experiment was then conducted in which the intestinal segments were first exposed maintained for 30 min in the absence of serosal $HCO_3^-$, followed by 70 min with RGN in the mucosal half-chamber (in the absence of serosal $HCO_3^-$), and then 70 min in the presence of serosal $HCO_3^-$. Note that the tissues were continually in the presence of RGN after the control flux, since the mucosal saline was never exchanged throughout an individual experiment.

*Intestinal Sac Preparations*

Intestinal sac preparations were used to examine fluid, $Cl^-$, and $Na^+$ fluxes across the posterior intestinal epithelium, following a similar protocol by Ruhr et al. (Ruhr *et al.*, 2014). The intestine of an adult Gulf toadfish was cut once at its midway point and once proximally to the rectal sphincter. A PE50 catheter was inserted into the posterior end of the excised intestine and tied off with a silk suture. Mucosal saline (Table 3.1) was then injected into the catheter to rinse the intestine of any debris, precipitates, and intestinal fluids. The intestine was then closed with a silk suture, approximately 1.5 cm away from the first suture, to form an intestinal sac, and was blot-dried and weighed. Intestinal sacs

from 35 and 60 ppt-acclimated Gulf toadfish were filled with either mucosal saline containing no RGN or 5 x $10^{-7}$ mol $l^{-1}$ RGN (Table 3.1). After an intestinal sac was filled, a subsample of mucosal saline was taken to measure the initial $Cl^-$ and $Na^+$ concentrations. The catheter was sealed and the volume of injected mucosal saline was determined by calculating the difference in mass between a filled and unfilled intestinal sac preparation. The intestinal sacs were immediately placed in scintillation vials filled with serosal saline and gassed with 0.3% $CO_2$ (Table 3.1), and underwent a 2-h flux period, after which the sacs were removed, blot-dried, and final masses weighed. The mucosal saline from each sac was then collected to measure final $Cl^-$ and $Na^+$ concentrations. Emptied intestinal sacs were cut in half and placed onto tracing paper for surface area measurements. Changes in volume were calculated by taking the difference in mass between the filled intestinal sacs at the beginning and end of the 2-h flux period. $Na^+$ concentrations were measured using flame spectrometry (Varian 220FS) and $Cl^-$ concentrations were measured using anion chromatography (DIONEX 120). Fluid, $Cl^-$, and $Na^+$ fluxes were determined by the difference between initial and final intestinal sac mass or ion concentration, divided by flux period and tissue surface area.

*Statistical analyses*

Data are presented as absolute means ± SEM. The following statistical tests were used to compare means. One- and two-way analysis of variances (ANOVAs), one- and two-way repeated measures ANOVAs, and Student's t-tests were used for parametric data. Kruskall-Wallis one-way and Friedman repeated measures ANOVAs on ranks, and the Mann-Whitney rank sum test were used for non-parametric data. Appropriate post-

hoc tests (Dunn's, Tukey, and Holm-Sidak tests) were used to reveal specific differences between groups. SigmaStat 3.5 and SigmaPlot 11.0 were used for statistical analyses, to calculate EC50 values, and to plot the data. Means were considered significantly different when $p \leq 0.05$. Additionally, for the pH-stat titration experiments, the average of the last thirty minutes of each exposure flux (i.e. 70-100 and 140-170 min) were compared to the average control flux (0-30 min).

## Results

*Gene distribution of Guanylin, Uroguanylin, and Guanylyl Cyclase-C*

A distinct, partial GC-C-like molecule was cloned from Gulf toadfish intestinal cDNA, revealing a protein of 252 amino acids, encoded by 756 base pairs (GenBank accession number: KP844723). The small, partial nucleotide sequences of putative NKCC1 and CFTR found in the Gulf toadfish intestinal transcriptome code for proteins of 117 and 95 amino acids, respectively. A basic local alignment search tool (BLAST), using both nucleotide and amino acid queries, confirmed that these molecules were partial sequences for a tfGC-C isoform, tfNKCC1 (accession number: KR360748), and tfCFTR (accession number: KR360747). The intestinal segments and the rectum expressed high levels of guanylin and uroguanylin mRNA ($n = 8$ for all tissues), while the other tissues analyzed displayed very low expression levels (Fig. 3.1). Analyzing only the intestinal segments and the rectum, it was revealed that the anterior intestine expressed uroguanylin mRNA at significantly lower levels than the posterior intestine (Fig. 3.1). As with the guanylin and uroguanylin, GC-C mRNA was highly expressed in the intestinal segments and in the rectum (Fig. 3.1).

Fig. 3.1. Relative transcription levels of guanylin (GN), uroguanylin (UGN), and guanylyl cyclase-C (GC-C) in various organs from Gulf toadfish held in 35 ppt. Expression levels for an individual gene are normalized to EF1α and scaled relative to the tissue with the lowest gene expression (kidney for guanylin, spleen for uroguanylin, and stomach for GC-C), which was assigned an expression value of one. Significant differences in uroguanylin mRNA expression were revealed by a two-way ANOVA followed by a Tukey test ($^{a, b}p \leq 0.05$).

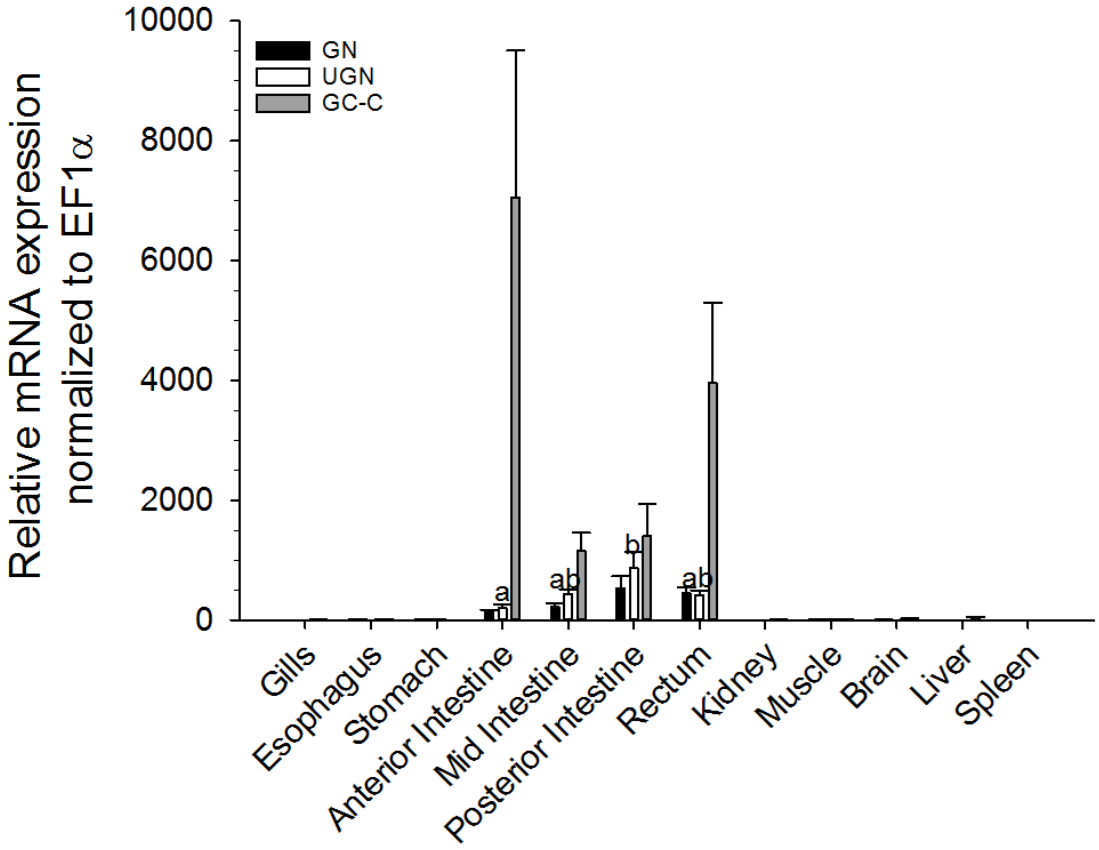


*Gene expression of intestinal tissues exposed to hypersalinity*

For the 60 ppt-acclimated Gulf toadfish, posterior intestinal tissues revealed significant increases in mRNA expression, relative to the control (0 h), of the following genes: GC-C at 96 h, NKCC1 at 96 h, and CFTR at 24 and 96 h (Fig. 3.2). Based on

these data, only the posterior intestine of the Gulf toadfish was subjected to further physiological study, following hypersalinity challenge.

Fig. 3.2. Relative transcription levels of guanylin (GN), uroguanylin (UGN), guanylyl cyclase-C (GC-C), NKCC1, and CFTR in the posterior intestine of Gulf toadfish exposed to 0, 6, 12, 24, and 96 h in 60 ppt SW. Expression levels are normalized to EF1α and scaled relative to the tissue with the lowest gene expression (0-h control), which was assigned an expression value of one. Values are means ± SEM (n=8). Statistically significant difference ($p \leq 0.05$) from the 0-h control (*), revealed by Kruskall-Wallis one-way ANOVAs, followed by Dunn's tests.

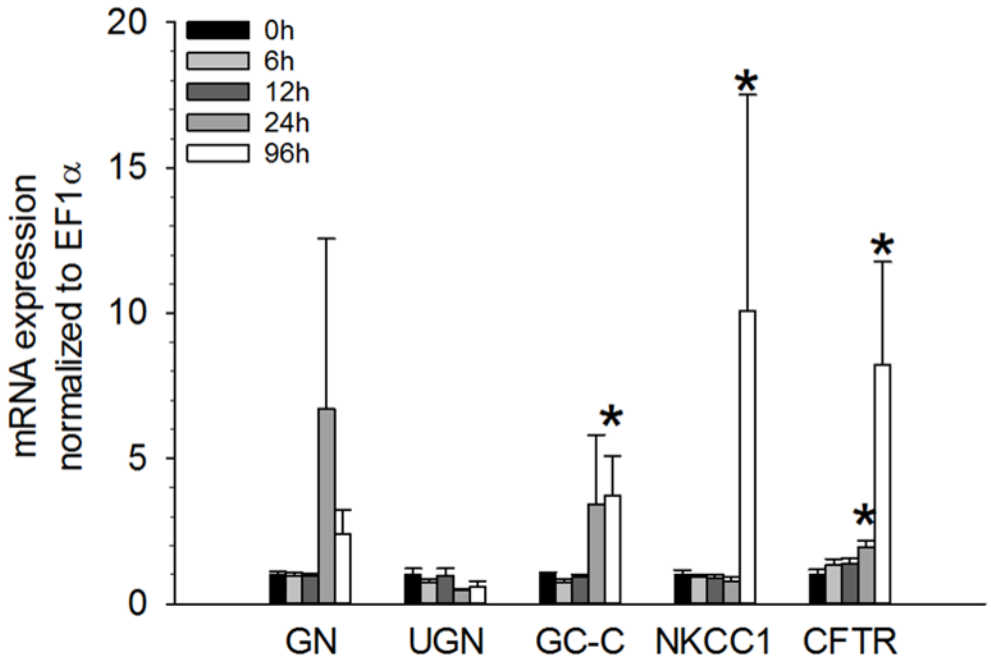


*Effects of renoguanylin on $I_{SC}$ of tissues exposed to hypersalinity*

For Gulf toadfish exposed to 35 ppt, mean $I_{SC}$ values were significantly greater than in the control (no dose) when tissues were exposed to $\geq 2.5 \times 10^{-8}$ mol $l^{-1}$ RGN, and reversed at concentrations of $\geq 10^{-7}$ mol $l^{-1}$ RGN (the point at which tissues switch from an absorptive/negative $I_{SC}$ values to secretory/positive) (Fig. 3.3A). For Gulf toadfish

exposed to 60 ppt, mean $I_{SC}$ values were significantly greater than in the control when tissues were exposed to $\geq 10^{-8}$ mol $l^{-1}$ RGN, and reversed at concentrations $\geq 10^{-7}$ mol $l^{-1}$ RGN (Fig. 3.3A). Furthermore, the mean $I_{SC}$ of the posterior intestine of Gulf toadfish exposed to 60 ppt was greater than tissues exposed to 35 ppt at 0 and $10^{-9}$ mol $l^{-1}$ RGN (Fig. 3.3A). Comparatively, the $\Delta I_{SC}$ of the posterior intestine of Gulf toadfish exposed to 60 ppt was greater than from those exposed to 35 ppt at concentrations $\geq 2.5 \times 10^{-8}$ mol $l^{-1}$ RGN (Fig 3.3B). The mean pooled EC50 value was $8.04 \pm 10.3 \times 10^{-8}$ mol $l^{-1}$ RGN (Fig. 3.3A). For the tissues from Gulf toadfish held in 35 and 60 ppt, significant differences in $G_{TE}$ occurred at concentrations $\geq 10^{-7}$ and $5 \times 10^{-8}$ mol $l^{-1}$ RGN, respectively (Fig. 3.3C).

All posterior intestinal tissues for subsequent experiments were dosed with $10^{-7}$ mol $l^{-1}$ RGN, with the exception of the intestinal sac preparations, which were fluxed with $5 \times 10^{-7}$ mol $l^{-1}$. At these concentrations, the mean $I_{SC}$ of both the 35 and 60 ppt SW-exposed tissues were reversed (mean $I_{SC}$ values > 0 μA $cm^{-2}$; Fig. 3A) and demonstrate maximal $\Delta I_{SC}$ readings (Fig. 3.3B).

Fig. 3.3. Log-scale of the dose-dependent effects of mucosal application of renoguanylin (RGN) on the (A) mean short-circuit current ($I_{SC}$), (B) $\Delta I_{SC}$, and (C) transepithelial conductance ($G_{TE}$) of the posterior intestine from Gulf toadfish held in 35 ppt (open circles) or 60 ppt (closed circles). $\Delta I_{SC}$ values were calculated as the difference in short-circuit current from the control (no dose), as a function of peptide concentration. (D) A representative trace of $I_{SC}$ from the posterior intestine of a Gulf toadfish exposed to 60 ppt. The concentration of RGN was increased once $I_{SC}$ values reached a stable reading (denoted by the vertical red lines in the representative trace), resulting in a range of time-course lengths: 35 ppt: 248.63-459.23 min, 60 ppt: 334.59-465.62. Positive and negative values on the mean $I_{SC}$ y-axis indicate secretory and absorptive currents, respectively. Values are mean ± SEM (n=5). Significant differences ($p \leq 0.05$) for the parameters $I_{SC}$, $\Delta I_{SC}$, and $G_{TE}$ were revealed by a Friedman repeated-measures ANOVA on ranks, followed by a Dunn's test (§35 ppt group), and a one-way repeated measures ANOVA, followed by a Holm-Sidak test (*60 ppt group). Differences between the 35 and 60 ppt groups (†) were revealed by a Student's t-test ($p \leq 0.05$).

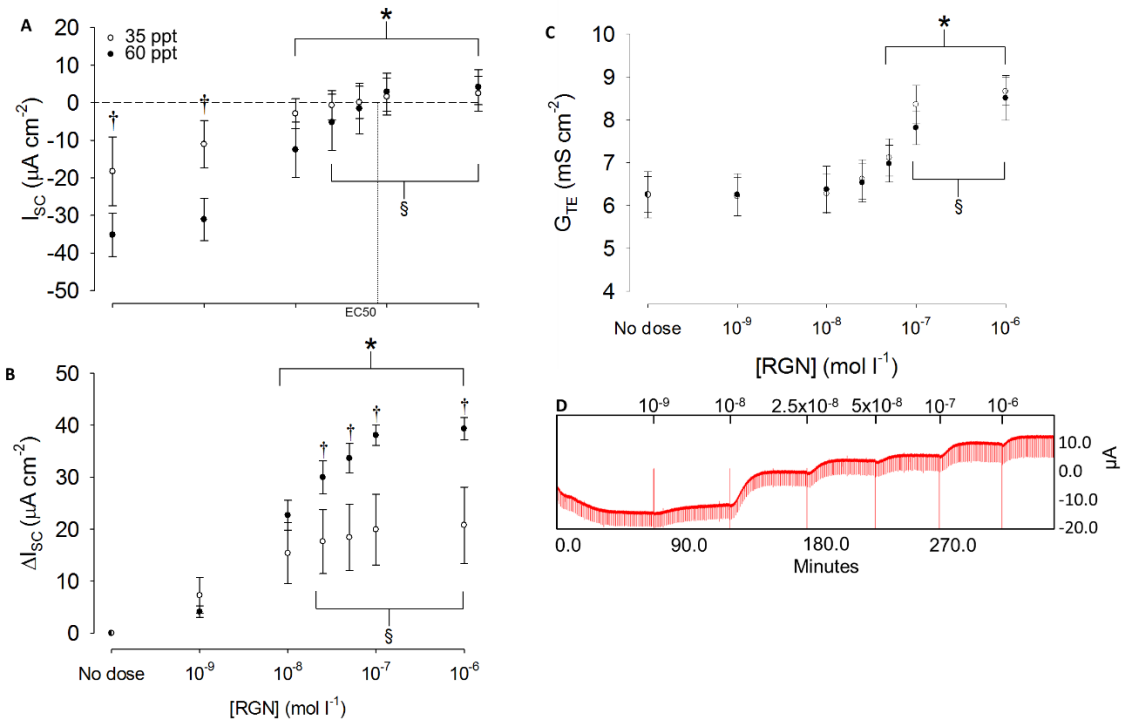

*Intestinal sac preparation experiments*

Corresponding with a previous study on the Gulf toadfish (Ruhr *et al.*, 2014), posterior intestinal tissues from fish exposed to 35 ppt and treated with RGN displayed net $Cl^-$ secretion compared to untreated tissues (Fig. 3.4A). Additionally, tissues from the 60 ppt-acclimated Gulf toadfish untreated with RGN had significantly greater net absorptive $Cl^-$ rates than tissues from untreated fish held in 35 ppt (Fig. 3.4A). In parallel to the $Cl^-$ measurements, tissues from both the 35 and 60 ppt-exposed Gulf toadfish treated with RGN displayed net $Na^+$ secretion, while untreated tissues were net $Na^+$-absorptive (Fig. 3.4B). In the posterior intestinal sac preparations of Gulf toadfish exposed to 35 ppt, tissues treated with RGN absorbed significantly less fluid than untreated intestinal sac preparations (Fig. 3.4C). Intestinal sac preparations from Gulf toadfish exposed to 60 ppt and treated with RGN also absorbed less fluid than untreated intestinal sac preparations from fish held in 60 ppt, and from fish held in 35 ppt and treated with RGN (Fig. 3.4C). There were no differences in absorption between the untreated intestinal sac preparations from fish held in 35 and 60 ppt.

*Effects of renoguanylin on $HCO_3^-$ secretion*

For tissues from Gulf toadfish acclimated to 35 ppt, treatment with RGN resulted in a significantly lower $HCO_3^-$ secretion rate compared to the control flux, and this rate was further decreased when tissues were simultaneously treated with RGN and the absence of serosal $HCO_3^-$ (Fig. 3.5A). In contrast, for tissues from the 60 ppt-acclimated Gulf toadfish, RGN significantly increased the $HCO_3^-$ secretion rate compared to the control flux, although the absence of serosal $HCO_3^-$ significantly decreased this rate (Fig.

3.5C). The TEP of tissues from the 35 and 60 ppt-acclimated fish was significantly decreased, and even reversed, by RGN, and this change was magnified by simultaneous treatment with RGN and the absence of serosal $HCO_3^-$ (Fig. 3.5B, D). In tissues from Gulf toadfish acclimated to 60 ppt, the conductance during the control flux was significantly lower than when tissues were simultaneously exposed to RGN and the absence of serosal $HCO_3^-$ (Table 3.3). In contrast, the tissue conductance from the 60 ppt-acclimated fish was significantly greater than those exposed to 35 ppt (Table 3.3). Control $HCO_3^-$ secretion rates of tissues from the 60 ppt-acclimated fish was greater than those exposed to 35 ppt (Fig. 5A, C).

When Gulf toadfish posterior intestinal tissues were alternatively exposed to 0 mmol $l^{-1}$ $HCO_3^-$ during the control flux, then to RGN, and, subsequently, to 5 mmol $l^{-1}$ serosal $HCO_3^-$, the tissues from the 35 ppt-acclimated Gulf toadfish treated with RGN displayed significantly lower $HCO_3^-$ secretion rates than in the presence of serosal $HCO_3^-$ (Fig. 3.6A). When considering the part of the experiment without serosal $HCO_3^-$, RGN treatment resulted in a significant decrease in $HCO_3^-$ secretion as expected. The $HCO_3^-$ secretion rate of the control flux was significantly greater for tissues from fish acclimated to 60 ppt SW than from fish acclimated to 35 ppt. The control TEP of tissues from Gulf toadfish acclimated to 35 ppt was significantly lower than when the tissues were simultaneously treated with RGN and the presence of serosal $HCO_3^-$ (Fig. 3.6B). Similarly, the TEP of tissues from the 60 ppt-acclimated fish was significantly less than in the RGN flux, and the TEP values of these two treatments were significantly less than when the tissues were simultaneously treated with RGN and the presence of serosal $HCO_3^-$ (Fig. 3.6D). In tissues from Gulf toadfish acclimated to 35 ppt, the conductance

of both the control and RGN fluxes were significantly lower than when tissues were simultaneously treated with RGN and in the presence of serosal $HCO_3^-$ (Table 3.3). For tissues from Gulf toadfish acclimated to 60 ppt, the conductance was significantly increased compared to the control, when tissues were treated with RGN and the presence of serosal $HCO_3^-$ (Table 3.3). As was the case in presence of serosal $HCO_3^-$ (Fig. 5A, B), $HCO_3^-$ secretion rates (Fig. 3.6A, B) and conductance (Table 3.3) of the control flux from the tissues obtained from 60 ppt-acclimated Gulf toadfish were significantly greater in tissues from those acclimated to 35 ppt.

Fig. 3.4. (A) $Cl^-$, (B) $Na^+$, and (C) fluid fluxes obtained from posterior intestinal sac preparations of Gulf toadfish held in 35 and 60 ppt SW, with and without luminal addition of 5 x $10^{-7}$ mol $l^{-1}$ renoguanylin (RGN). Negative and positive values indicate secretion and absorption, respectively. Values are means ± SEM (n = 6-8). Significant differences in $Cl^-$, $Na^+$, and fluid fluxes were revealed by Student's t-tests (*$p \leq 0.05$). Significant differences between the 35 and 60 ppt groups were revealed by a Mann-Whitney rank sum test (†$p \leq 0.05$).

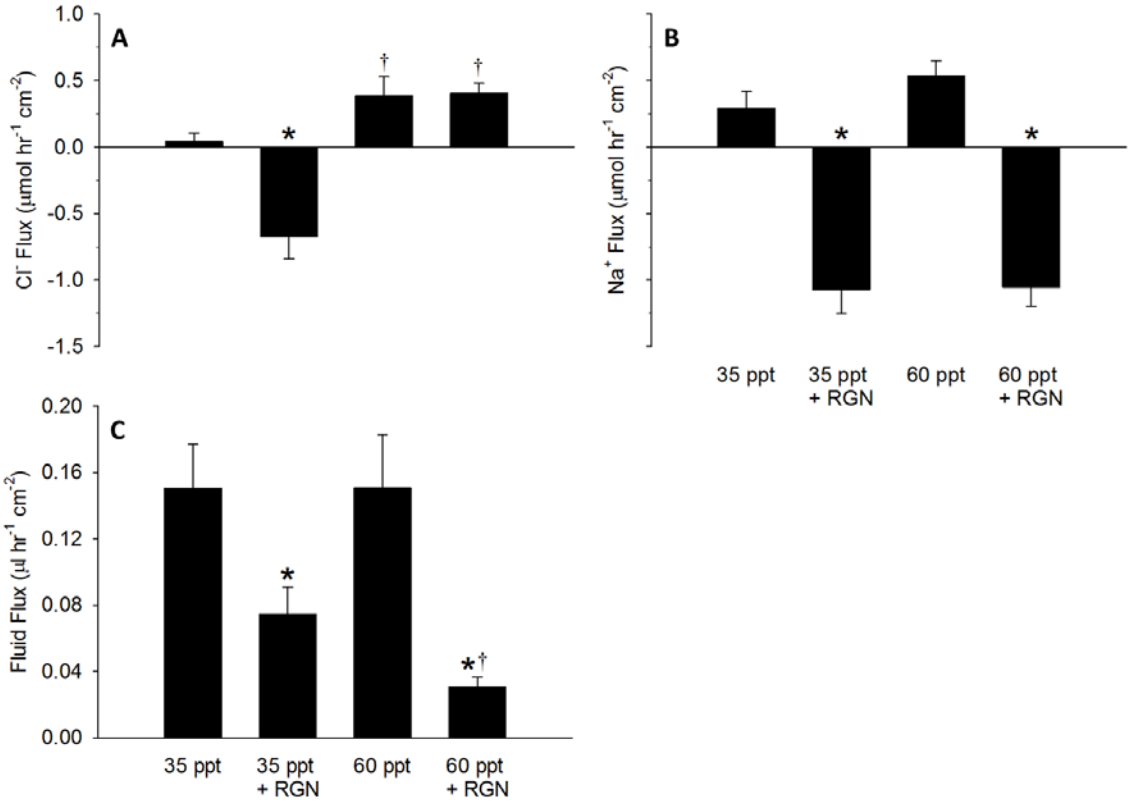

Fig. 3.5. (A) $HCO_3^-$ secretion and (B) transepithelial potential (TEP) of posterior intestinal tissues from Gulf toadfish held in 35 ppt. (C) $HCO_3^-$ secretion and (D) TEP of posterior intestinal tissues from Gulf toadfish acclimated to 60 ppt. After a 30-min control flux in the presence of 5 mmol l-1 serosal $HCO_3^-$, renoguanylin (RGN; 10-7 mol l-1) was added to the mucosal half-chamber of an Ussing chamber. The serosal saline was exchanged for a serosal saline containing 0 mmol l-1 $HCO_3^-$ after a combined 100 min. Filled bars and circles indicate the presence of serosal $HCO_3^-$, white bars and circles indicate the absence of serosal $HCO_3^-$. Values are means ± SEM (n = 9). Horizontal bars represent 30-min mean values. Significant differences ($p \leq 0.05$) in HCO3- secretion and TEP within the 35 or 60 ppt groups were revealed by one-way repeated measures ANOVAs, followed by Holm-Sidak tests (a, b, c). Significant differences between the 35 and 60 ppt groups were revealed by a Mann-Whitney rank sum test (†).

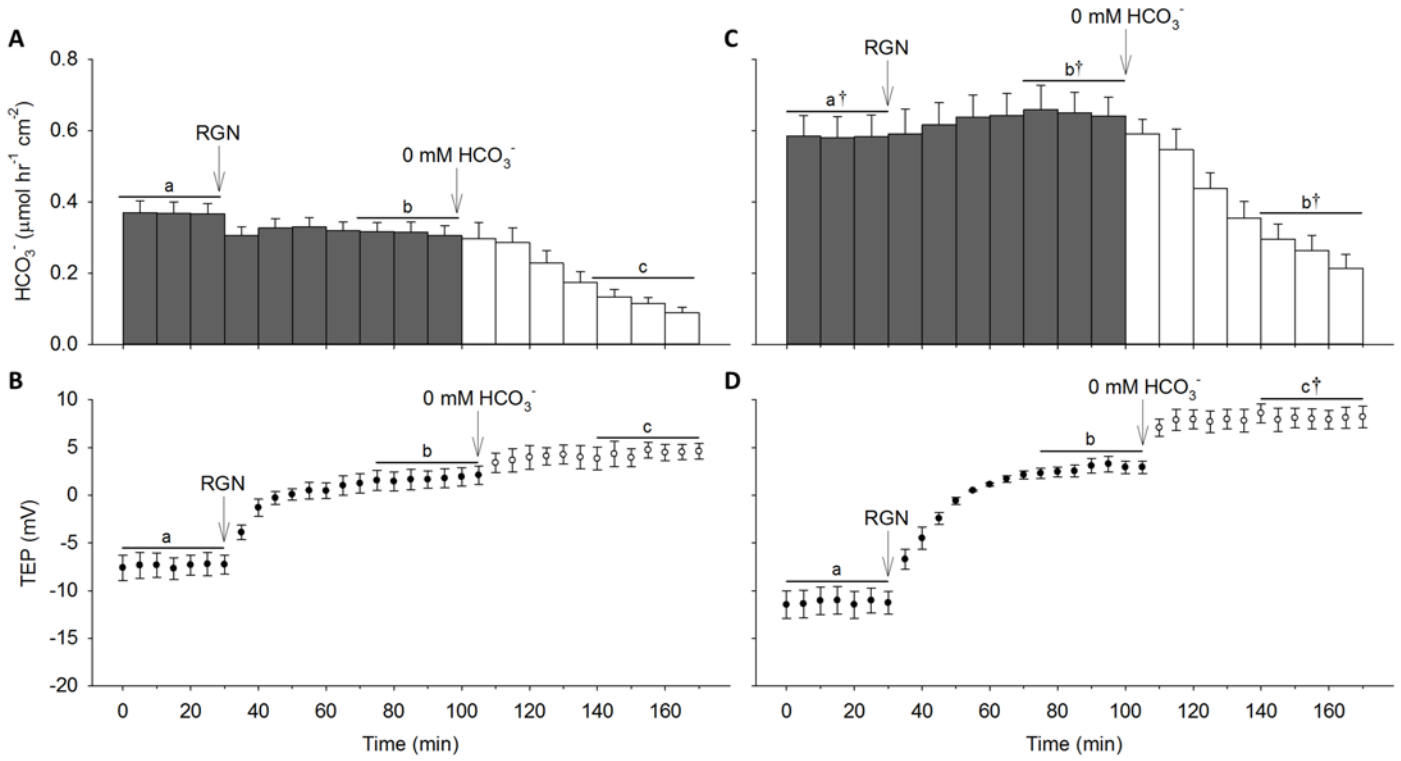

Table 3.3. Transepithelial conductance ($G_{TE}$) of the posterior intestine in response to renoguanylin (RGN) and $HCO_3^-$/$CO_2$-free serosal saline.

| Corresponding Figure | $G_{TE}$ (mS $cm^{-2}$) | | Saline | | |
|---|---|---|---|---|---|
| | 35 ppt | 60 ppt | Mucosal | Serosal | Time (min) |
| | 3.9±0.4 | 2.7±0.2[a]† | | + | 0-30 |
| 5 | 3.9±0.3 | 3.4±0.5[ab] | RGN | + | 70-100 |
| | 3.7±0.2 | 4.2±0.5[b] | RGN | - | 140-170 |
| | 3.1±0.3[a] | 3.3±0.2[ab]† | | - | 0-30 |
| 6 | 2.9±0.2[a] | 2.9±0.3[a] | RGN | - | 70-100 |
| | 5.4±0.8[b] | 6.0±0.4[b] | RGN | + | 140-170 |

Values are means ± SEM (n = 5-9) for the response of the posterior intestine to $HCO_3^-$/$CO_2$-free serosal saline (0 mmol $l^{-1}$ $HCO_3^-$) and/or RGN ($10^{-7}$ mol $l^-$). RGN was applied to the mucosal half-chamber (2 mL volume) of an Ussing chamber. † indicates significant differences ($p \leq 0.05$) between the 35 and 60 ppt exposures, and [a, b,]* indicate significant effects within the 35 or 60 ppt exposures. The presence or absence of $HCO_3^-$/$CO_2$ is indicated by + or -, respectively.

Fig. 3.6. (A) $HCO_3^-$ secretion and (B) transepithelial potential (TEP) of posterior intestinal tissues from Gulf toadfish held in 35 ppt. (C) $HCO_3^-$ secretion and (D) TEP of posterior intestinal tissues from Gulf toadfish acclimated to 60 ppt. After a 30-min control flux in the absence of serosal $HCO_3^-$ (0 mmol $l^{-1}$), renoguanylin (RGN; $10^{-7}$ mol $l^{-1}$) was added to the mucosal half-chamber of an Ussing chamber. The serosal saline was exchanged for a serosal saline containing 5 mmol $l^{-1}$ $HCO_3^-$ after a combined 100 min. Filled bars and circles indicate the presence of serosal $HCO_3^-$, white bars and circles indicate the absence of serosal $HCO_3^-$. Values are means ± SEM (n = 5). Horizontal bars represent 30-min mean values. Significant differences ($p \leq 0.05$) in $HCO_3^-$ secretion and TEP within the 35 ppt groups were revealed by a Friedman repeated measures ANOVA on ranks, followed by a Tukey test ($^{a, b}$). For the 60 ppt group, significant differences were revealed by a one-way repeated measures ANOVA, followed by Holm-Sidak test ($^{a, b, c}$). Significant differences between the 35 and 60 ppt groups were revealed by a Mann-Whitney rank sum test (†).

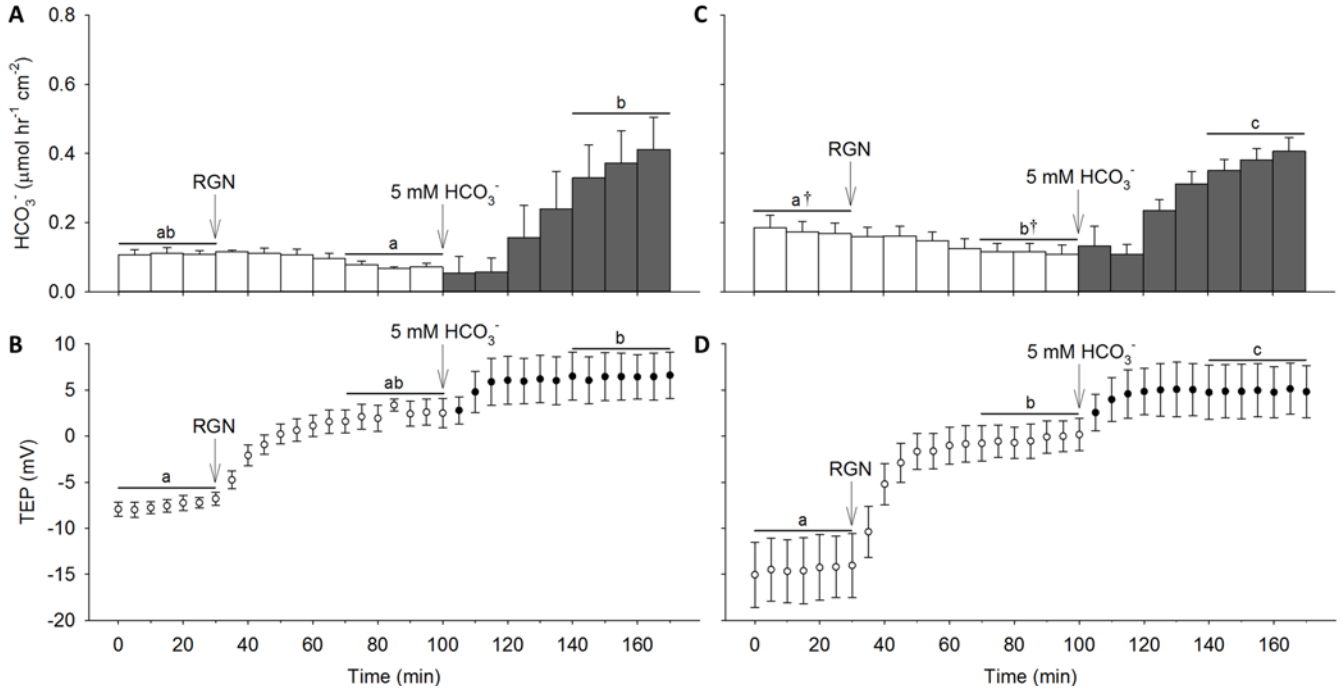

## Conclusions

The present study demonstrates transcriptional upregulation of tfGC-C, tfNKCC1, and tfCFTR in the posterior intestine of Gulf toadfish acclimated to 60 ppt, and a parallel increase in the secretory response of this tissue to RGN. Moreover, guanylin and uroguanylin is shown to be present in all the intestinal segments and in the rectum of the Gulf toadfish, as well as in European and Japanese eels (Kalujnaia *et al.*, 2009; Yuge *et al.*, 2003), despite the fact that only the mid and posterior intestine appear to respond to these peptides (Ando *et al.*, 2014; Ruhr *et al.*, 2014; Yuge and Takei, 2007). The present study also confirms the expression of at least one isoform of GC-C in all the intestinal segments and in the rectum of the Gulf toadfish. The existence of two or more GC-C isoforms is likely, as is the case with other teleosts (Comrie *et al.*, 2001b; Iio *et al.*, 2005; Yuge *et al.*, 2006). The partial clone of tfGC-C sequenced in the present study spans a highly conserved region of vertebrate GC-C, which does not allow for differentiation between possible tfGC-C isoforms that might otherwise be evident from less conserved regions found in the full-length sequences. It is perhaps surprising that tfGC-C is expressed roughly equally throughout the intestine, since the anterior intestine lacks a physiological response to guanylin-peptide stimulation, at least for the parameters measured in the present and a previous study (Ruhr *et al.*, 2014). This implies the possibility that GC-C and the guanylin peptides play a different, untested role in the anterior intestine. Moreover, the absence of apical CFTR in the anterior intestine most likely prevents the switch from net $Cl^-$ absorption to secretion. This contrasts to the posterior intestine, in which RGN stimulation leads to activation of apical CFTR and, subsequently, $Cl^-$ secretion into the intestine (Ruhr *et al.*, 2014).

In support of our hypothesis, that the guanylin-induced $Cl^-$-secretory response might facilitate the removal of $CaCO_3$ precipitates from the intestine, the present study demonstrates that tfGC-C, tfNKCC1, and tfCFTR are transcriptionally upregulated in the posterior intestine of Gulf toadfish after 96 h in 60 ppt. These observations suggest the potential of a greater secretory response at 60 ppt than at 35 ppt. Similar changes in NKCC1 and CFTR mRNA expression have also been shown in the intestine of hypersaline-acclimated Mozambique tilapia (*Oreochromis mossambicus*) (Li *et al.*, 2014) and sea bream (*Sparus aurata* L.) (Gregorio *et al.*, 2013). The potential for a larger secretory response is important when considering that Gulf toadfish transferred from 35 to 50 ppt increase the formation of $CaCO_3$ by 2.3-fold (Genz *et al.*, 2008). Consequently, a greater secretory response by intestinal tissues from the 60 ppt-acclimated Gulf toadfish, mediated by transcriptional upregulation of the $Cl^-$-secretory pathway (apical CFTR and basolateral NKCC1), would be expected to facilitate the removal of the increased production of $CaCO_3$ precipitates. The lack of transcriptional upregulation of guanylin and uroguanylin in the posterior intestine suggests that these peptides do not limit the intracellular guanylin-stimulated signaling pathway. The absence of transcriptional upregulation of guanylin and uroguanylin (Carrithers *et al.*, 2002) and their secretion (Kita *et al.*, 1999) has also been observed in the intestine of salt-loaded rats. Accordingly, it is likely that some combination of GC-C, NKCC1, and apical CFTR limits the tissue response to guanylin-peptide stimulation.

Correlating with increases in tfGC-C, tfNKCC1, and tfCFTR mRNA expression in the posterior intestine is the roughly twofold larger $\Delta I_{SC}$ of RGN-treated tissues from Gulf toadfish acclimated to 60 ppt. This would indicate that the posterior intestine from

Gulf toadfish held in 60 ppt, relative to those held in 35 ppt, could produce a greater secretory response after RGN stimulation. When guanylin peptides inhibit the absorptive $I_{SC}$, either net fluid absorption should be inhibited or net fluid secretion stimulated (Ando *et al.*, 2014; Forte and Hamra, 1996; Ruhr *et al.*, 2014)]. In the present study, the absorptive $I_{SC}$ of the tissues from the 35 and 60 ppt-acclimated Gulf toadfish was modestly, but significantly, reversed, which led to inhibited fluid absorption. Despite this inhibition of net ion absorption, the conductance of these tissues increased in the presence of RGN, possibly due to the opening of apical CFTR channels, as has been observed previously in marine teleosts (Ando *et al.*, 2014; Ruhr *et al.*, 2014; Yuge and Takei, 2007). In a previous study on the Gulf toadfish posterior intestine from fish held in 35 ppt (Ruhr *et al.*, 2014), guanylin, uroguanylin, and RGN reversed the absorptive $I_{SC}$, which corresponded to net $Cl^-$ and fluid secretion. In contrast, RGN in the present study and guanylin in the Japanese eel posterior intestine (Ando *et al.*, 2014) also reversed the absorptive $I_{SC}$, with fluid absorption being inhibited rather than reversed to secretory. In the case of the wild-caught Gulf toadfish, these contrasts could reflect seasonal differences in transport physiology. Indeed, the previous study on the Gulf toadfish was performed in the spring and early summer, while the present study was conducted in late summer and in early autumn. Nevertheless, it is the presence of fluid in the intestinal lumen that would be necessary to help move solids from the intestine during peristalsis. Increased fluid volume, in combination with mucus lining the intestinal wall and the mechanical motions that help grind solids, would facilitate the passage of a solid though the intestine (Schulze, 2015). In any case, it should be noted that net fluid movement of the intestinal tissues is the sum of simultaneous secretory and absorptive processes, and

that the reduced absorption, seen in the present study, is likely attributable to the stimulation by RGN of the $Cl^-$-secretory pathway, comprised of basolateral NKCC1 and apical CFTR.

The observed inhibition of $Na^+$ absorption, by RGN might possibly be due to the inhibition of the apical NKCC2 co-transporter that seems to occur in the Japanese eel (Ando and Takei, 2015; Ando *et al.*, 2014; Yuge and Takei, 2007). Inhibition of NKCC2 would facilitate a secretory response by the tissues, as occurs in mammals [reviewed in Arshad & Visweswariah (Arshad and Visweswariah, 2012)]. However, paracellular secretion of $Na^+$ is entirely possible, as suggested to occur in the GN-treated Japanese eel intestine (Ando and Takei, 2015). The fact that RGN produces a larger secretory $I_{SC}$ and the observation of transcriptional upregulation of tfGC-C, tfCFTR, and tfNKCC1 would suggest that RGN-treated tissues from fish acclimated to 60 ppt should secrete more $Cl^-$ than RGN-treated tissues held in 35 ppt. Unexpectedly, RGN-treated and -untreated sac preparations from Gulf toadfish acclimated to 60 ppt did not differ in $Cl^-$ flux. This unanticipated result might be explained by elevated $HCO_3^-$ secretion, via anion exchange, of tissues from Gulf toadfish acclimated to 60 ppt (and treated with RGN). Greater $HCO_3^-$ secretion would result from increased apical $Cl^-/HCO_3^-$ exchange activity, and not by transport via CFTR, as has been previously shown in the Gulf toadfish (Ruhr *et al.*, 2014), leading to complete reabsorption of the $Cl^-$ secreted as part of the RGN-induced response of the tissues. The complete reabsorption of $Cl^-$ could be useful for maintaining the drinking rate for two important reasons. First, to compensate for increased branchial fluid loss in hypersalinity, and second, because elevated intestinal

$Cl^-$ concentration has been shown to reduce drinking behaviour (Ando and Nagashima, 1996).

The apical membrane of the marine teleost intestine expresses the SLC26a6 antiporter, a $Cl^-/HCO_3^-$ exchanger [(Grosell *et al.*, 2009b; Kurita *et al.*, 2008), for review in Grosell (Grosell, 2010)] and its transporting activity is limited by $HCO_3^-$ (Grosell *et al.*, 2005; Tresguerres *et al.*, 2010) and not by $Cl^-$ (Grosell *et al.*, 2001; Ruhr *et al.*, 2014). In hypersalinity, the Gulf toadfish and sea bream intestine display the tendency to secrete $HCO_3^-$ at a higher rate than in 35 ppt [present study, (Gregorio *et al.*, 2013; Guffey *et al.*, 2011)]. In the Gulf toadfish, it does so, to a certain extent, by increasing the expression of the NBCe1 (SLC4a4), a basolateral $Na^+/HCO_3^-$ symporter (Taylor *et al.*, 2010), and cytosolic carbonic anhydrase ($CA_C$) (Sattin *et al.*, 2010), but not of SLC26a6 (Grosell *et al.*, 2009b). The exchange activity of SLC26a6 is limited, in part, by the availability of intracellular $HCO_3^-$, which, itself, is limited by the protein expression of NBCe1 and $CA_C$. However, the expression of NBCe1 and $CA_C$ is not elevated in the posterior intestine of the 60 ppt-exposed Gulf toadfish (Sattin *et al.*, 2010; Taylor *et al.*, 2010), suggesting that any contribution of NBCe1 and $CA_C$ is posttranslational, and that intracellular regulation by RGN might mediate the increased $HCO_3^-$ secretion rate. Indeed, certain regions of mammalian tissues, such as in the kidneys and pancreas, also express isoforms of basolateral NBCs in order to reabsorb or secrete $HCO_3^-$, respectively [for review in Sabbatini (Sabbatini *et al.*, 2014)]. In the pancreas, for example, activation of a transmembrane adenylyl cyclase (tmAC) leads to intracellular increases in cAMP formation and PKA phosphorylation, which leads to the opening of apical CFTR [for review in Sabbatini (Sabbatini *et al.*, 2014)]. Activation of CFTR increases $Cl^-$ secretion

across the apical membrane and depolarizes both apical and basolateral membranes, resulting in a favourable gradient for $HCO_3^-$ influx across the basolateral membrane via NBC [for review (Arshad and Visweswariah, 2013; Sabbatini *et al.*, 2014)]. A similar situation may also occur in the posterior intestine of Gulf toadfish acclimated to 60 ppt and treated with RGN, in which activation of apical CFTR leads to the depolarization of enterocytes, as $Cl^-$ is excreted across the apical membrane. Concurrently, acclimation to 60 ppt leads to increased $HCO_3^-$ secretion by the enterocytes; combined with depolarization by the guanylin peptides, this could produce a more favourable gradient that would increase the influx of negatively charged ions, namely $HCO_3^-$, through the basolateral NBCe1, resulting in the increased $HCO_3^-$ secretion rate observed. As stated above, the exchange activity of SLC26a6 is limited by $HCO_3^-$, thus, it is plausible that increased $HCO_3^-$ secretion in 60 ppt and in the presence of RGN could enhance $Cl^-$ absorption via SLC26a6, which results in the absence of $Cl^-$ flux differences in tissues from 60 ppt-acclimated Gulf toadfish, despite clear differences in $\Delta I_{SC}$, and fluid and $Na^+$ fluxes.

One objective of the present study was to determine how RGN might inhibit $HCO_3^-$ secretion in the posterior intestine of Gulf toadfish held in 35 ppt. The reduction in $HCO_3^-$ secretion occurs when either endogenous $CO_2$ is solely responsible for intracellular $HCO_3^-$, or when both endogenous $CO_2$ as well as serosal $HCO_3^-$ contribute to $HCO_3^-$ secretion. The most parsimonious interpretation of these observations is that RGN downregulates the exchange activity of SLC26a6 through some unknown intracellular mechanism. Conversely, posterior intestinal tissues from Gulf toadfish acclimated to 60 ppt and in the presence of both mucosal RGN and serosal $HCO_3^-$ show

elevated $HCO_3^-$ secretion, indicating that RGN enhances the transport of $HCO_3^-$ by NCBe1 to provide additional substrate for apical anion exchange by SLC26a6. Moreover, it is unlikely that apical CFTR contributes to $HCO_3^-$ secretion, and is primarily responsible for $Cl^-$ secretion, which is the primary cause of the $I_{SC}$ reversal (Ruhr *et al.*, 2014). In mammals, the guanylin-peptide activation of GC-C can lead to increases in cAMP formation and PKA phosphorylation that stimulate apical CFTR channels [for review in Arshad and Visweswariah (Arshad and Visweswariah, 2013)]. In the mammalian intestine, guanylin, uroguanylin, and forskolin (which also elevates cAMP levels) act to increase $HCO_3^-$ secretion, supporting the above suggestion. In contrast, forskolin and IBMX, a PDE inhibitor, decrease $HCO_3^-$ secretion, fluid absorption, and the absorptive $I_{SC}$ in the intestine and rectum of the sea bream, due to tmAC stimulation or inhibition of soluble adenylyl cyclase (sAC) (Carvalho *et al.*, 2012). This response appears analogous to what is observed when the posterior intestine of Gulf toadfish held in 35 ppt is treated with RGN. It is clear that the transfer of the Gulf toadfish from 35 to 60 ppt modifies the intracellular pathways that are regulated by the guanylin peptides.

From the studies mentioned above, future investigations on the intracellular regulation of the posterior intestine of the Gulf toadfish (from fish held in both 35 and 60 ppt) by the guanylin peptides should focus on the secondary messengers mentioned above, to elucidate their roles in $HCO_3^-$ flux. Indeed, there is evidence that protein kinase C regulates the transport activity of SLC26a6 in mammals, by altering its interactions with CA (Alvarez *et al.*, 2005). It is plausible that guanylin peptide-induced activation of PKG and PKA could have similar effects on SLC26a6. Moreover, the present findings from the Gulf toadfish also demonstrate significantly reduced fluid absorption by the

posterior intestine from fish acclimated to 35 and 60 ppt, likely due to $Cl^-$ secretion by SLC26a6 and NKCC2. However, it remains to be seen if these observations apply to marine teleosts in general.

*Significance and Perspectives*

The transcriptional upregulation of tfGC-C, tfCFTR, and tfNKCC1 in the posterior intestine of Gulf toadfish exposed to 60 ppt, and the corresponding enhanced secretory response, further demonstrates the important function the guanylin peptide system has in osmoregulation. The present study demonstrates that fluid absorption and the absorptive $I_{SC}$ are inhibited, or even reversed, by RGN in the posterior intestine of Gulf toadfish from 35 ppt (the latter to a greater extent than the former), and that these parameters are more impacted in posterior intestinal tissues from fish acclimated to 60 ppt. These observations support the hypothesis that the RGN-stimulated secretory response may serve the role of eliminating $CaCO_3$ precipitates from the intestine. In 35 ppt, $Cl^-$ secretion by the posterior intestine treated with RGN correlated with a modest, but significant, reversal of the absorptive $I_{SC}$ (from mucosa-to-serosa to serosa-to-mucosa). However, in 60 ppt, there was no net change in $Cl^-$ absorption in the presence of RGN, despite a greater inhibition of the absorptive $I_{SC}$ and fluid absorption, relative to that in 35 ppt. This is explained by possible membrane depolarization initiated by RGN, in combination with increased baseline $HCO_3^-$ secretion that occurs in 60 ppt. Studies on the Japanese eel suggest that the $Cl^-$ concentration in the intestinal lumen modulates drinking rate; when $Cl^-$ levels in the lumen become elevated, drinking rate is reduced (Ando and Nagashima, 1996). In the context of the present study, it appears that the

posterior intestine of Gulf toadfish held in 35 ppt and treated with RGN, secretes $Cl^-$ and reduces $HCO_3^-$ secretion in order to limit the formation of $CaCO_3$ precipitates and to promote their removal from the intestine. In contrast, $Cl^-$ secreted by intestinal tissues from Gulf toadfish held in 60 ppt, due to RGN stimulation, is completely reabsorbed by elevated apical $Cl^-/HCO_3^-$ exchange activity, perhaps serving to preserve the drinking behaviour of the fish. Increased drinking rate by marine teleosts held in hypersalinity is important for counteracting increased fluid loss through the gills. guanylin and uroguanylin have also been linked to relaxation of the smooth muscles surrounding the guinea pig caecum (Ochiai *et al.*, 1997) and bronchioles (Ohbayashi *et al.*, 1998), and those of the human corpora cavernosa (Sousa *et al.*, 2010). If this smooth muscle relaxation also occurs in the Gulf toadfish intestine, it may serve as an important adaptation in preventing intestinal blockages that would inhibit the drinking behaviour of a marine teleost. Increased fluid secretion into the intestine could work synergistically with smooth muscle relaxation to allow solids to be more easily removed from the intestine.

The present study employed *in vitro* techniques, but nothing is known about the effects of the guanylin peptides *in situ* in teleost fish. Furthermore, the present study raises the intriguing questions about the intracellular control that the guanylin peptides have in the Gulf toadfish intestine. Further studies should be carried out on the possible roles secondary messengers play in intestinal physiology, specifically PKG, PKA, and PDEs (which break down cAMP and cGMP), whose phosphorylation levels are regulated by GC-C activity, and that of sAC, a $HCO_3^-$-sensing protein, which produces cAMP and

is suggested to regulate NKCC2 in marine teleosts (Carvalho *et al.*, 2012; Tresguerres *et al.*, 2010).

Fig. 3.7. Proposed effects of guanylin peptides in the posterior intestinal epithelia of Gulf toadfish (*Opsanus beta*). (A) In tissues from 35 ppt-acclimated fish, guanylin (GN), uroguanylin (UGN), or renoguanylin (RGN) bind to an (i) apical guanylin cyclase-C (GC-C) receptor, which has intrinsic GC activity. GC-C initiates an intracellular transduction cascade that (ii) stimulates the opening and/or increased insertion of apical cystic fibrosis transmembrane conductance regulator (CFTR) $Cl^-$ channels and upregulates the transport activity of NKCC1. Net ion absorption is inhibited by the activation of GC-C by the guanylin peptides, leading to either decreased fluid absorption or net fluid secretion. (iii) An unknown intracellular pathway is modulated and decreases the activity of the apical SLC26a6 anion exchanger, limiting the enterocyte's ability to secrete $HCO_3^-$. (B) In tissues from 60 ppt-acclimated fish, guanylin, uroguanylin, or RGN bind to (i') GC-C and initiate the intracellular signals described above, including (ii') upregulation in the activity of the $Cl^-$-secretory pathway. In 60 ppt, the posterior intestine has both an elevated $HCO_3^-$ secretion rate and a stronger response to the guanylin peptides (leading to greater $Cl^-$ secretion via CFTR), relative to 35 ppt. Increased $Cl^-$ secretion in 60 ppt leads to greater cell depolarization than what occurs in 35 ppt, leading to a more favourable gradient for the influx of negative charges (i.e. increased basolateral $HCO_3^-$ uptake). (iii') Combined, the guanylin peptides further elevate $HCO_3^-$ secretion in 60 ppt by elevating the transport activity of both SLC26a6 and NBCe1 (see text for the role of NBCe1). In the present study, Japanese eel RGN was used as a research tool, but the presence of tfR guanylin, in the Gulf toadfish intestine, remains to be established. Symbols: (+) stimulatory effects, (-) inhibitory effects. NKA: the $Na^+/K^+$-ATPase. TJ: tight junctions. Cell diagrams modified from Grosell (Grosell, 2010) and Ruhr et al. (Ruhr *et al.*, 2014).

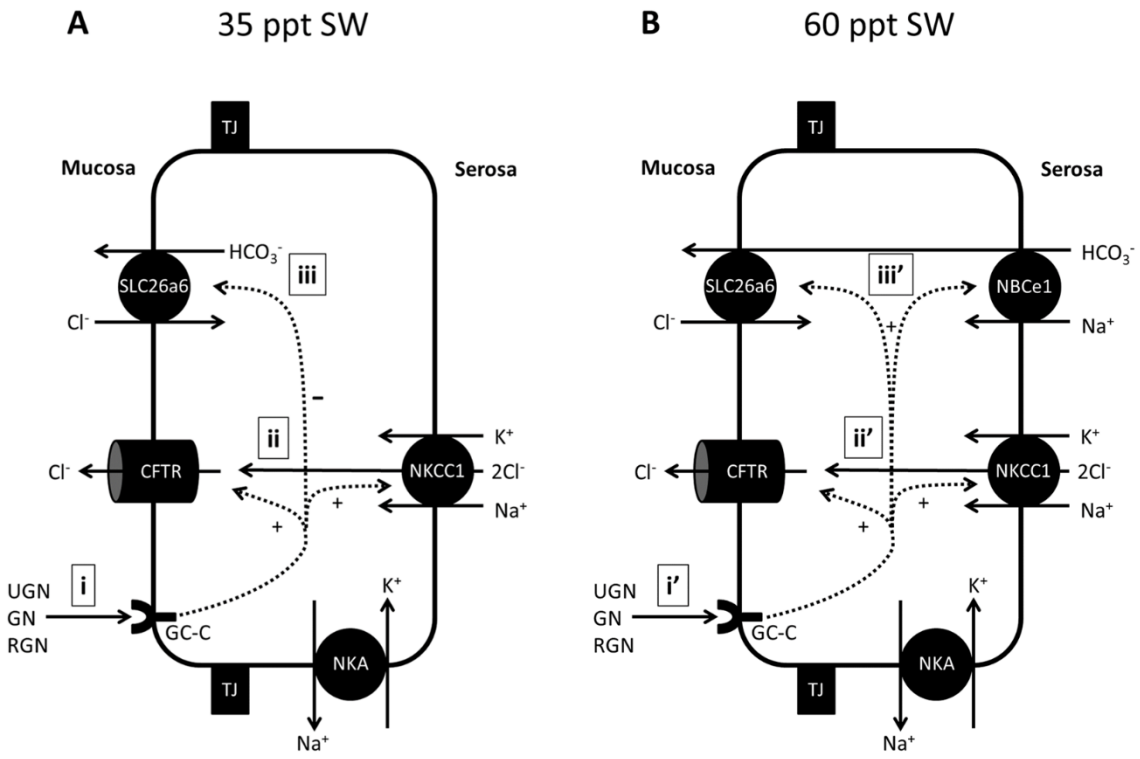


*Acknowledgements*

We thank Drs. M. Danielle McDonald, Douglas L. Crawford, and Marjorie F. Oleksiak from the Rosenstiel School of Marine and Atmospheric Science at the University of Miami for the generous use of their equipment. We also thank Drs. Patrick J. Walsh and Christophe M. R. LeMoine from the University of Ottawa for providing us with the annotated intestinal transcriptome of the Gulf toadfish. MG is Maytag Professor of Ichthyology and is supported by NSF (IOS 1146695).

## Chapter 4

## The role of the rectum in osmoregulation and the potential effect of renoguanylin on SLC26a6 transport activity in the Gulf toadfish (*Opsanus beta*)


### Summary

Teleosts living in seawater continually absorb water across the intestine to compensate for branchial water loss to the environment. The present study reveals that the Gulf toadfish (*Opsanus beta*) rectum plays a comparable role to the posterior intestine in ion and water absorption. However, the posterior intestine appears to rely more on SLC26a6 (a $HCO_3^-/Cl^-$ antiporter) and the rectum on NKCC2 (SLC12a1) for the purposes of solute-coupled water absorption. The present study also demonstrates that the rectum responds to renoguanylin (RGN) by decreasing water absorption (which occurs more greatly than in the posterior intestine) due to net $Na^+$ and $Cl^-$ secretion, corresponding to a reversal of the absorptive short-circuit current ($I_{SC}$). It is hypothesized that maintaining a larger fluid volume within the distal segments of intestinal tract facilitates the removal of $CaCO_3$ precipitates and other solids from the intestine. Indeed, the expression of the components of the $Cl^-$-secretory response, apical CFTR and basolateral NKCC1 (SLC12a2), are upregulated in the rectum of the Gulf toadfish after 96 h in 60 ppt, an exposure that increases $CaCO_3$ precipitate formation relative to 35 ppt. Moreover, the downstream intracellular effects of RGN appear to directly inhibit ion absorption by NKCC2 and anion exchange by SLC26a6. Overall, the present findings elucidate key electrophysiological differences between the posterior intestine and rectum of Gulf toadfish and the potent regulatory role renoguanylin plays in osmoregulation.

## Background

Marine teleost fish live in an environment that is hypertonic to their blood plasma, resulting in continual water loss through the gills (Marshall and Grosell, 2006). To compensate for this, marine teleosts drink copious volumes of water that are continually desalinated by the esophagus and gastrointestinal tract to produce a fluid that is roughly isotonic to blood plasma (Grosell, 2010; Marshall and Grosell, 2006). The constant absorption of ions, by the intestine, is critical as it lowers luminal osmolality and allows for solute-coupled water absorption, and, thereby, compensating for branchial water loss (Skadhauge, 1969; Skadhauge, 1974). The decrease in luminal osmolality is achieved by ion transport mechanisms that not only favour salt absorption, but also results in the precipitation of osmolytes in the intestinal lumen that further reduce osmotic pressure. Enterocytes express the apical electrogenic $HCO_3^-/Cl^-$-antiporter (SLC26a6) that secretes multiple molecules of $HCO_3^-$ in exchange for a single $Cl^-$, although the exact ratio is unknown (Grosell *et al.*, 2009b; Kurita *et al.*, 2008). Secreted $HCO_3^-$ binds to luminal $Ca^{2+}$ (and to a lesser extent with $Mg^{2+}$) to form $CaCO_3$ (and $MgCO_3$) precipitates, resulting in a 70-100 mOsm reduction in luminal osmolality (Wilson *et al.*, 2002). In addition, the titration of $HCO_3^-$ by $H^+$, secreted by apical V-type $H^+$-ATPase (VHA), can further decrease luminal osmolality by up to 30 mosm/kg $H_2O$ (Grosell, 2006; Grosell, 2010; Grosell *et al.*, 2009a; Grosell *et al.*, 2005; Guffey *et al.*, 2011; Wilson and Grosell, 2003; Wilson *et al.*, 2002). $Na^+$ is primarily taken up by the apical $Na^+/K^+/2Cl^-$-cotransporter, NKCC2 (SLC12a1), and the apical $Na^+/Cl^-$cotransporter, NCC (SLC12a3) (Hiroi *et al.*, 2008). Water absorption occurs through aquaporins (Wood and Grosell, 2012), a process coupled to the ion transport mechanisms described above.

The marine teleost rectum also plays a role in water absorption. For instance, in the sea bream (*Sparus aurata*) and Japanese eel (*Anguilla japonica*), fluid absorption by the rectum also occurs via aquaporins, but the rate of absorption is less than in the intestine (Carvalho *et al.*, 2012; Gregorio *et al.*, 2013; Kim *et al.*, 2008; Martos-Sitcha *et al.*, 2015). The rectum of the Gulf toadfish (*Opsanus beta*) also expresses intestinal ion transporters and enzymes involved in solute-coupled water absorption, such as SLC26a6, the basolateral electrogenic $Na^+/HCO_3^-$-cotransporter [NBCe1 (SLC4a4)], apical VHA, and cytosolic carbonic anhydrase ($CA_C$) (Grosell *et al.*, 2009b; Guffey *et al.*, 2011; Sattin *et al.*, 2010; Taylor *et al.*, 2010). These cellular components are essential for fluid absorption by the marine teleost intestine, but there is a large gap in knowledge concerning their osmoregulatory role in the rectum.

The hydration mechanisms described above are vital to a marine teleost's survival. However, recent studies have demonstrated the potential for inhibited fluid absorption by the intestine, initiated by the guanylin family of intestinal peptides [guanylin, uroguanylin, and renoguanylin (RGN)] (Ando and Takei, 2015; Ando *et al.*, 2014; Ruhr *et al.*, 2014; Ruhr *et al.*, 2015). These short-length hormones are expressed in the intestine and rectum of the Japanese eel, European eel (*A. anguilla*), and Gulf toadfish (Ruhr *et al.*, 2015; Takei, 2008; Takei and Yuge, 2007), and are upstream regulators of apical guanylyl cyclase-C1 and -C2 (GC-C) receptors in the intestine, which have intrinsic GC activity (Yuge *et al.*, 2006). GC-C activation leads to increases in intracellular cGMP, whose downstream effects stimulate $Cl^-$ secretion by activation of the apical cystic fibrosis transmembrane conductance regulator (CFTR) and greatly inhibit ion and water absorption (Ando and Takei, 2015; Ando *et al.*, 2014; Arshad and

Visweswariah, 2012; Ruhr *et al.*, 2014). In the Gulf toadfish and Japanese eel, the guanylin peptide effect appears restricted to the mid and posterior intestine, by reversing the absorptive short-circuit current ($I_{SC}$) (from mucosa-to-serosa to serosa-to-mucosa), mediated primarily by a switch from net $Cl^-$ absorption to net secretion (Ando *et al.*, 2014; Ruhr *et al.*, 2014; Ruhr *et al.*, 2015; Yuge and Takei, 2007). This reversal leads to either fluid secretion or inhibited fluid absorption (Ando and Takei, 2015; Ando *et al.*, 2014; Ruhr *et al.*, 2014; Ruhr *et al.*, 2015; Yuge and Takei, 2007). Moreover, the guanylin peptides, GC-C1, and GC-C2 are transcriptionally upregulated when freshwater-acclimated European and Japanese eels are transferred from freshwater to seawater (SW) (Comrie *et al.*, 2001a; Cramb *et al.*, 2005; Kalujnaia *et al.*, 2009; Yuge *et al.*, 2003; Yuge *et al.*, 2006), which suggests that the guanylin peptide system is important for seawater acclimatization. There is also immunohistochemical and molecular evidence for a putative $Cl^-$-secretory pathway comprised of an apical CFTR and basolateral NKCC1 (SLC12a2) in the posterior intestine of Gulf toadfish, killifish (*Fundulus heteroclitus*), and sea bream (Gregorio *et al.*, 2013; Marshall *et al.*, 2002; Ruhr *et al.*, 2014; Singer *et al.*, 1998).

It is hypothesized that the guanylin-stimulated $Cl^-$-secretory response is essential for removing solids (e.g. $CaCO_3$ precipitates or undigested food) from the intestine (Ruhr *et al.*, 2014; Ruhr *et al.*, 2015). The mechanical activity (*e.g.* peristalsis) along with presence of fluids in the intestinal lumen facilitates the movement of solids along the intestine (Schulze, 2015). The presence of fluid in the intestinal lumen likely facilitates clearance of $CaCO_3$ precipitates from the intestine. In support of this hypothesis, transcription of CFTR and NKCC1 is upregulated in the posterior intestine of Gulf

toadfish (Ruhr *et al.*, 2015) and Mozambique tilapia (*Oreochromis mossambicus*) (Li *et al.*, 2014) exposed to hypersalinity. Further support for the above hypothesis is the observation that RGN causes a larger reversal of the absorptive $I_{SC}$ and inhibits water absorption more greatly in the posterior intestine of Gulf toadfish exposed to hypersalinity (Ruhr *et al.*, 2015). Although the above hypothesis remains to be fully validated, an important consideration is the fate of the fluid that is either secreted or not absorbed by the distal intestine of marine teleosts, due to guanylin peptide stimulation.

The retention of water is vital for the survival of a marine teleost, yet, the inhibition of absorptive mechanisms in the intestine that occurs by guanylin peptide stimulation exists. Either this water is lost by expulsion into the environment or reabsorbed by the rectum. To our knowledge, the duration of the *in vivo* guanylin peptide response in marine teleosts is unknown. It is also unknown if the duration of the guanylin peptide stimulation is long enough that it prevents the distal intestine and rectum from being able to absorb water secreted by the more proximal segments.

The purpose of this study was twofold. First, we sought to rectify the gap of knowledge with respect to transport physiology of the rectum by characterizing the normal osmoregulatory mechanisms of the Gulf toadfish rectum. Second, we wished to determine if the rectum responded to RGN, and compared this response to that of the posterior intestine. A third, objective was to determine the mechanisms that decrease $HCO_3^-$ secretion in the intestinal tract by RGN.

## Materials and Methods

*Experimental animals*

Gulf toadfish (*Opsanus beta*) were caught as bycatch from Biscayne Bay, FL, by shrimp fishermen, and placed in a 3-min freshwater bath and treated with malachite green for ectoparasite removal, upon arrival to the laboratory. Individuals were separated by size and placed into 62-litre aerated tanks (33-36 ppt, 20-26°C), with continuous flow-through of sand-filtered SW from Key Biscayne. Gulf toadfish were fed squid, to satiation once per week, but food was withheld for three days prior to experimentation. For the hypersalinity (60 ppt) studies, Gulf toadfish were held in experimental tanks in groups of 6-10, with recirculating biofilters containing charcoal. The tanks sat in a temperature-controlled water bath at 26°C. Individuals were acclimated to 35 ppt and 60 ppt (adjusted with Instant Ocean; SpectrumBrands, Inc, Madison, WI, USA) for up to four days for the real-time, quantitative polymerase chain reaction (qPCR) study and at least seven days for the physiological studies. Tanks were siphoned regularly and topped up with SW adjusted to the proper salinity. Water chemistry was monitored daily (temperature and salinity) and twice weekly (pH). Fish husbandry and experimental procedures followed an approved University of Miami Animal Care Protocol (IACUC no. 13-225, renewal 02). Gulf toadfish were sacrificed using 0.2 g $l^{-1}$ MS-222 (Argent, Redmond, WA, USA) solution buffered with 0.3 g $1^{-1}$ $NaHCO_3^-$ (Sigma-Aldrich, St. Louis, MO, USA), followed by severing the spinal cord at the cervical vertebra and pithing of the brain.

*Composition of salines, hormones, and inhibitors*

Mucosal (pH = 7.8) and serosal (pH = 7.8) salines were prepared as described in (Table 4.1), and were used to bathe intestinal and rectal tissues of Gulf toadfish acclimated to both 35 and 60 ppt. The osmolalities of plasma, posteror intestinal, and rectal fluids from Gulf toadfish at these two salinities are not significantly different (Genz *et al.*, 2011; McDonald and Grosell, 2006) and, accordingly, would influence neither cell volume nor osmotic transepithelial water movement. Eel RGN (Peptide Institute, Inc., Osaka, Osaka Prefecture, Japan) was used in the present study for two reasons. First, the sequence for eel RGN (ADLCEICAFAACTGCL, accession number: BAC76010.1) is nearly identical to that of Gulf toadfish (tf) guanylin (MDVCEICAFAACTGC, accession number: AIA09902.1). Second, because of its close homology with tf guanylin, eel RGN has the greatest physiological effects on Gulf toadfish intestinal tissues (Ruhr *et al.*, 2014). Ethoxzolamide (Sigma-Aldrich) was dissolved in dimethyl sulfoxide (DMSO, Sigma-Aldrich) and administered at a concentration of 100 μmol $l^{-1}$ in saline containing 0.1% DMSO. Vehicle controls for 0.1% DMSO have been shown not to affect the physiological parameters tested in the present study (Ruhr *et al.*, 2014). Bumetanide (Sigma-Aldrich) was dissolved in ethanol (Sigma-Aldrich) and administered at 10 μmol $l^{-1}$ in saline containing 0.05% ethanol. Control experiments revealed that at this concentration, ethanol does not affect the physiological parameters tested in the present study (data not shown).

Table 4.1. Composition of salines for short-circuit current, pH-stat titration, and sac preparation experiments

| Compound | Mucosal* | Serosal† | $HCO_3^-/CO_2$-free serosal |
|---|---|---|---|
| NaCl, mmol/l | 169.0 | 151.0 | 151.0 |
| KCl, mmol/l | 5.0 | 3.0 | 3.0 |
| $MgSO_4$, mmol/l | 77.5 | 0.88 | 0.88 |
| $MgCl_2$, mmol/l | 22.5 | | |
| $Na_2HPO_4$, mmol/l | | 0.5 | 0.5 |
| $KH_2PO_4$, mmol/l | | 0.5 | 0.5 |
| $CaCl_2$, mmol/l | 5.0 | 1.0 | 1.0 |
| $NaHCO_3$, mmol/l | | 5.0 | |
| HEPES, free acid, mmol/l | | 11.0 | 11.0 |
| HEPES, $Na^+$ salt, mmol/l | | 11.0 | 11.0 |
| Urea, mmol/l | | 4.5 | 4.5 |
| Glucose, mmol/l | | 5.0 | 5.0 |
| Osmolality§, mosmol/kg $H_2O$ | 330 | 330 | 330 |
| pH | 7.8† | 7.8 | 7.8 |
| Gas‡ | 100% $O_2$ | 0.3% $CO_2$ in $O_2$ | 100% $O_2$ |

*Mucosal application of blockers and pharmaceuticals: Renoguanylin was added for a final concentration of $10^{-7}$ and 5 x $10^{-7}$ mol/l in Ussing chamber and sac preparation experiments, respectively. Bumetanide and ethoxzolamide were added to Ussing chambers for final concentrations of 10 and 100 µmol/l, respectively. Salines were adjusted for osmolality with mannitol (§). When measuring $HCO_3^-$ secretion, mucosal pH in Ussing chambers was maintained at 7.8 by pH-stat titration (†). Salines were gassed for at least 1 h prior to experiments (‡).

*RNA isolation and molecular cloning*

Tissues were collected from Gulf toadfish kept in 33-35 ppt seawater for the tissue distribution study and from Gulf toadfish acclimated to 0 (control), 6, 12, 24, and 96 h in 60 ppt for the hypersalinity study. Collected tissues were homogenized with an Ultra-Turrax T8 homogenizer (Ika-Werke, Breisgau, Baden-Württemberg, Germany) and 50-100 mg $ml^{-1}$ of total RNA was extracted with RNA STAT-60 (Tel-Test, Friendswood, TX, USA). Traces of genomic DNA were removed with DNase I (Turbo DNA-free kit, Ambion, Foster City, CA, USA) from each isolate (10 µg per sample). A spectrophotometer (NanoDrop 1000 Spectrophotometer, Thermo Scientific, Grand

Island, NY, USA) was used to quantify total RNA at 260 nm. A subsample of isolates was spot-checked using gel electrophoresis to confirm RNA integrity. Isolated RNA (1 μg) was reversed transcribed into cDNA using SuperScript First-Strand Synthesis System (Invitrogen, Carlsbad, CA, USA) according to the manufacturer's protocol. Genes coding for tf guanylin, tf uroguanylin, tf guanylyl cyclase-C (GC-C), tfNKCC1, and tfCFTR were previously cloned (Ruhr *et al.*, 2014; Ruhr *et al.*, 2015) by polymerase chain reaction (PCR).

*Real-time, quantitative polymerase chain reaction*

Gene expression levels of tf guanylin, tf uroguanylin, tfGC-C, tfNKCC1, tfNKCC2, and tfCFTR were detected using qPCR. Gulf toadfish tissues were dissected and immediately snap-frozen in liquid nitrogen, after which RNA was isolated and cDNA produced, as described above. Gene expression was measured using gene-specific primers (Table 4.2) and Power SYBR Green (Applied BioSystems, Foster City, CA, USA) as the reporter dye, for qPCR in an Mx4000 cycler (Stratagene, San Diego, CA, USA). Cycling parameters were as follows: 95°C for 10 min, 40-50 cycles of 95°C for 30s, 55-60°C for 30s, and 72°C for 30s. The specificity for all PCR products was confirmed by observing a distinct, corresponding melting peak for each product following each qPCR run using a melting curve analysis (guanylin: 79-85, uroguanylin: 81-86, GC-C: 80-86, NKCC1: 81-86, NKCC2: 77-83, and CFTR: 80-85 in °C), as reported previously (Ruhr *et al.*, 2015). Gene expression was normalized to EF-1α and scaled relative to the lowest expressing tissue (tissue distribution study) and the 0-h control (hypersalinity study), which were given a value of 1.0, as described by Pfaffl

(Pfaffl, 2001). Primers for tfNKCC1, tfNKCC2, tfCFTR were designed from an annotated Gulf toadfish intestinal transcriptome (unpublished data, C.M.R. LeMoine, N. Corradi, P.J. Walsh).

*General experimental protocol: short-circuit current and $HCO_3^-$ secretion*

Short-circuit current ($I_{SC}$), transepithelial potential (TEP), and transepithelial conductance ($G_{TE}$) of Gulf toadfish tissues were measured by Ussing chambers (model 2400; Physiologic Instruments, San Diego, CA, USA). These experiments were paired, with the posterior intestine and the rectum of an individual Gulf toadfish (15-30 g) measured in parallel. The posterior intestine and rectum were excised, cut open along the midline, and mounted onto P2413 tissue holders (Physiologic Instruments), which exposed 0.71 $cm^2$ of tissue, and placed between the two half-chambers of the Ussing apparatus. $I_{SC}$ and TEP were measured by silver (Ag) current and Ag/AgCl voltage electrodes, respectively, and were connected to an amplifier (model VCC600, Physiologic Instruments).

$I_{SC}$ studies were performed under symmetrical conditions, in which 2 ml of serosal saline (Table 4.1) was added to both the mucosal (apical membrane/luminal side) and serosal (basolateral membrane/blood side) half-chambers. The salines were continually mixed by airlift gassing (0.3% $CO_2$ in $O_2$) and maintained at 25 °C by a recirculating bath (model 1160S, VWR, Radnor, PA, USA), as described in Grosell and Genz (Grosell and Genz, 2006). $I_{SC}$ was measured by current electrodes under voltage-clamp conditions (0.0 mV), with 3 s of 2-mV pulses (mucosal-to-serosal) every 60 s. TEP studies were performed under asymmetrical conditions, in which 2 ml each of mucosal and serosal saline (Table 4.1) were added to the mucosal and serosal half-chamber,

respectively. The mucosal saline was continually mixed by airlift gassing (100% $O_2$) and the serosal saline as described above, and maintained at 25 °C. TEP was measured by voltage electrodes under current-clamp conditions (0.0 μA), with 3 s of 30-μA pulses (mucosal-to-serosal) every 60 s. $G_{TE}$ was calculated by Ohm's law and was determined from the deflections in $I_{SC}$ and TEP during pulsing. Acqknowledge software (v. 3.8.1, BIOPAC Systems, Goleta, CA, USA) recorded $I_{SC}$ and TEP onto a computer.

A pH-stat titrator (Radiometer, model TIM 854 or 856, Brea, CA, USA) was set up in tandem with an Ussing chamber to measure $HCO_3^-$ secretion along with TEP (described above), respectively, on the isolated tissues, following the protocol in Grosell and Genz (Grosell and Genz, 2006). A pH electrode (Radiometer, model PHC4000.8) and a microburette tip (from which acid is delivered) were immersed in the mucosal saline bath and maintained a pH of 7.8, allowing for symmetrical pH conditions on either side of the epithelium. Titramaster software (Radiometer, v. 5.1.0), installed on a computer, recorded pH and the volume of acid titrant (0.005 mol $l^{-1}$ HCl) injected into the mucosal bath. The $HCO_3^-$ secretion rate from a tissue preparation was calculated from the rate of titrant secreted and its concentration, as described in Grosell and Genz (Grosell and Genz, 2006).

*Experimental set 1:* To determine baseline $I_{SC}$ and $HCO_3^-$ secretion rates, as well as the effects of RGN, on posterior intestinal and rectal tissues of Gulf toadfish acclimated to 35 and 60 ppt. RGN ($10^{-7}$ mol $l^{-1}$) was added to mucosal half-chamber once baseline values stabilized.

*Experimental set 2*: To determine the source of decreased $HCO_3^-$ secretion rates by RGN, bicarbonate was removed from the serosal saline, leaving $CA_C$ as the sole

source of intracellular $HCO_3^-$. As before, RGN was added to the mucosal half-chamber once the $HCO_3^-$ secretion rates of the posterior intestine and rectum stabilized (of fish acclimated to 35 ppt). A subsequent experiment tested the potential influence of RGN on $CA_C$ with ethoxzolamide ($10^{-4}$ mol $l^{-1}$) [a known inhibitor of $CA_C$ (Grosell and Genz, 2006)]. This experimental set served to elucidate the role of RGN on the transport rates of $HCO_3^-$ by apical SLC26a6 and basolateral NBCe1, and on $HCO_3^-$ formation by $CA_C$.

*Experimental set 3:* To determine the effects of mucosally applied bumetanide on $I_{SC}$ and $HCO_3^-$ secretion. In the Japanese eel and Gulf toadfish, $Na^+$ absorption is inhibited by guanylin peptide stimulation, suggesting altered NKCC2 activity (Ando and Takei, 2015; Ando *et al.*, 2014; Ruhr *et al.*, 2015; Yuge and Takei, 2007). To test for this in the Gulf toadfish, bumetanide (10 μmol $l^{-1}$), which specifically binds to and inhibits NKCC isoforms, was added to the mucosal half-chamber, and either $I_{SC}$ or $HCO_3^-$ and TEP were measured.

*Intestinal and rectal sac preparations*

Sac preparations were used to determine the effects of RGN on water, $Cl^-$, and $Na^+$ fluxes. The posterior intestine (1.5-3 cm) and rectum (1.5-2 cm) from Gulf toadfish (50-80 g) were excised as described above. The flared end of a PE50 catheter was inserted into either the posterior intestine or rectum and tied off with a silk suture. Mucosal saline (Table 4.1) was then injected into the catheter to rinse the tissue of any debris. The tissue was then tied off at the open end with a silk suture to form either an intestinal or rectal sac. The sac preparations were then injected with mucosal saline (control or containing 5 x $10^{-7}$ mol $l^{-1}$ RGN). A subsample of injected mucosal saline was

collected from which initial $Na^+$ and $Cl^-$ concentrations were measured. The catheter was sealed, and the sac preparations were blot-dried and initial masses weighed. The sac preparations were then placed in a scintillation vial containing serosal saline and continually gassed with 0.3% $CO_2$ (Table 4.1) and underwent a 2-h flux period. At the end of the flux period, the sac preparations were removed from the serosal saline, blot-dried once again, and final masses weighed. The sealed catheter was opened and the fluid collected. The silk sutures of an empty sac preparation were cut, the tissue was cut down its midline, thoroughly dried, weighed, and its surface area outlined onto tracing paper. Water, $Na^+$, and $Cl^-$ flux rates were calculated by the differences in the product between final and initial volumes and concentrations (volume x concentration), divided by the flux period and surface area. $Na^+$ and $Cl^-$ concentrations were measured using flame spectrometry (Varian 220FS, Palo Alto, CA, USA) and anion chromatography (DIONEX 120, Sunnyvale, CA, USA), respectively.

*Statistical analyses*

The data are presented as means ± the standard error of the mean (SEM) and were evaluated using parametric and non-parametric statistical tests, as described in the figure legends. The half effective concentration ($EC_{50}$) was calculated with a non-linear regression using a global curve fitting. All data were analyzed and plotted onto graphs with SigmaPlot 13.0. Means were considered significantly different with $P \leq 0.05$. Control measurements for $I_{SC}$, TEP, and $HCO_3^-$ secretion were calculated from the final 30 min of the control fluxes and treatment values were calculated from the final 30 min of a 70-min treatment exposure. One-tailed tests were used to analyze the qPCR results; a

previous study in the Gulf toadfish (Ruhr *et al.*, 2015) revealed that tfGC-C, tfCFTR, and tfNKCC1 levels of expression increased in 60 ppt. One-tailed tests were also used to analyze changes in $Na^+$, $Cl^-$, and fluid absorption, which have been shown to be inhibited after RGN stimulation in the Gulf toadfish (Ruhr *et al.*, 2014; Ruhr *et al.*, 2015).

Table 4.2. Primer used for qPCR experiments.

| Name | Sequence |
|---|---|
| tfGN-F | 5'-AGCAAAGGGCAGCATCTGCA-3' |
| tfGN-R | 5'-TGGCAAGATGTTTGTGGCTTTGC-3' |
| tfUGN-F | 5'-CCGACCCTCTCATGCCGCAGG-3' |
| tfUGN-R | 5'-TGCACGGAGGCATCGAGCTG-3' |
| tfGC-C-F | 5'-CAGAGGCCACCATGCGGCGTCACCTA-3' |
| tfGC-C-R | 5'-TTCACCAAGCGCTGCTCCGACCAA-3' |
| tfNKCC1-F | 5'-TCCTGCAGCAGCTCGTTGAG-3' |
| tfNKCC1-R | 5'-GAGCACGTGGCGGCCTTCGAGGAT-3' |
| tfNKCC2-F | 5'-AAGGCACCATAGACGTGTGG-3' |
| tfNKCC2-R | 5'-CCTCAACCGACAGTCCTTCC-3' |
| tfCFTR-F | 5'-GTTTCATCACCGGCATGAACG-3' |
| tfCFTR-R | 5'-GTGCCTTTCTGTAGATGGCTCCAA-3' |
| EF-1α-F | 5'-AGGTCATCATCCTGAACCAC-3' |
| EF-1α-R | 5'-GTTGTCCTCAAGCTTCTTGC-3' |
| Universal Primer* | 5'-CTAATACGACTCACTATAGGGCAAGCGTGGTATCAACGCAGAGT-3' |
| | 5'-CTAATACGACTCACTATAGGGC-3' |

* Universal primer (Clontech SMARTer RACE cDNA Amplification Kit) consists of both a long and short sequence. Abbreviations: tf (Gulf toadfish), F (forward), R (reverse), GN (guanylin), UGN (uroguanylin), GC-C (guanylyl cyclase-C-associated receptor), NKCC1 ($Na^+/K^+/2Cl^-$-cotransporter type 1, SLC12a2), NKCC2 ($Na^+/K^+/2Cl^-$-cotransporter type 2, SLC12a1) CFTR (cystic fibrosis transmembrane conductance regulator), and EF-1α (elongation factor 1-alpha).

## Results

*Tissue density*

Tissue masses and surface areas collected for the sac preparations revealed that the rectum of the Gulf toadfish is significantly denser than the posterior intestine (16.16 ± 1.29 v. 20.59 ± 2.36 mg $cm^{-2}$). There were no differences in tissue densities of fish acclimated to 35 and 60 ppt. Significant differences were revealed by Mann-Whitney rank sum tests.

*Dose response of the rectum to renoguanylin*

Stimulation of rectal tissues with increasing RGN concentrations ($10^{-9}$→$10^{-6}$ mol $l^{-1}$) resulted in pronounced decreases in the absorptive $I_{SC}$ in a sigmoidal, dose-dependent manner. On average, the absorptive $I_{SC}$ was reversed (mucosa-to-serosa to serosa-to-mucosa) at a concentration of 2.5 x $10^{-8}$ mol $l^{-1}$ RGN, with an $EC_{50}$ of 6.12 x $10^{-9}$ mol $l^{-1}$ RGN (Fig. 4.1A). $G_{TE}$ also increased significantly at RGN concentrations ≥ 5.0 x $10^{-8}$ mol $l^{-1}$ (Fig. 4.1B).

**Quantitative PCR analysis**

Gene expression levels were normalized to elongation factor (EF)-1α expression. NKCC1, NKCC2, and CFTR gene expression was present in all intestinal segments and the rectum (Fig. 4.2). Increased levels of rectal NKCC1 and CFTR gene expression occurred after a 96-h exposure to 60 ppt; conversely, a decreased level of rectal UGN gene expression occurred after 96 h in 60 ppt (Fig. 4.3).

*Effects of renoguanylin on bicarbonate secretion, transepithelial potential, and conductance.*

*Tissues bathed in a serosal saline containing 5 mmol $l^{-1}$ $HCO_3^-$.* In the posterior intestine, RGN significantly reduced $HCO_3^-$ secretion, reversed the TEP (on average), and significantly increased the $G_{TE}$ (Fig. 4.5A, B, C). Conversely, RGN had no effect on $HCO_3^-$ secretion in the rectum, but did significantly reduce the magnitude of the TEP (Fig. 4.5B, C). The control TEP of the posterior intestine was significantly more negative than that of the rectum (Fig. 5B).

*Tissues bathed in a serosal saline devoid of $HCO_3^-$.* In both the posterior intestine and rectum, RGN significantly reduced both $HCO_3^-$ secretion and the TEP (Fig. 4.5D, E). All control and RGN-treated tissues bathed in the serosal saline devoid of $HCO_3^-$ displayed significantly lower $HCO_3^-$ secretion rates than their counterparts bathed with 5 mmol $l^{-1}$ $HCO_3^-$ (Fig. 4.5A, D). The TEP of the RGN-treated rectum was significantly more negative than that of the RGN-treated posterior intestine (Fig. 4.5E).

Fig. 4.1. Changes in short-circuit current ($I_{SC}$) (A) and transepithelial conductance ($G_{TE}$) (B) in rectal tissues as a function of renoguanylin (RGN) dose after mucosal application (log scale). The concentration of RGN was increased every 30 min when $I_{SC}$ values became stable. Values are means ± SEM (n = 6). Significant differences from the control (no dose) were revealed by one-way, repeated measures ANOVAs, followed by Holm-Sidak tests (*P ≤ 0.05). The half effective concentration ($EC_{50}$) of RGN was calculated using a non-linear regression, global curve fitting (n = 6, P ≤ 0.05). Positive and negative $I_{SC}$ values indicate secretory and absorptive currents, respectively.

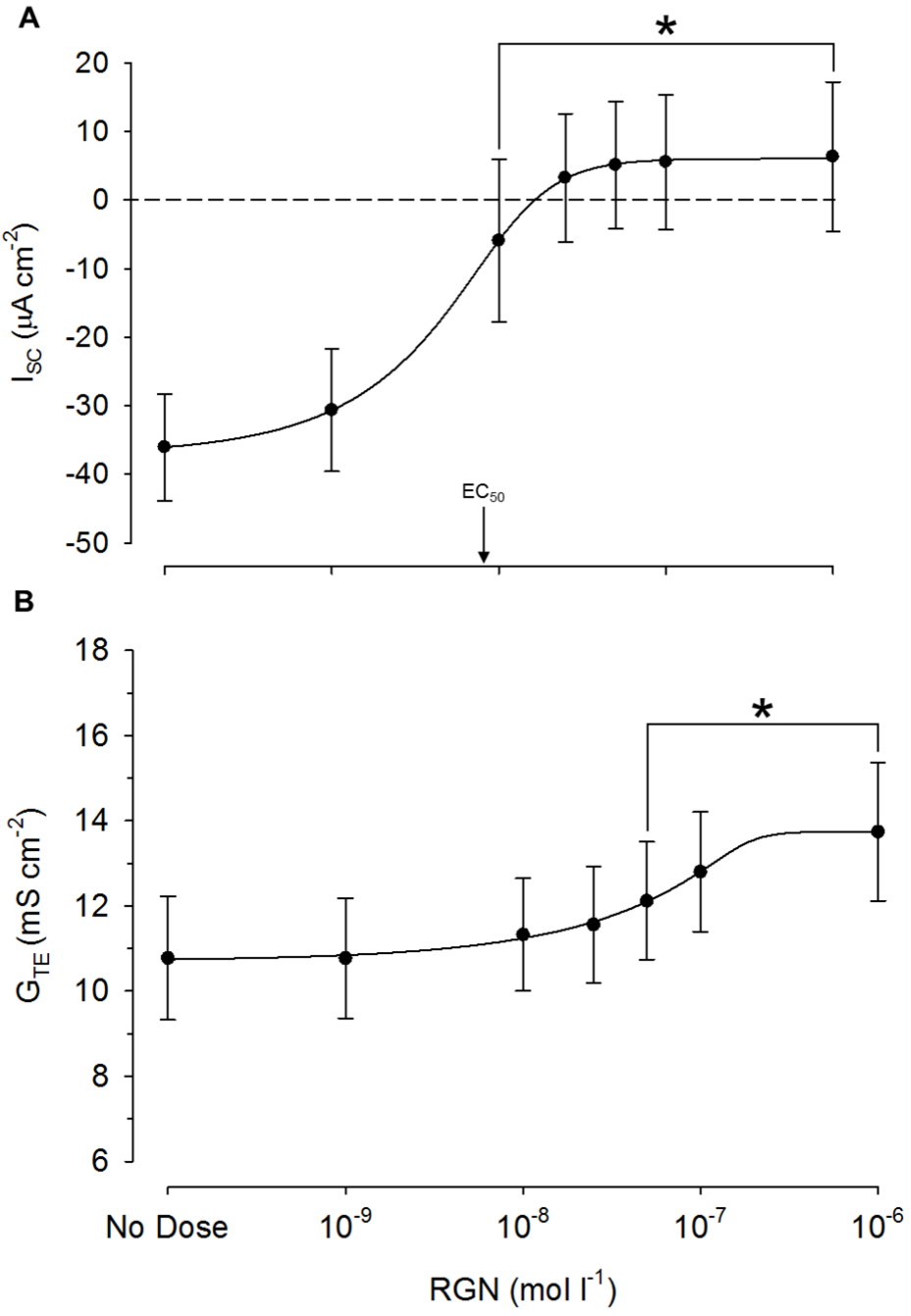

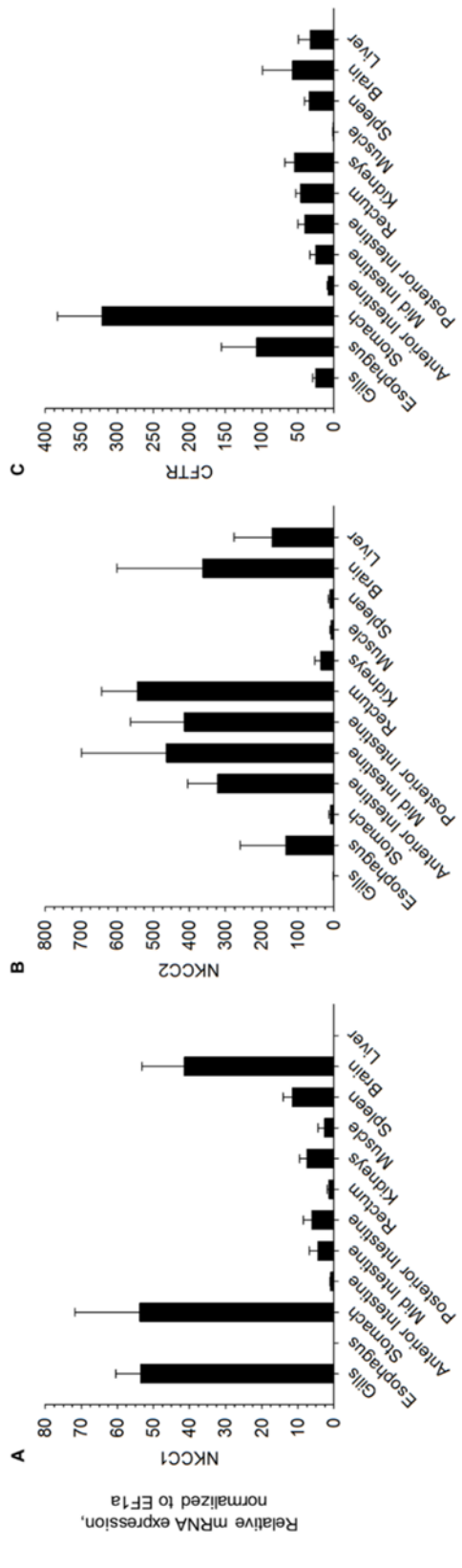


Fig. 4.2. Relative gene expression levels of NKCC1 (A), NKCC2 (B), and CFTR (C) in various tissues of the Gulf toadfish. Transcription for each gene is normalized to elongation factor (EF)-1α and scaled relative to the tissue with the lowest expression value (NKCC1: anterior intestine, NKCC2: gills, and CFTR: anterior intestine), which was given a value of 1.0. NKCC1 gene expression was not detected in the esophagus and liver. Values are means ± SEM (n = 8).

Fig. 4.3. Relative gene expression levels of guanylin (GN), uroguanylin (UGN), guanylyl cyclase-C (GC-C), NKCC1, CFTR, and NKCC2 in the rectum of Gulf toadfish acclimated to 0 (control) and 96 h in 60 ppt seawater. The level of expression for each gene is normalized to elongation factor (EF)-1α and scaled relative to the 0-h control, which was given a value of 1.0. Values are means ± SEM (n = 8). Significant differences between the 0 and 96 h groups were revealed by one-tailed Student's t-tests (*P ≤ 0.05).

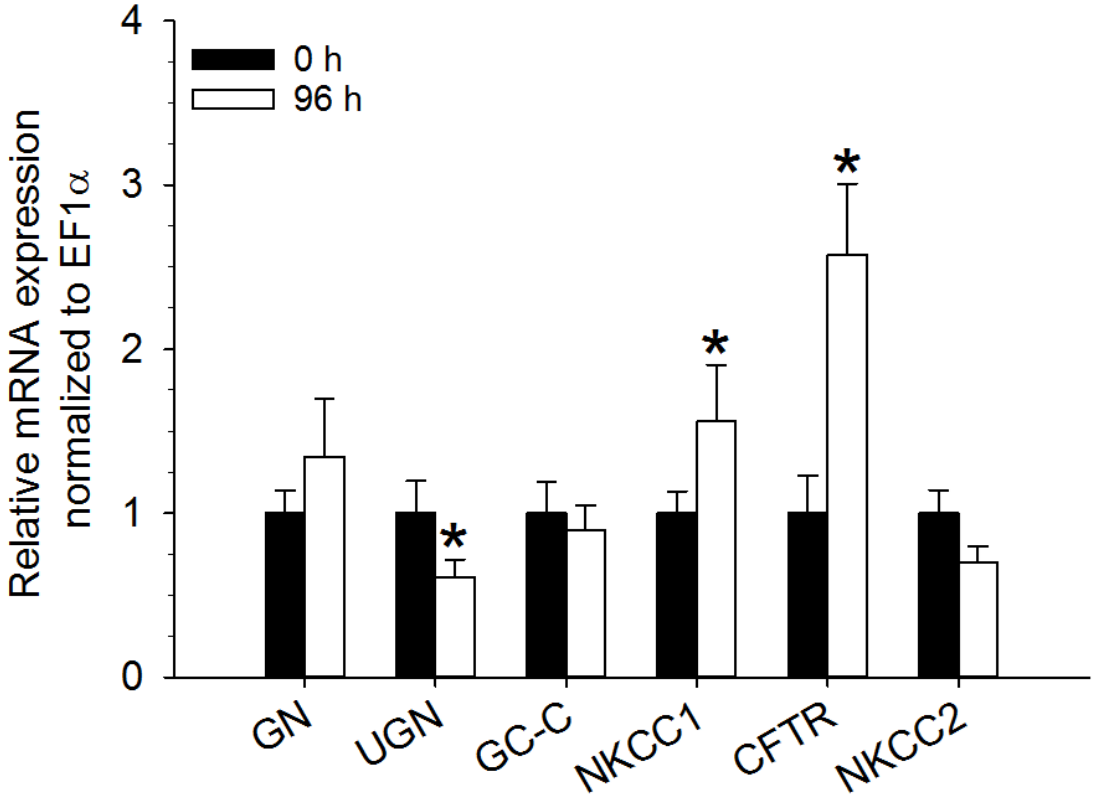

*Baseline parameters: posterior intestine v. rectum*

The posterior intestine and rectum of the Gulf toadfish both displayed an absorptive $I_{SC}$, which was significantly greater in the rectum (Fig. 4.4). The basal TEP of both the posterior intestine and rectum was negative, and significantly more so in the posterior intestine (Fig. 4.4).

Fig. 4.4. Baseline (control) values of the short-circuit current ($I_{SC}$), transepithelial potential (TEP), and transepithelial conductance ($G_{TE}$) displayed by the posterior intestine and rectum of Gulf toadfish. Values are means ± SEM and were pooled from various experiments in the present study ($I_{SC}$: n = 11 and 13, TEP: 13 and 13, and $G_{TE}$: 25 and 27, posterior intestine and rectum, respectively). Significant differences were revealed by Student's t-tests (*P ≤ 0.05). Positive and negative $I_{SC}$ values indicate secretory and absorptive currents, respectively. Positive and negative TEP values indicate net anion secretion and absorption, respectively.

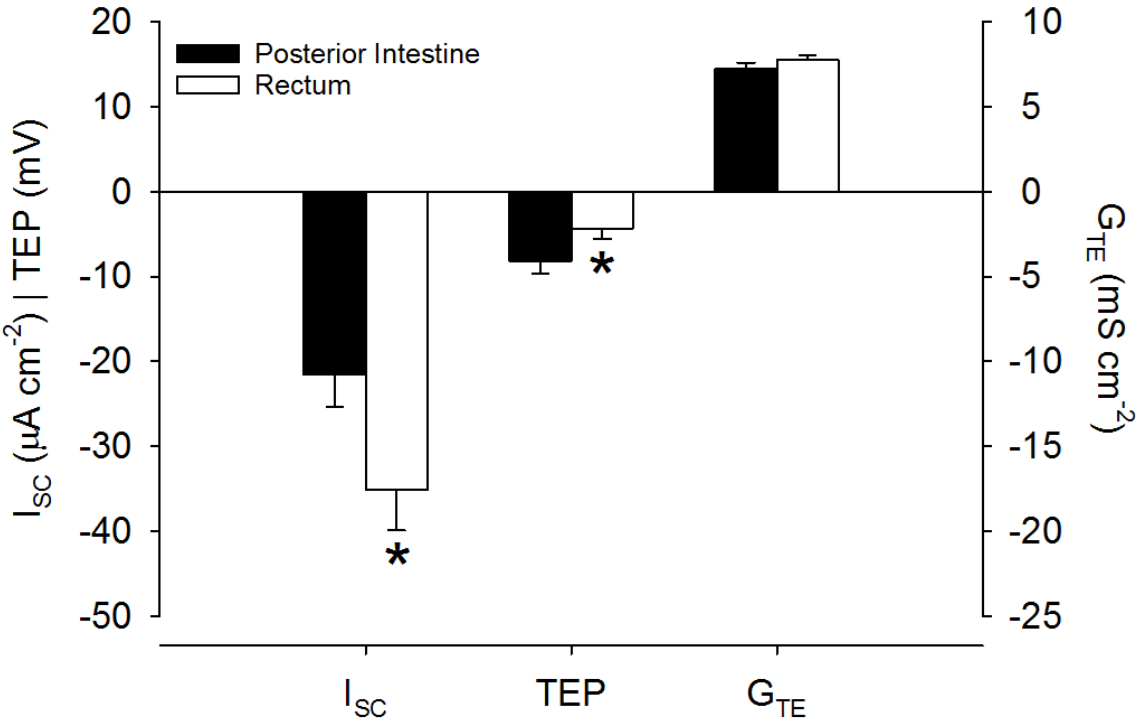

Fig. 4.5. $HCO_3^-$ (Bic) secretion (A, D), transepithelial potential (TEP) (B, E), and transepithelial conductance ($G_{TE}$) (C, F) displayed by the posterior intestine and rectum of Gulf toadfish before and after treatment with renoguanylin (RGN). Pre-treatment values were taken from the final 30 min of the control flux and post-treatment values were taken from the final 30 min of a 70-min treatment flux. Values are means ± SEM (n = 7 and 8, 5 and 0 mM Bic groups, respectively). Significant differences: control v. RGN revealed by paired t-tests (*$P \leq 0.05$), posterior intestine v. rectum revealed by Student's t-tests (†$P \leq 0.05$), and 5 mM Bic v. 0 mM (within tissue and within treatment) revealed by Student's t-tests (§$P \leq 0.05$). The presence (5 mM Bic) and absence (0 mM Bic) of serosal $HCO_3^-$ is indicated by solid and open bars, respectively. Mucosally administered renoguanylin (RGN) treatment is indicated by hashed bars.

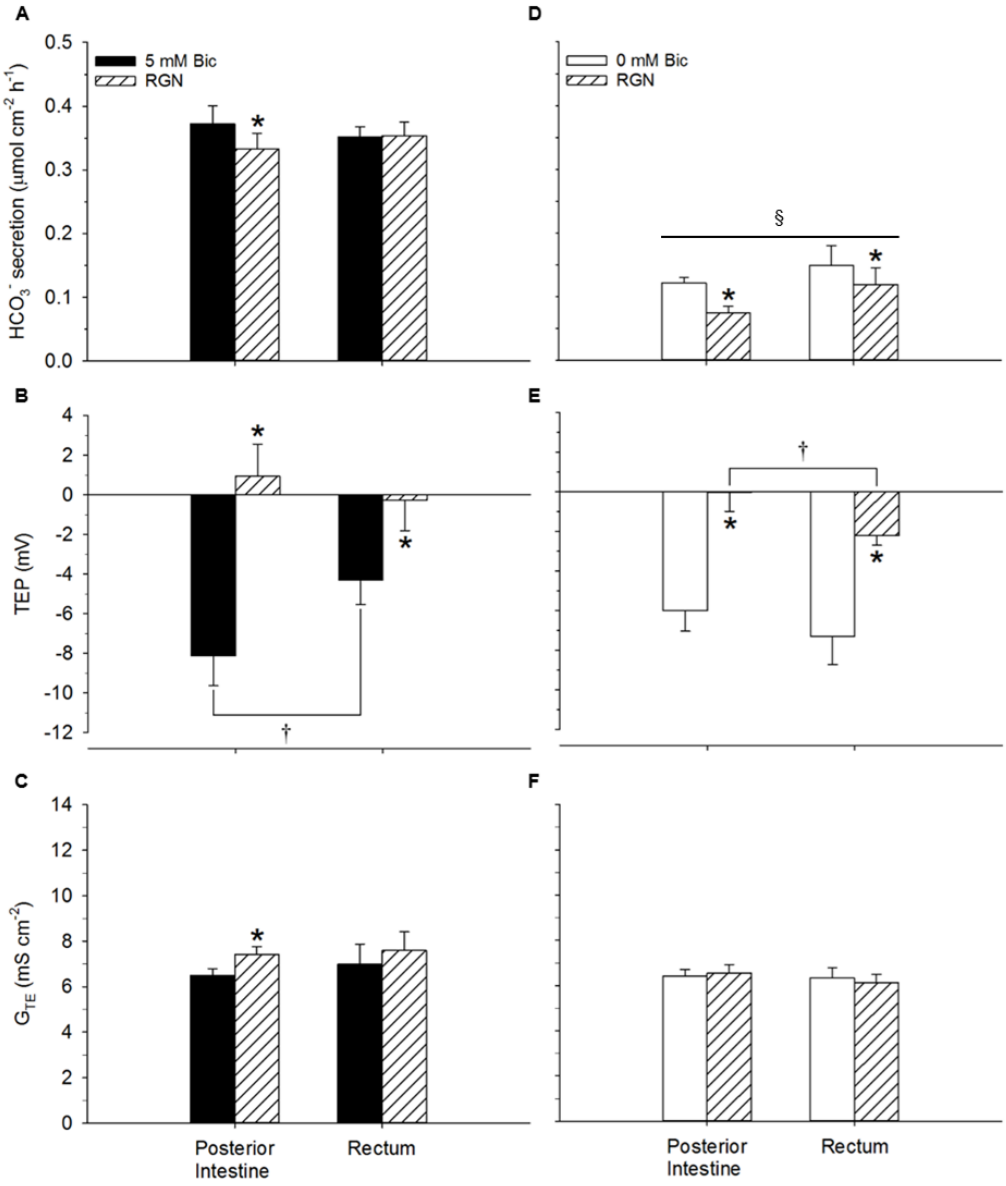

*Effects of renoguanylin and bumetanide on short-circuit current and transepithelial conductance*

On average, RGN reversed the absorptive $I_{SC}$ (from mucosa-to-serosa to serosa-to-mucosa) and significantly increased the $G_{TE}$ of both the posterior intestine and rectum of the Gulf toadfish (Fig. 4.6A, B); these results are in line with previous reports (Ruhr *et al.*, 2014; Ruhr *et al.*, 2015). Bumetanide had similar effects as RGN; in both tissues, it significantly increased $G_{TE}$, and reduced the magnitude of the absorptive $I_{SC}$ of the posterior intestine and, on average, reversed it in the rectum (Fig. 4.6C, D).

*Effects of bumetanide and renoguanylin on bicarbonate secretion, transepithelial potential, and conductance.*

In the posterior intestine, $HCO_3^-$ secretion was significantly decreased in the presence of combined bumetanide and RGN treatment, but not with bumetanide alone (Fig. 4.7A). Bumetanide reversed the TEP (on average), and this effect was not enhanced by RGN (Fig. 4.7B). $G_{TE}$ significantly increased in the presence of combined bumetanide and RGN treatment, but not with bumetanide alone (Fig. 4.7C). In the rectum, only the TEP was affected by bumetanide, with a significant decrease, and this effect was not enhanced by RGN (Fig. 4.7B).

Fig. 4.6. Short-circuit current ($I_{SC}$) (A, C) and transepithelial potential (TEP) (B, D) displayed by the posterior intestine and rectum of Gulf toadfish before and after treatment with renoguanylin (RGN) or bumetanide (Bum). Pre-treatment values were taken from the final 30 min of the control flux and post-treatment values were taken from the final 30 min of a 70-min treatment flux. Values are means ± SEM (n = 6 and 6-7, RGN and Bum experiments, respectively). Significant differences: control v. treatment revealed by paired t-tests (*$P \leq 0.05$) and posterior intestine v. rectum revealed by Student's t-tests (†$P \leq 0.05$). Control and treatment values are indicated by filled and open bars, respectively. Positive and negative $I_{SC}$ values indicate secretory and absorptive currents, respectively.

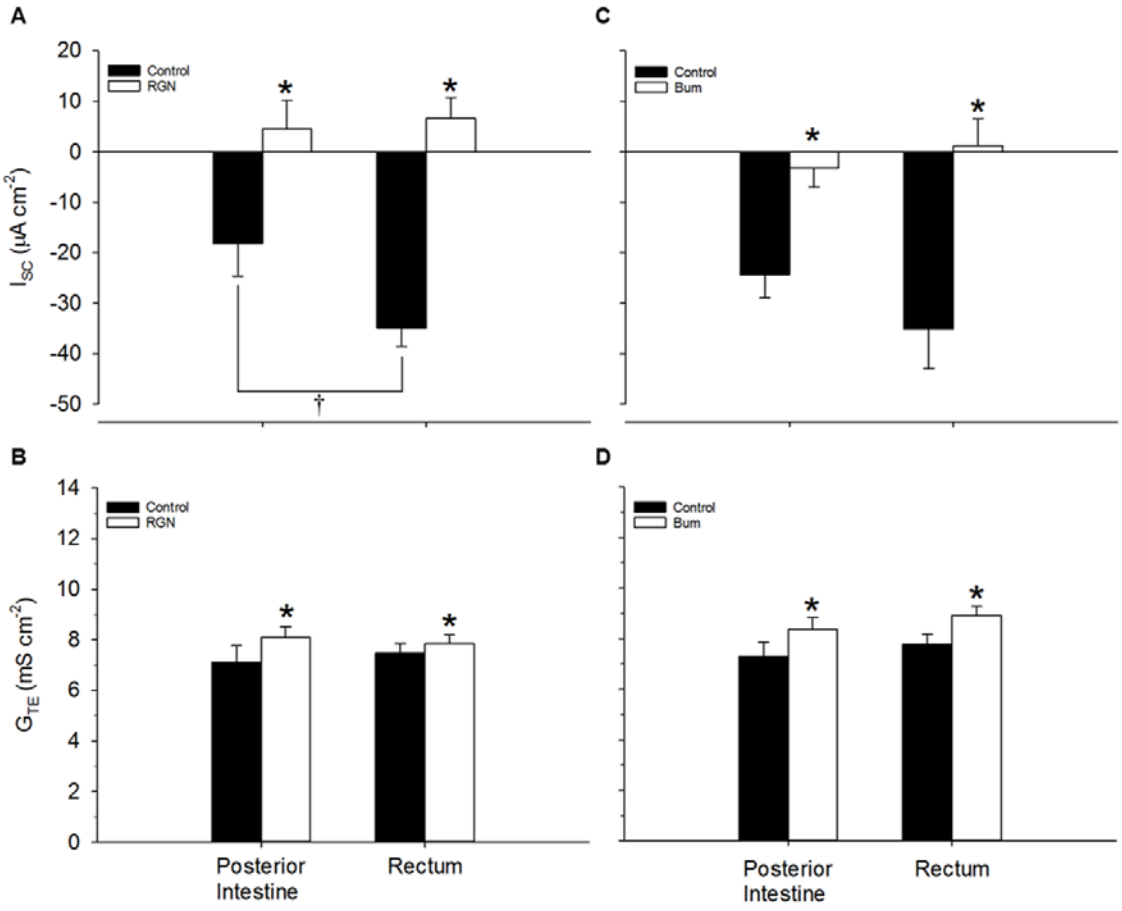


Fig. 4.7. $HCO_3^-$ secretion (A), transepithelial potential (TEP) (B), and transepithelial conductance ($G_{TE}$) (C) displayed by the posterior intestine and rectum of Gulf toadfish. Control values (solid bars) were taken from the final 30 min of the control flux, bumetanide (Bum) (open bars) was then added and its effects were measured from the final 30 min of a 70-min treatment flux, and, finally, renoguanylin (RGN) (shaded bars) was added in combination with Bum and its effects were measured from the final 30 min of a 70-min treatment flux ($t_{total}$ = 170 min). Values are means ± SEM. Significant

differences were revealed by one-way, repeated measures ANOVAs, followed by Holm-Sidak tests ($^{a, b}P \leq 0.05$). Positive and negative TEP values indicate net anion secretion and absorption, respectively.

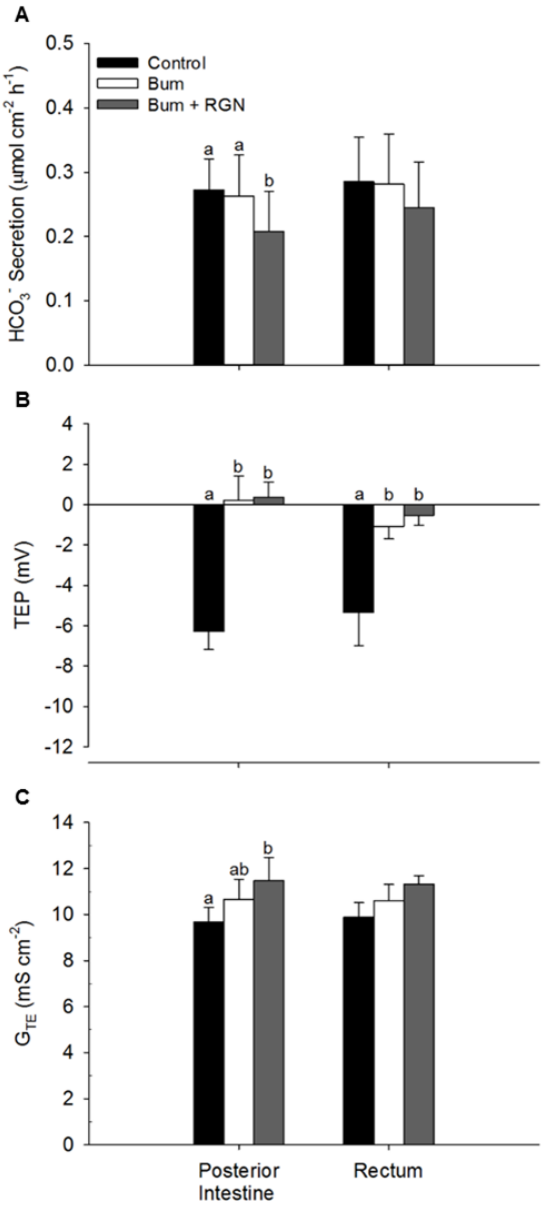


*Effects of ethoxzolamide on bicarbonate secretion in the posterior intestine and rectum, when bicarbonate/$CO_2$ is absent from the serosal saline.*

Under bicarbonate-free conditions, ethoxzolamide decreased bicarbonate secretion in both the posterior intestine and rectum (Fig. 4.8A, D). As expected, RGN

decreased bicarbonate secretion in both the posterior intestine and rectum, and further by the administration of ethoxzolamide into the mucosal saline (Fig. 4.8B, E). The effects of RGN and ethoxzolamide were equal when applied individually and additive when applied together (Fig. 4.8C, F).

*Effects of renoguanylin on water, $Cl^-$, and $Na^+$ fluxes in posterior intestinal and rectal sac preparations of Gulf toadfish exposed to 35 and 60 ppt.*

In the posterior intestine, RGN treatment led to net water secretion of fish exposed to 35 ppt, and decreased water absorption in fish exposed to 60 ppt (Fig. 4.9A). RGN caused net $Na^+$ secretion in posterior sac preparations of fish exposed to both 35 and 60 ppt (Fig. 4.9B), and led to net $Cl^-$ secretion in posterior sac preparations of fish exposed to 35 ppt, but not from the 60 ppt group (Fig. 4.9C). In the rectum, RGN led to net water secretion in rectal sac preparations of fish exposed to 35 ppt, and decreased water absorption in fish exposed to 60 ppt (Fig. 4.9A). Moreover, the response to RGN of the rectum was greater than in the posterior intestine of fish exposed to 60 ppt (Fig. 4.9A). RGN led to net $Na^+$ and $Cl^-$ secretion in the rectal sac preparations of fish exposed to both 35 and 60 ppt (Fig. 4.9B, C).

Fig. 4.8. Absolute (A, B, D, E) and relative (C, F) $HCO_3^-$ secretion rates displayed by the posterior intestine and rectum of Gulf toadfish when exposed in the absence (0 mmol $l^{-1}$) of serosal $HCO_3^-$ (Bic). A, D: Ethoxzolamide (Ethox) was added alone to the mucosal saline (n = 7 and 8, posterior intestine and rectum, respectively; $t_{total}$ = 100 min). Values are means ± SEM. Significant differences were revealed by paired t-tests (*P ≤ 0.05). B, E: renoguanylin (RGN) was initially added to the mucosal saline, after which Ethox was also added to the mucosal saline (n = 6 and 7, posterior intestine and rectum, respectively; $t_{total}$ = 170 min). Significant differences were revealed by one-way, repeated measures ANOVAs, followed by Holm-Sidak tests ($^{a, b, c}$P ≤ 0.05). C, F: The combined effects of RGN and Ethox were compared to their individual treatments. Significant differences: RGN v. RGN + Ethox revealed by paired t-tests and Ethox v. RGN + Ethox revealed by Student's t-tests (*P ≤ 0.05). Control values were taken from the final 30 min of the control flux. Treatment values were taken from the final 30 min of a 70-min treatment flux.

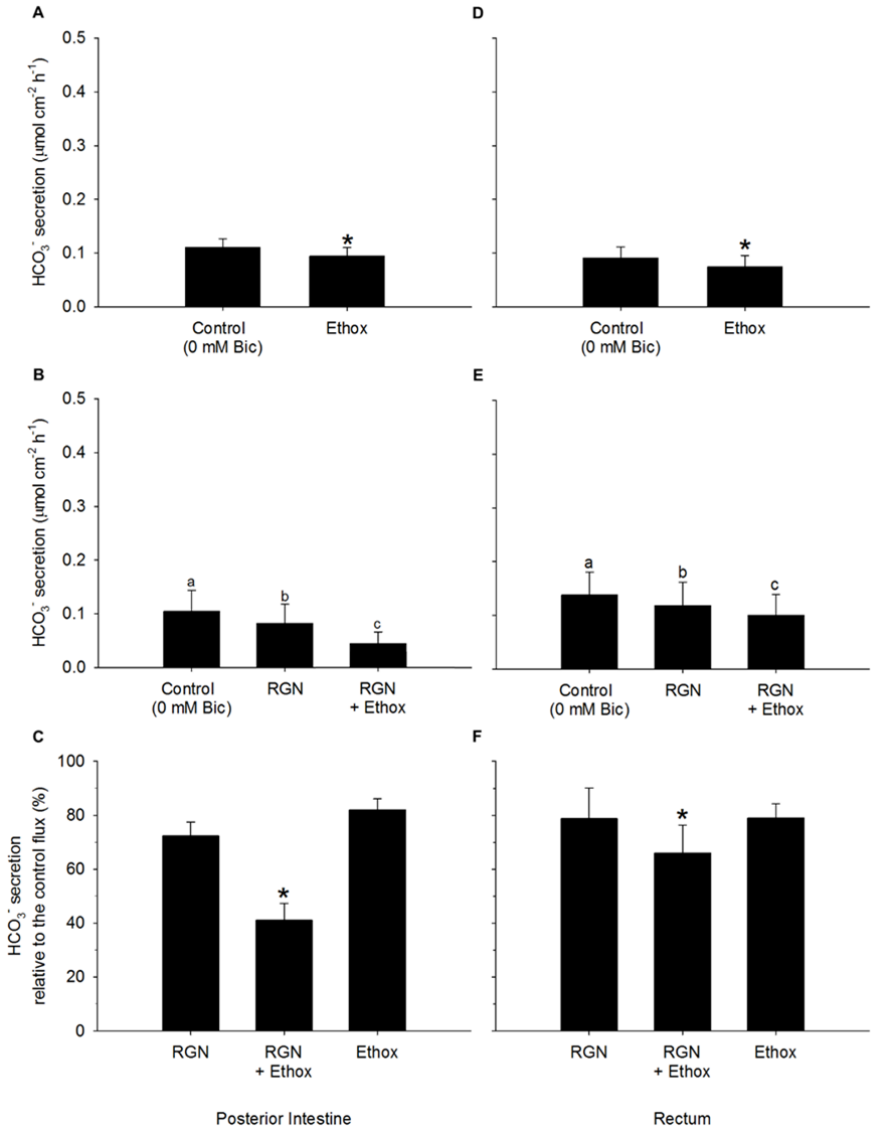

Fig. 4.9. Water (A), $Na^+$ (B), and $Cl^-$ (C) fluxes displayed by the posterior intestine (PI) and rectum (Rec) of Gulf toadfish acclimated to 35 or 60 ppt and treated with renoguanylin (RGN). Values are means ± SEM. Three-way ANOVAs, followed by one-tailed Holm-Sidak tests revealed significant differences in $Na^+$, $Cl^-$, and water fluxes ($p \leq 0.05$; $n_{total} = 55$). Symbols: control v. RGN (*), PI: 35 v. 60 ppt (†), and 35 or 60 ppt: PI v. Rec (§). Positive and negative values indication net absorption or net secretion, respectively.

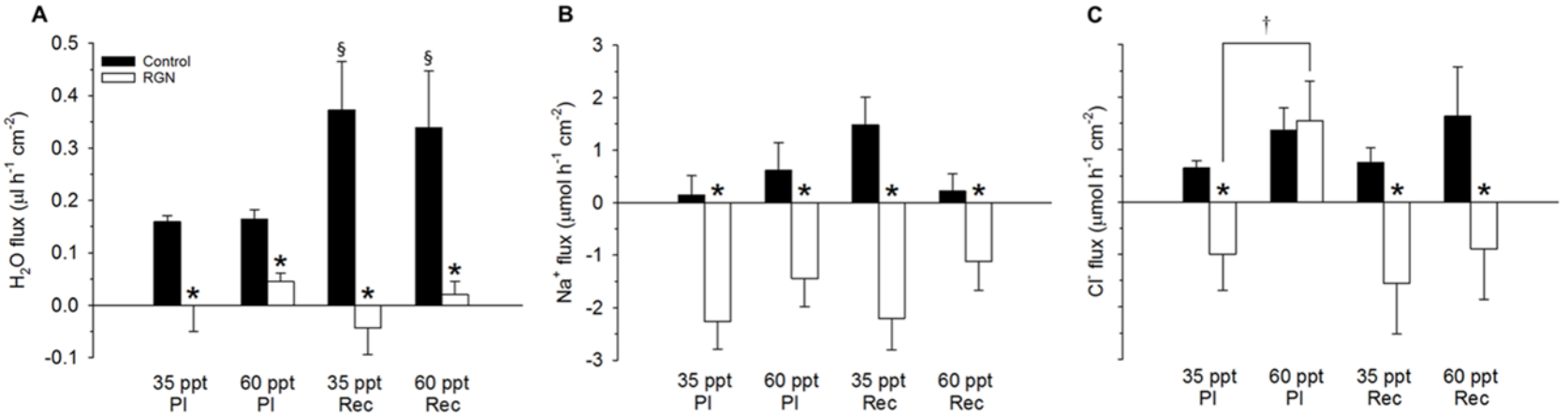

Fig. 4.10. Simplified proposed effects of the guanylin peptides in the posterior intestinal and rectal epithelia of Gulf toadfish (*Opsanus beta*) acclimated to 35 ppt seawater. Guanylin (GN), uroguanylin (UGN), and renoguanylin (RGN) bind to a guanylyl cyclase-C (GC-C) receptor (which have intrinsic GC activity) on the apical membrane of an enterocyte (A). The stimulation of GC-C leads to enhanced formation of cGMP, whose downstream effects increase the phosphorylation of PKA and PKG, both of which can activate CFTR and, perhaps, NKCC1 (B). The downstream effects of cGMP also lead to inhibited ion transport activity by NKCC2 and decreased anion exchange activity by SLC26a6 (C). The combined effects of GC-C stimulation results in the reversal of ion flux, from net ion absorption (mucosa-to-serosa) to net ion secretion (serosa-to-mucosa), which results in either inhibition of water absorption or net water secretion. Abbreviations/symbols: NKA: $Na^+/K^+$-ATPase (maintains electrochemical gradients that enables ion transport), TJ: tight junction, stimulatory (+) and inhibitory (-) effects. Cell diagram modified from: (Ruhr *et al.*, 2015).

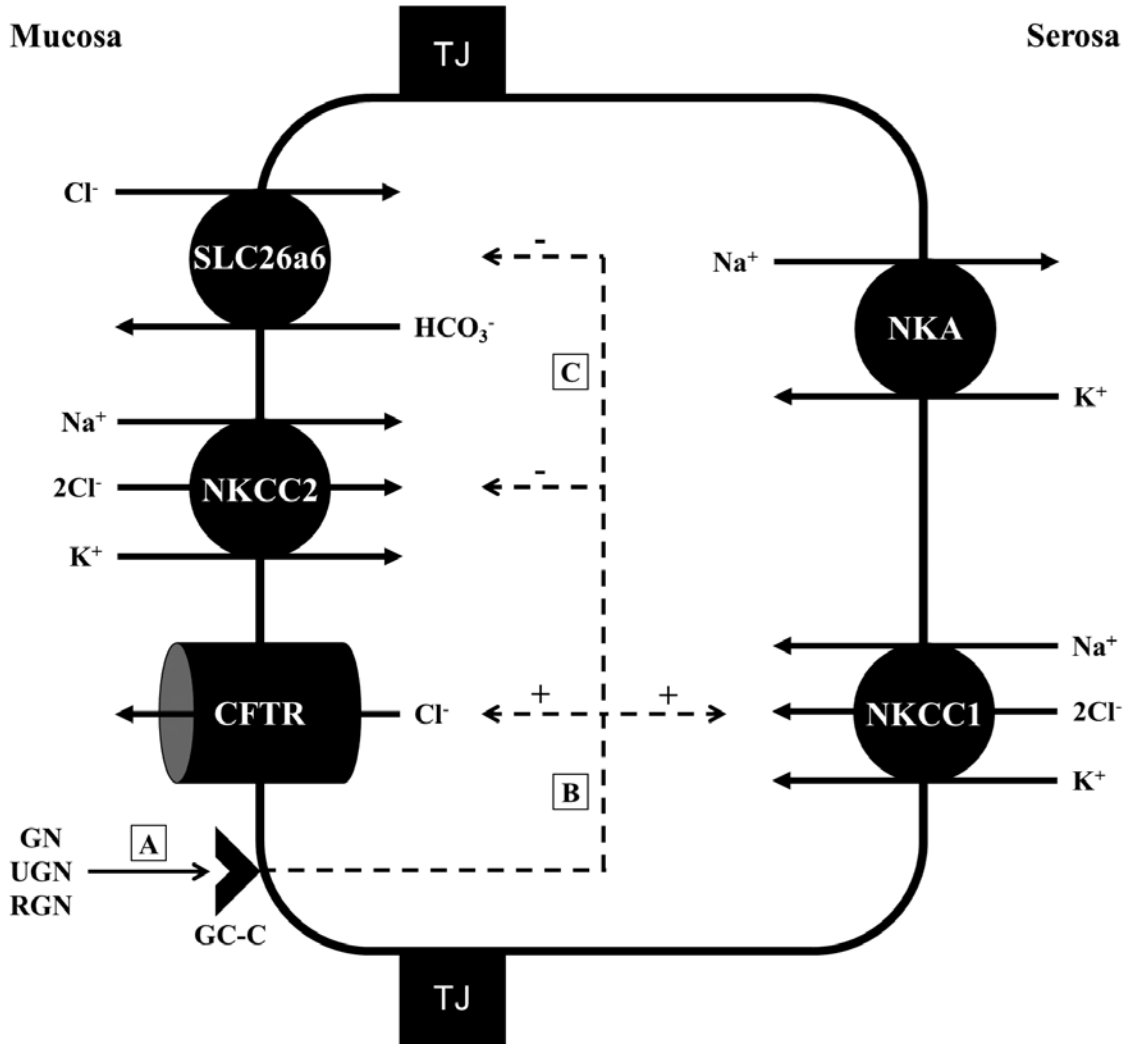

## Conclusions

The present study reveals that the absorptive $I_{SC}$ of the rectum is greater than that of the posterior intestine, yet, the TEP of the posterior intestine is more negative than that of the rectum. Furthermore, it is demonstrated that RGN affects the rectum similarly to the posterior intestine. However, in the rectum, RGN inhibits water absorption more greatly than in the posterior intestine and, in contrast to the posterior intestine, does not reduce $HCO_3^-$ secretion when bicarbonate is present in the serosal saline. The present study also shows that the downstream effects of RGN likely act on SLC26a6 and lead to the observed reduction of the $HCO_3^-$ secretion from endogenous $CO_2$, in addition to stimulating the $Cl^-$-secretory pathway, apical CFTR and basolateral NKCC1 (Fig. 4.10).

*Comparative physiology of the posterior intestine and rectum*

The present study reinforces the current knowledge on the tissue distribution patterns of NKCC1, NKCC2, and CFTR gene expression in marine teleosts. The high relative mRNA expression of CFTR and NKCC1 in gill tissues is not surprising. In the seawater teleost gill, CFTR and NKCC1 are located on the apical and basolateral membranes, respectively, and constitute a $Cl^-$-secretory pathway that excretes excess $Cl^-$ for the purposes of maintaining homeostasis of plasma osmolality [for review (Marshall and Grosell, 2006)]. Conversely, NKCC1 transcripts were not detected in the esophagus of the Gulf toadfish, a result that is unsurprising given the importance of esophageal desalination, rather than salt secretion, for the purposes of decreasing the osmolality of imbibed seawater (from ~1000 to ~500 mosm/kg $H_2O$) [for review (Grosell, 2010)]. It is interesting to note relatively high CFTR gene expression in the esophagus, which could

be expressed in the apical membrane as an absorptive isoform or on the basolateral membrane as a secretory transporter. In any case, the Gulf toadfish likely takes advantage of the large inward electrochemical gradient for $Cl^-$ that permits for its passive absorption from the esophageal lumen and into the interstitial fluid. The high mRNA expression of CFTR and NKCC1 in the stomach is also unsurprising given the role of HCl plays as a component of gastric juices used to break down food. All of the intestinal segments and the rectum displayed relatively lower CFTR and NKCC1 gene expression, although they appear to be expressed at the protein level, as evidenced by their immunofluorescent-like reactivity [CFTR in the posterior intestine and NKCC1 in the anterior and posterior intestine (Ruhr *et al.*, 2014)]. The anterior intestine is the site of the greatest ion absorption in the marine teleost intestine, while the mid and posterior intestine are the sites of high water absorption (Grosell, 2010; Marshall and Grosell, 2006). Accordingly, it is not surprising that the entire intestine displays rather low relative mRNA expression of CFTR and NKCC1, since its primary osmoregulatory role is ion and fluid absorption for the purposes of maintaining whole-body hydration. Indeed, the marine teleost intestine expresses absorptive-type ion transporters important for fluid absorption (Grosell, 2010), including NKCC2 shown in the present and previous studies (Frizzell *et al.*, 1979; Halm *et al.*, 1985; Hiroi *et al.*, 2008; Musch *et al.*, 1982). Moreover, in the Gulf toadfish rectum, absorptive-type ion transporters and proteins necessary for ion absorption, including NKCC2, as well as CFTR and NKCC1, are also expressed at the mRNA level. These consist of SLC26a6 (Grosell *et al.*, 2009b), VHA (Guffey *et al.*, 2011), NBCe1 (Taylor *et al.*, 2010), and $CA_C$ (Sattin *et al.*, 2010). Consequently, the Gulf

toadfish rectum has absorbing and secretory ion transporters that enable it to absorb and secrete water, respectively, much like in the posterior intestine.

Indeed, the present study shows that the posterior intestine and rectum of Gulf toadfish acclimated to 35 ppt absorbed $Na^+$ and $Cl^-$ at roughly the same rates. Interestingly, the rectum displayed a greater absorptive $I_{SC}$ (under symmetrical conditions) and absorbed more water (under asymmetrical, *in vivo*-like conditions) than the posterior intestine, while the magnitude of the TEP of the posterior intestine was roughly twice of the rectum. These data suggest that the posterior intestine relies more on $nHCO_3^-/Cl^-$ exchange by SLC26a6 and the rectum on $Na^+/K^+/2Cl^-$-cotransport by NKCC2. This is due to the electrogenic nature of SLC26a6 (Grosell *et al.*, 2009b), which exchanges multiple bicarbonate anions for a single $Cl^-$, as opposed to the electroneutral transport of NKCC2. The differences in the electrophysiological and osmoregulatory properties between the posterior intestine and rectum are likely not due to transcriptional differences of proteins involved in ion absorption [i.e. SLC26a6, VHA, NBCe1, $CA_C$, and NKCC2 (present study)], which are expressed equally (Grosell *et al.*, 2009b; Guffey *et al.*, 2011; Sattin *et al.*, 2010; Taylor *et al.*, 2010).

An objective of the present study was to determine if the rectum would respond to RGN stimulation. The present study confirms the presence of the components of the $Cl^-$-secretory pathway, CFTR and NKCC1 by qPCR, which seem necessary for responding to RGN, at least for the parameters measured in previous studies (Ando and Takei, 2015; Ando *et al.*, 2014; Ruhr *et al.*, 2014; Ruhr *et al.*, 2015). In prior studies on the Gulf toadfish and Japanese eel, inhibited water absorption and, in some instances, water secretion has been observed in the mid and posterior intestine, but not in the anterior

intestine, after the mucosal administration of guanylin, uroguanylin, or RGN (Ando and Takei, 2015; Ando *et al.*, 2014; Yuge and Takei, 2007). It should first be noted that the rectum seems to be more sensitive to RGN than the posterior intestine, with the $EC_{50}$ of the rectum ($6.12 \times 10^{-9}$ mol $l^{-1}$ RGN) being significantly lower than that of the posterior intestine [$11.6 \times 10^{-9}$ mol $l^{-1}$ RGN (Ruhr *et al.*, 2014)]. Moreover, RGN causes a significant decrease and a reversal of the absorptive $I_{SC}$ in the rectum at $10^{-8}$ and $2.5 \times 10^{-8}$ mol $l^{-1}$ (present study), respectively, and at $2.5 \times 10^{-8}$ mol $l^{-1}$ (for both measurements) in the posterior intestine (Ruhr *et al.*, 2014). These differences might be related to a combination of the greater tissue density of the rectum (which could express greater GC-C on the apical membrane) and a greater affinity for RGN by rectal GC-C than in the posterior intestine.

The present study shows that the posterior intestine and rectum of Gulf toadfish acclimated to 35 ppt respond to RGN by inhibiting water absorption, and displaying net secretion of $Cl^-$ and $Na^+$. However, their electrophysiological responses to RGN are distinct: RGN decreases the absorptive $I_{SC}$ of the rectum more greatly than that of the posterior intestine; conversely, RGN decreases the TEP of the posterior intestine more greatly than that of the rectum. These differences might be due to the proposed reliance on SLC26a6 by the posterior intestine and NKCC2 by the rectum for ion absorption (see above). The larger decrease in the TEP of the posterior intestine is likely the result of SLC26a6 being inhibited more greatly than in the rectum, in contrast to the more tissue-dense rectum, where the effects of RGN might be more pronounced on the overall ion-absorptive capacity of the tissue. In both tissues, however, $G_{TE}$ was significantly increased, despite inhibition of ion absorption. It has been suggested that anion secretion

by the opening of CFTR (Ruhr *et al.*, 2014; Ruhr *et al.*, 2015) and, possibly, increased paracellular cation secretion (Ando and Takei, 2015) might be responsible for the increases in conductance when intestinal tissues are treated with the guanylin peptides. Inhibition of water absorption partially occurs as a result of $Cl^-$ secretion, likely by CFTR activation, which is fueled, in part, by NKCC1 that takes up $Cl^-$ from the blood (Ando and Takei, 2015; Ando *et al.*, 2014; Ruhr *et al.*, 2014; Ruhr *et al.*, 2015; Yuge and Takei, 2007) and is necessary to inhibit water absorption. Although counterintuitive, decreased water absorption is a strategy that would benefit the removal of $CaCO_3$ precipitates that naturally form along the intestine (as part of the normal osmoregulatory processes). It has been demonstrated that the retention of water in the guinea pig ileum can make digested food more aqueous and allow it to be moved out of the intestinal tract more easily by muscle contractions (Schulze, 2015). A similar mechanism would allow the removal of $CaCO_3$ precipitates from the intestine and reduce the occurrence of intestinal blockages. Consequently, the trade-off between decreasing water absorption in the posterior intestine, and the risk of dehydration associated with this behaviour, is made by decreasing the risk of harmful obstructions in the narrow intestinal passage. Nevertheless, the osmoregulatory mechanisms necessary for water absorption are maintained in the anterior intestine of the seawater teleost, as it does not seem to be affected by the guanylin peptides (Ruhr *et al.*, 2014; Yuge and Takei, 2007).

*The effects of renoguanylin on NKCC2 and SLC26a6 transport activity*

Another objective of the present study was to determine if the downstream effects of RGN affected the transport activity of NKCC2 and SLC26a6. To test the effects of

RGN on NKCC2, bumetanide (a specific blocker of NKCC isoforms) was used to determine if its effects on electrophysiological characteristics were similar to that of RGN. Indeed, the reductions to the absorptive $I_{SC}$ and TEP of the posterior intestine and rectum by bumetanide were similar to those of RGN. Of particular interest, however, is the failure of bumetanide to increase tissue conductance in the posterior intestine and rectum under *in vivo*-like conditions (asymmetrical saline exposures), as opposed to RGN. This suggests that RGN does not inhibit NKCC2 as greatly as bumetanide, and the reductions to the absorptive $I_{SC}$ and TEP, as well as the increases in $G_{TE}$, are the sum effects of NKCC2 inhibition, apical CFTR activation, and possible paracellular $Na^+$ secretion, that leads to net $Na^+$ and $Cl^-$ secretion observed in tissues of fish acclimated to 35 ppt. Evidence from the Japanese eel supports this suggestion, because the magnitude of the decreases to the absorptive $I_{SC}$ and TEP of the mid and posterior intestine were similar for both guanylin and bumetanide (Ando *et al.*, 2014).

Bumetanide also had no effect on $HCO_3^-$ secretion in the posterior intestine and rectum of fish acclimated to 35 ppt (under *in vivo*-like, asymmetrical conditions). Upon the administration of RGN, however, the posterior intestine displayed reduced $HCO_3^-$ secretion and increased $G_{TE}$, without further reductions to the TEP. This suggests that, at least in the Gulf toadfish intestine, $Cl^-$ does not recirculate across the apical membrane through NKCC2 and SLC26a6 for the purposes of preserving ion and fluid absorption, which is hypothesized to occur in the Japanese eel (Ando *et al.*, 2014; Yuge and Takei, 2007). Interestingly, the present study shows that RGN does not reduce $HCO_3^-$ secretion in the Gulf toadfish rectum as it does in the posterior intestine (when $HCO_3^-$ is present in the serosal saline). A previous study demonstrated that the downstream effects of RGN

inhibited the exchange activity of SLC26a6, when $CO_2$ was the only source of $HCO_3^-$ (via $CO_2$ hydration and $CA_C$) with which to fuel SLC26a6 (Ruhr *et al.*, 2015). By removing bicarbonate from the serosal saline, the basolateral $HCO_3^-$ transporter, NBCe1, was rendered functionless and, as before, $CO_2$ was the sole source of $HCO_3^-$ fuelling SLC26a6. Under these conditions, RGN reduced $HCO_3^-$ secretion in both the posterior intestine and rectum. These observations support the previous study's conclusions (Ruhr *et al.*, 2015) that the transport activity of SLC26a6 is being directly affected by the downstream effects of RGN.

We also tested a possible mechanism in mammals that is proposed to decrease $HCO_3^-$ secretion, via SLC26a6, when PKC phosphorylates SLC26a6 at a site that decreases its ability to bind $CA_C$, and, thereby, disrupts the SLC26a6-$CA_C$ metabolon (Alvarez *et al.*, 2005). It is possible that the effects of RGN could lead to PKG or PKA [which are both phosphorylated downstream of GC-C activation (Arshad and Visweswariah, 2013)] binding to Gulf toadfish intestinal SLC26a6 at a location on or near the $CA_C$ binding site and limit the exchange capacity of SLC26a6 as well. To test this in the Gulf toadfish intestine, the $CA_C$-specific inhibitor, ethoxzolamide [tested in Gulf toadfish previously (Grosell and Genz, 2006)], was used along with RGN in tissues bathed with a serosal saline absent of $HCO_3^-$, to determine their individual and combined effects on $HCO_3^-$ secretion. With this approach, as with the previous experiment (see above), $CO_2$ was the only source of $HCO_3^-$ to fuel SLC26a6. The results of the present study reveal that in both the posterior intestine and rectum, the individual doses of RGN and ethoxzolamide significantly decreased $HCO_3^-$ secretion equally, and the combined doses were additive and different than the individual doses. Consequently, these data do

not suggest that the downstream effects of RGN stimulation affects SLC26a6 by interfering with the binding of $CA_C$ and disrupting the SLC26a6-$CA_C$ metabolon. Instead, the data support the idea that the downstream effects of RGN have a direct effect on the transport capacity of SLC26a6 for $HCO_3^-$ that leads to decreased exchange activity in the posterior intestine (in both the presence and absence of serosal $HCO_3^-$) and in the rectum (in the absence of $HCO_3^-$). Moreover, three previous studies (including one on the Gulf toadfish) also demonstrate that CFTR does not seem to transport $HCO_3^-$ (Ko *et al.*, 2002; Ruhr *et al.*, 2014; Wang *et al.*, 2006), and that Gulf toadfish SLC26a6 transport activity is limited by $HCO_3^-$ and not $Cl^-$ (Ruhr *et al.*, 2014). With respect to the guanylin peptide system in the Gulf toadfish intestine observed in the present and previous studies (Ruhr *et al.*, 2014; Ruhr *et al.*, 2015), it is possible that inhibition of SLC26a6 (and $HCO_3^-$ secretion) and activation of CFTR due to RGN stimulation leads to a maximal $Cl^-$ current that manifests itself, physiologically, as a reversal of the absorptive $I_{SC}$.

*Increased response to renoguanylin in hypersalinity*

The present study reveals changes in gene expression for NKCC1 and CFTR in the rectum after Gulf toadfish are transferred from 35 to 60 ppt and these results are comparable to what is seen in the posterior intestine (Ruhr *et al.*, 2015). The data from both tissues show that gene expression of NKCC1 and CFTR is upregulated in 60 ppt, but differ concerning the expression of GC-C, which is upregulated in the posterior intestine (Ruhr *et al.*, 2014), but not in the rectum. The previous study suggested that the response to RGN in the posterior intestine of Gulf toadfish acclimated to 60 ppt was limited by the level of GC-C, NKCC1, and/or CFTR gene expression. At least in the rectum of the Gulf

toadfish, the response to RGN is likely limited to NKCC1 and/or CFTR. Despite acclimation to 60 ppt, the current and previous studies (Ruhr *et al.*, 2015) demonstrate that water absorption by the posterior intestine and rectum of Gulf toadfish does not increase as expected, as opposed to the sea bream intestine when acclimated to 55 ppt (Gregorio *et al.*, 2013). Moreover, both the posterior intestine and rectum of fish exposed to 35 and 60 ppt displayed decreased water absorption in response to RGN that correlates with net $Na^+$ and $Cl^-$ secretory fluxes (a switch from mucosa-to-serosa to serosa-to-mucosa), with the exception of the posterior intestine from the 60 ppt. When considering our hypothesis, that the guanylin peptide-induced inhibition of water absorption is necessary to facilitate the removal of solids (such as $CaCO_3$ precipitates from the intestine), the occurrence of water absorption being inhibited more greatly in 60 ppt (in response to RGN) would be more important. In 50 ppt, intestinal $CaCO_3$ precipitation in Gulf toadfish increases 2.3-fold (Genz *et al.*, 2008). Thus, by upregulating gene expression of the components of the $Cl^-$-secretory pathway (apical CFTR and basolateral NKCC1), and inhibiting NKCC2 transport activity by RGN (which seems to occur at 35 ppt as well), more fluid can remain in the intestine to facilitate the removal of increased $CaCO_3$ precipitates formed as a result of hypersalinity.

A notable difference in $Cl^-$ flux between the posterior intestine and rectum of Gulf toadfish exists, as mentioned above, in response to RGN. In the present and previous study, net $Cl^-$ secretion does not occur in the posterior intestine of fish acclimated to 60 ppt when treated with RGN and this is observed in parallel with increased $HCO_3^-$ secretion (Ruhr *et al.*, 2015). It has been suggested that this occurs to maintain the drinking rate of the fish (Ando and Nagashima, 1996). In hypersalinity, there is even

greater branchial fluid loss relative to normal seawater. Consequently, in order to stave off dehydration, a seawater teleost must increase its rate of drinking concurrently with the increases in branchial water loss. In 35 ppt, decreases in $HCO_3^-$ secretion by the posterior intestine is beneficial to promote net $Cl^-$ secretion and inhibit both water absorption and $CaCO_3$ precipitation (Ruhr *et al.*, 2014; Ruhr *et al.*, 2015). Conversely, in 60 ppt, stimulating net $Cl^-$ secretion and limiting the posterior intestine's ability to absorb water and secrete $HCO_3^-$ could be detrimental. The consequence of limiting $HCO_3^-$ secretion in 60 ppt is the reduction of $CaCO_3$ precipitation that is essential for the absorption of water in marine teleosts. Likewise, increases in luminal $Cl^-$ concentration in fish decreases their drinking rate in parallel (Ando and Nagashima, 1996). Accordingly, the RGN response with respect to $HCO_3^-$ secretion (Ruhr *et al.*, 2015) and $Cl^-$ in the posterior intestine of Gulf toadfish acclimated to 60 ppt is a possible adaptation for maintaining a high rate of drinking to compensate for increases in branchial fluid loss. In this fascinating process, $Cl^-$ secretion likely still occurs in response to RGN (as evidenced by inhibited water absorption), but is completely reabsorbed by SLC26a6 in exchange for $HCO_3^-$. Yet, these mechanisms are not observed in the rectum of fish acclimated to 60 ppt, with $Cl^-$ secretion occurring equally to what is seen in both the posterior intestine and rectum of fish acclimated to 35 ppt. The adaptive benefit of this response might be to ensure that enough water is present in the rectum (via inhibited water absorption/stimulation of water secretion) in order to removed $CaCO_3$ precipitates (or other solids) from the intestine.

*Significance and perspectives*

The posterior intestine and rectum of Gulf toadfish display comparable osmoregulatory physiologies with respect to $Na^+$, and $Cl^-$ fluxes, yet, they possess key distinct mechanisms by which they regulate ion and fluid movement. The posterior intestine appears to rely more on electrogenic anion exchange by SLC26a6 than the rectum (as evidence by the larger magnitude of its TEP), while the rectum appears to rely more on ion cotransport by NKCC2 than the posterior intestine (as evidenced by the large magnitude of its absorptive $I_{SC}$ and the greater absolute change in $I_{SC}$ when bumetanide is applied). In addition, the rectum absorbs more water than the posterior intestine, and this observation correlates with the greater absorptive $I_{SC}$ and tissue density of the intestine. The rectum responds more strongly to RGN than the posterior intestine in reversing the absorptive $I_{SC}$ and inhibiting water absorption. In support of the hypothesis that the tissue response of the intestine to the guanylin peptides is necessary to facilitate the removal of solids from the intestine, limiting water absorption would permit more water to remain in the rectum with which solids could be move along out of the intestinal tract (at least in response to RGN from the Japanese eel).

The downstream effects of cGMP formation, due to RGN binding to GC-C, might act to inhibit both NKCC2 and SLC26a6, in addition to stimulating the opening of apical CFTR. If these intracellular effects do occur, it elevates the guanylin peptides as potent modulators of intestinal physiology due to their modification of the osmoregulatory processes. The intracellular mechanisms that regulate these changes should be investigated further and be focussed on the roles that cGMP/PKG and cAMP/PKA might play.

The present study also reveals that uroguanylin gene expression significantly decreases in the rectum of fish exposed to 60 ppt and compares well to what is seen in the posterior intestine in 60 ppt (Ruhr *et al.*, 2015). This suggests that Gulf toadfish guanylin and uroguanylin might have different functions. Indeed, in the rat intestine and in T84 cells expressing rat GC-C, uroguanylin was most effective in a pH of 5.5 and guanylin in a pH of 7.4 and 8.0 (Hamra *et al.*, 1997; Joo *et al.*, 1998). In mammals, guanylin and uroguanylin cause increased $HCO_3^-$ secretion into the intestinal lumen, accordingly, it has been suggested that uroguanylin might play a role in defending the pH of the intestine as acidic chyme enters from the stomach (Forte and Hamra, 1996). Conversely, guanylin transcription and secretion are increased in rat intestinal tissues when perfused with high salt concentrations and decreased with low salt intake (Carrithers *et al.*, 2002; Kita *et al.*, 1999; Li *et al.*, 1996). Conceivably, in marine teleosts, uroguanylin plays a more prominent role in digestion and guanylin takes a more active part in osmoregulatory processes.

It should be emphasized that the guanylin peptide system in Gulf toadfish has, so far, been studied on fasted fish. The potential interactions between osmoregulation and digestion in the context of guanylin peptide function is an interesting avenue for further study.

*Acknowledgements*

We thank Dr. M. Danielle McDonald from the Rosenstiel School of Marine and Atmospheric Science at the University of Miami for the generous use of her equipment. We also thank Drs. Patrick J. Walsh, Nicolas Corradi, and Christophe M. R. LeMoine

from the University of Ottawa for providing us with the annotated intestinal transcriptome of the Gulf toadfish. Grants: M. Grosell is Maytag Professor of Ichthyology and is supported by NSF (IOS 1146695).

# Chapter 5

## Discussion

In its entirety, this dissertation contributes new, revelatory findings to the field of fish physiology by elucidating the poorly studied area of secretion in the seawater teleost intestine. An interdisciplinary approach was implemented to describe the response of the intestine to guanylin peptide stimulation, using isolated tissues and gene expression markers that revealed corresponding cellular and molecular changes. The findings contained within this dissertation have translational relevance for the field of comparative physiology for two important reasons. First, the study of teleost intestinal physiology has dramatically increased over the past 20 years. In expanding this knowledge, this dissertation demonstrates that the seawater teleost intestine is a much more dynamic tissue than was previously thought. This is showcased within the findings of Chapters 2, 3, and 4, which describe newly identified secretory mechanisms and physiological differences along the Gulf toadfish intestine. Second, the study of guanylin peptide function in mammals has also increased substantially. These peptides have been linked to colitis, adipocyte lipolysis, regulation of renal NKA and VHA activity, oncogenesis (when guanylin, uroguanylin, or GC-C are not expressed), and smooth muscle relaxation (Arnaud-Batista *et al.*, 2016; Bosse, 2014; da Silva Lima *et al.*, 2014; Lan *et al.*, 2016; Ochiai *et al.*, 1997; Ohbayashi *et al.*, 1998; Rodriguez *et al.*, 2016; Sousa *et al.*, 2010; Tanday, 2014). Thus, the findings described in this dissertation can be used to elucidate the cellular response of these various mammalian tissue systems to guanylin peptide stimulation.

*Identification of secretory mechanisms in the Gulf toadfish intestine*

Prior to the onset of this dissertation, very few studies had investigated secretory mechanisms in the seawater teleost intestine, and none had demonstrated intestinal fluid secretion by an endogenous hormone. The majority of these studies were conducted in the 1980s and early 1990s and demonstrated that hormones and stimulants (e.g. VIP, ANF, cAMP, cGMP) could alter intestinal tissue conductance and lead to large reversals of the absorptive $I_{SC}$ (Bakker *et al.*, 1993; Bakker and Groot, 1989; O'Grady S, 1989; O'Grady *et al.*, 1988; O'Grady *et al.*, 1985; O'Grady and Wolters, 1990; Rao and Nash, 1988; Rao *et al.*, 1984). However, these studies did not pursue the identity of the ion transporters responsible for these secretory fluxes, which are suggested to cause fluid secretion or greatly inhibit water absorption. In subsequent years, it has been demonstrated that apical CFTR is involved, at least partly, for these types of secretory responses in the seawater teleost intestine (Marshall *et al.*, 2002; Singer *et al.*, 1998). The findings presented in Chapter 2 of this dissertation, using immunofluorescence and electrophysiology, provide further evidence for a secretory response driven by apical CFTR, along with basolateral NKCC1. In addition, the presence of membrane-bound CFTR in the posterior intestine of the Gulf toadfish has been confirmed by Western blot analyses (Fig. 5.1, unpublished data). Together, CFTR and NKCC1 likely serve as a conduit for $Cl^-$ secretion that is stimulated by renoguanylin. In support of the suggested conduit, inhibition of CFTR in the Gulf toadfish and Japanese eel (Ando *et al.*, 2014) negated the tissue response to renoguanylin and guanylin, respectively. These findings

confirm that CFTR is activated by the guanylin peptide secretory response of the teleost intestine, similarly to what is observed in mammals (Chao *et al.*, 1994).

Fig. 5.1. Western blot for CFTR (169 kDa) in isolated plasma membrane fraction of the posterior intestine of the Gulf toadfish. A monoclonal mouse CFTR antibody (R&D Systems) raised against human CFTR was used to identify CFTR.

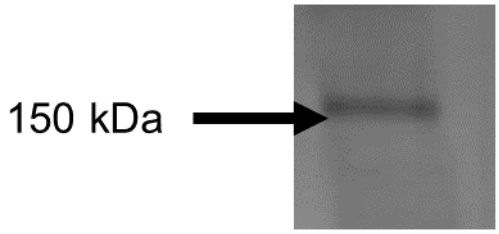


Yet, the notion that a teleost living in seawater would possess cellular mechanisms that enable intestinal fluid secretion is counterintuitive. Seawater teleosts must continually drink water and absorb it by the intestine in order to prevent dehydration, due to their hypertonic environment (Grosell, 2010; Marshall and Grosell, 2006). In the killifish intestine, it was hypothesized that possessing secretory mechanisms could help dilute and remove harmful toxins or parasites from the intestine (Marshall *et al.*, 2002). Although this might hold true for teleosts living in brackish water or polluted environments (e.g. killifish), the vast majority of seawater teleosts, such as the Gulf toadfish, live in relatively cleaner, non-brackish coastal waters, where there are relatively smaller concentrations of toxins or parasites (Rohde, 2002). However, as stated previously throughout this dissertation, it is hypothesized that a secretory response might be useful for removing solids from the intestine, but could also include toxin removal as a secondary function. In general, intestinal secretory mechanisms ensure that enough fluid is present in order to facilitate the movement of solids through the intestinal tract and

increase the efficiency of peristalsis (Schulze, 2015; Weems, 1981). Nevertheless, the purpose of intestinal secretory mechanisms described by this dissertation remain to be validated for seawater teleosts.

Whatever the purpose of inhibited water absorption might be, it is clear that the guanylin peptides have potent control over intestinal physiology in vertebrates (Forte, 1999; Forte, 2003; Forte and Hamra, 1996; Takei and Yuge, 2007). The guanylin peptides are suggested to have a more prominent role in seawater because their gene expression, as well as that of GC-C, are more highly expressed in seawater than in freshwater (Comrie *et al.*, 2001a; Cramb *et al.*, 2005; Yuge *et al.*, 2003). In addition to this, Chapters 3 and 4 describe how GC-C, CFTR, and NKCC1 gene expression in the posterior intestine and rectum of Gulf toadfish are elevated in hypersalinity, a treatment that has been shown to increase carbonate precipitate formation in the Gulf toadfish (Genz *et al.*, 2008). Elevated gene expression of GC-C, CFTR, and NKCC1 would suggest a potentially larger secretory response. Indeed, in parallel to these increases in gene expression, the functional response of the posterior intestine to renoguanylin from fish acclimated to 60 ppt was significantly greater. Specifically, water absorption by the posterior intestine from fish acclimated to 60 ppt, when more carbonate precipitates are formed, display significantly less fluid absorption than tissues from the 35 ppt group. These findings, at the very least, indicate that the guanylin peptide response becomes more important as teleosts encounter increasingly hypertonic environments.

*Regulation of intestinal $HCO_3^-$ transporters by renoguanylin stimulation*

In addition to the stimulatory effects on CFTR in the Gulf toadfish posterior intestine, renoguanylin seems to affect other osmoregulatory proteins. Chapter 2 describes inhibited $HCO_3^-$ secretion by the posterior intestine in response to renoguanylin. In the Gulf toadfish, SLC26a6 is responsible for the majority of $Cl^-$ uptake and $HCO_3^-$ secretion (Grosell *et al.*, 2009b), which is fueled by basolateral $HCO_3^-$ absorption via NBCe1 and by the hydration of intracellular $CO_2$ by $CA_C$ (Gilmour and Perry, 2009; Taylor *et al.*, 2010). These findings led to the speculation that the downstream effects of renoguanylin stimulation act on either one or more of SLC26a6, $CA_C$, or NBCe1. Indeed, the findings described in Chapter 3 provide evidence that either SLC26a6 or $CA_C$ are regulated by renoguanylin, and that NBCe1 is secondarily modified. In the posterior intestine from Gulf toadfish acclimated to 35 ppt, the use of a $HCO_3^-$ /$CO_2$-free serosal saline (which knocks down NBCe1 function) along with the addition of renoguanylin results in decreased $HCO_3^-$ secretion as before, suggesting downstream modification of $CA_C$ and SLC26a6

In contrast, in tissues exposed to $HCO_3^-$/$CO_2$-free conditions and treated with renoguanylin, the subsequent addition of $HCO_3^-$/$CO_2$ to the serosal saline dramatically increases $HCO_3^-$ secretion. These findings suggest that NBCe1 is not modified by the downstream effects of renoguanylin stimulation, because the addition of $HCO_3^-$/$CO_2$ should have no effect on $HCO_3^-$ transport activity. However, the transport activity of NBCe1 does seem to be secondarily upregulated. Chapter 3 reveals that renoguanylin treatment of the posterior intestine from fish acclimated to 60 ppt leads to increased, rather than decreased, $HCO_3^-$ secretion. NBCe1 is an electrogenic transporter that is

driven by a favourable inward electrochemical gradient for $Na^+$ (Taylor *et al.*, 2010). In hypersalinity, seawater teleosts display greater rates of $HCO_3^-$ secretion than they do in normal seawater (Genz *et al.*, 2008; Gregorio *et al.*, 2013; Guffey *et al.*, 2011), due to greater NBCe1 ion transport and hydration of $CO_2$ by $CA_C$. Thus, in tissues from the 60 ppt group, stimulation of $Cl^-$ secretion by renoguanylin, through the $Cl^-$-secretory pathway of CFTR and NKCC1, creates a favourable inward electrochemical gradient for $Na^+$ absorption into the cell. This leads to even greater basolateral $HCO_3^-$ influx (due to NBCe1 co-transport) that is eventually secreted by SLC26a6 at an elevated rate, relative to tissues from fish acclimated to 35 ppt. Thus, the findings in Chapter 3 suggest that $HCO_3^-$ secretion is decreased by renoguanylin (in the 35 ppt group) by modulation of either SLC26a6 or $CA_C$, a suggestion that was further elucidated in Chapter 4.

The findings in Chapter 4 describe how the rectum of the Gulf toadfish does not display decreased $HCO_3^-$ secretion after renoguanylin stimulation under normal conditions, but that $HCO_3^-$ efflux is depressed when rectal tissues are exposed to $HCO_3^-$ /$CO_2$-free serosal saline and treated with renoguanylin. This latter exposure effectively knocks down NBCe1 ion transport, leaving $CA_C$ as the only source of $HCO_3^-$ as substrate for SLC26a6. Chapter 4 describes that the combined effects of renoguanylin and $CA_C$ inhibition by ethoxzolamide are additive in reducing $HCO_3^-$ secretion. These findings suggest that renoguanylin has no effects on $CA_C$ and inhibits SLC26a6 via the downstream effects of cGMP. Consequently, in the Gulf toadfish intestine, the incremental approach described by this dissertation reveals that the cellular effects of renoguanylin downregulate SLC26a6 transport activity, and do not affect NBCe1 or $CA_C$.

*Heterogeneity in Gulf toadfish intestinal physiology*

Differences in anatomy, morphology, and physiology along the length of the vertebrate gastrointestinal tract are common. In mammals, such differentiation is noticeable in development (Menard, 2004) and carries on into adulthood (Bowcutt *et al.*, 2014; Cats *et al.*, 1996). In teleost fish, on the other hand, the anatomical and morphological differences of the intestine exist, but are much more modest (Wilson and Castro, 2010). Nevertheless, studies on the Japanese eel and sea bream intestine and rectum demonstrate differences in physiology, particularly with respect to water, salt, and $HCO_3^-$ fluxes (Gregorio *et al.*, 2013; Kim *et al.*, 2008). At the onset of this dissertation, no physiological heterogeneity studies had been conducted on the Gulf toadfish intestine. The only segment that had been thoroughly studied was the anterior intestine, while the mid and posterior intestine, as well as the rectum, had not been investigated. A review of studies on intestinal osmoregulatory proteins in the anterior and posterior intestine of the Gulf toadfish does not reveal major differences in $CA_C$; NBCe1; NHE1, -2, or -3; SLC26a6; and VHA gene expression, which would suggest that there are no variations in osmoregulatory performance (Esbaugh and Grosell, 2014; Esbaugh *et al.*, 2012; Grosell *et al.*, 2009b; Guffey *et al.*, 2011; Sattin *et al.*, 2010; Taylor *et al.*, 2010). The findings in Chapter 2 describe, for the first time, baseline $I_{SC}$, $G_{TE}$, ion ($Na^+$ and $Cl^-$) and water absorption, and $HCO_3^-$ secretion values in the posterior intestine of the Gulf toadfish. Although these findings do not reveal significant differences in baseline parameters between the anterior and poster intestine, subsequent investigations (personal observations, unpublished data) reveal that the posterior intestine displays ion-absorptive rates that are twice the size of the anterior intestine, while the anterior intestine [where

the majority of water absorption takes place (Marshall and Grosell, 2006)] displays significantly greater tissue conductance than the posterior intestine.

The decision to take a comparative approach to study the intestine of the Gulf toadfish in Chapter 2 was made because the anterior intestine, by itself, would have made a poor candidate for studying the general physiological effects of the guanylin peptides. A previous study on the Japanese eel revealed that the guanylin peptides have no physiological effect on the anterior intestine (Yuge and Takei, 2007), and, comparatively to this study, Chapter 2 also describes the lack of physiological response by the anterior intestine of the Gulf toadfish to the guanylin peptides, in contrast to the large stimulatory effect the peptides have on the posterior intestine. Accordingly, even when ion and water absorption are being inhibited in the posterior intestine by guanylin peptide stimulation, the important function of water absorption is still taking place in the anterior intestine.

However, the events that lead to the guanylin peptides becoming active in the intestine and the length of stimulatory response are still unknown (Forte, 1999). In isolated intestinal tissues from Gulf toadfish, the guanylin peptides can elicit a response that can be maintained for more than 6 hours. Conversely, because these studies are conducted on excised tissues, rather than on intact animals, other biological factors that might regulate the guanylin peptide response are not present. Consequently, it is not known if the water involved in the guanylin peptide secretory response is absorbed after the termination of the stimulatory event or if it is lost to the environment. Thus, Chapter 4 also investigated whether the rectum would respond to renoguanylin treatment by inhibited water absorption.

The findings presented in Chapter 4 reveal that basal water absorption by the rectum of the Gulf toadfish is greater than in the posterior intestine and is driven by greater ion absorption (i.e. a larger absorptive $I_{SC}$). This reveals further physiological heterogeneity in the Gulf toadfish intestine and supports the idea that the rectum is also important for maintaining hydration in seawater teleosts (Carvalho *et al.*, 2012; Gregorio *et al.*, 2013; Kim *et al.*, 2008; Martos-Sitcha *et al.*, 2013). Subsequent treatment with renoguanylin stimulates a greater inhibitory effect on water absorption in the rectum than in the posterior intestine of the Gulf toadfish. This difference might exist to ensure that there is enough water present in the rectum for facilitating the removal of solids, such as carbonate precipitates, from the intestine, in support of this dissertation's hypothesis.

An interesting finding revealed in Chapter 4 is the preference of SLC26a6 by the posterior intestine and NKCC2 by the rectum for $Cl^-$ absorption. In many seawater teleosts, either SLC26a6 (Grosell, 2011; Kurita *et al.*, 2008) or NKCC2 (Ando, 1980; Musch *et al.*, 1982) is the preferred $Cl^-$-uptake pathway. In the context of the guanylin peptide response in the Gulf toadfish, perhaps NKCC2 is the preferred $Cl^-$-uptake pathway in order to reduce rectal $HCO_3^-$ secretion/carbonate precipitation and facilitate the removal of the intestinal precipitates. Additionally, these findings also suggest that NKCC2 is inhibited by the downstream effects of renoguanylin stimulation. Indeed, Chapter 4 describes findings that inhibition of NKCC2 in the posterior intestine and rectum lead to ion-inhibitory effects that are similar to those of renoguanylin and closely resemble the findings in the Japanese eel (Ando *et al.*, 2014; Yuge and Takei, 2007).

*Significance and perspectives*

As a whole, the findings described by this dissertation contain several implications for the field of teleost physiology. Most important among them is the revelation of a secretory response in the intestine that is initiated by guanylin peptide stimulation. Although secretory mechanisms have been described previously in the seawater teleost intestine (Marshall *et al.*, 2002; O'Grady S, 1989; O'Grady *et al.*, 1988; O'Grady *et al.*, 1985; O'Grady and Wolters, 1990; Yuge and Takei, 2007), the findings contained within this dissertation more fully elucidate the effects of renoguanylin and, furthermore, provides evidence that a secretory response is important for osmoregulation in hypersaline environments. This dissertation is focused on a number of physiological parameters, such as ion flux, that are necessary to inhibit water absorption and initiate ion secretion. Although a secretory response in the seawater teleost intestine seems counterintuitive, particularly since intestinal water absorption is vital to survival, the findings described in this dissertation provide evidence that a secretory response is important for hypersaline osmoregulation, perhaps because it facilitates the removal of solids from the intestine. In support of this hypothesis, acclimation of Gulf toadfish to hypersalinity, when carbonate precipitation increases (Genz *et al.*, 2008), results in greater gene expression of the components of a $Cl^-$-secretory response (GC-C, CFTR, and NKCC1) and a larger inhibition of water absorption in the posterior intestine.

There is a need to further study the integrative function of guanylin peptide stimulation in the seawater intestine, but evidence in mammals reveals a possible synergistic effect for stimulating secretion and solid removal. Guanylin and uroguanylin have been shown to cause smooth muscle relaxation in mammals, including those

surrounding intestinal tissues (Ochiai *et al.*, 1997; Ohbayashi *et al.*, 1998; Sousa *et al.*, 2010). Smooth muscle relaxation enables food and other solids to pass through the intestine more easily. In addition to this, increasing the fluid content, when solids are present in the intestine, facilitates their removal via peristalsis (Schulze, 2015). A similar, combined process might also exist in the Gulf toadfish (and seawater teleosts in general) for removing solids from the intestine. Undoubtedly, despite the evidence presented by this dissertation, the guanylin peptide response in the seawater teleost requires further investigation.

Avenues currently being pursued in the Gulf toadfish are the intracellular effects renoguanylin has in the enterocytes of the Gulf toadfish posterior intestine. Several studies reveal the effects of phosphorylation on ion transporter activity. In the sea bream, for instance, elevated cAMP leads to decreases in $HCO_3^-$ secretion and water absorption (Carvalho *et al.*, 2012). In mammals, activation of GC-C, by guanylin, increases cGMP formation that can either elevate or reduce cAMP concentrations (Arshad and Visweswariah, 2013). Moreover, both cGMP and cAMP modulate the activities of PKG and PKA which act on CFTR and other ion transporters involved in the intestinal guanylin peptide response [(Golin-Bisello *et al.*, 2005), for review (Arshad and Visweswariah, 2012)]. In the Gulf toadfish intestine, it seems that PKA plays a larger role than PKG in stimulating CFTR activity, increasing CFTR membrane trafficking, and reducing $HCO_3^-$ secretion (personal observations, unpublished data).

What is currently lacking are studies on the guanylin peptide system in intact fish. Future studies ought to investigate the conditions by which guanylin peptide secretion and composition are modulated. These studies should focus on the both the concentration and

ratio of guanylin and uroguanylin under conditions that are predicted to stimulate the secretory response, such as hypersalinity and feeding. Indeed, Chapters 2, 3, and 4 describe studies conducted on isolated tissues from unfed Gulf toadfish. Due to this type of experimental design, the ability to interpret the results of these studies is limited, since many biological factors regulating intestinal physiology are excluded. The function of the secretory response initiated by the peptides is hypothesized to remove solids, such carbonate precipitates, from the intestine. Although the data presented in the dissertation provide support for this hypothesis, our understanding of the data is, at best, speculative. Studies on the intestine in intact fish would add much needed value to our understanding of guanylin-peptide function in seawater teleosts. It would be worthwhile to expose unfed fish to hypersalinity (to increase carbonate precipitation formation) or feed them (to increase solid content in the intestine), then testing the effects of the guanylin peptides or measuring their concentrations from intestinal fluids. These types of experiments would provide important information because (1) the effects of the guanylin peptides on the intestine of an intact fish could be compared to those already performed on isolated studies (where a greater secretory response would be expected by fish acclimated to hypersalinity or those who have been fed) and (2) the we would expect greater secretion of the guanylin peptides from intact fish acclimated to hypersalinity or after feeding. Moreover, observed differences in the ratio of guanylin and uroguanylin secretion under these two conditions could reveal functional differences between the guanylin peptides. Thus, although the dissertation does not contain these sorts of studies, a fruitful avenue of research in the field of fish physiology has been opened with the potential for exciting findings.

*Acknowledgments*

The research conducted for this dissertation could not have been accomplished without the generous use of equipment provided by Drs. M. Danielle McDonald, Douglas L. Crawford, Marjorie F. Oleksiak, and Michael C. Schmale from the Rosenstiel School of Marine and Atmospheric Science (RSMAS) at the University of Miami. The dissemination of this dissertation's findings to members of the scientific community were partly funded by the RSMAS Student Travel Fund, and travel funding awarded by the Society for Experimental Biology, the International Congress on the Biology of Fish, and the Society for Integrative and Comparative Biology to Ilan M. Ruhr. Funding for this research was made possible by a National Science Foundation grant (IOS 1146695) to Dr. Martin Grosell, Maytag Professor of Ichthyology at the University of Miami.

**Bibliography**


1. **Akiba, Y., Jung, M., Ouk, S., and Kaunitz, J. D.** (2005). A novel small molecule CFTR inhibitor attenuates $HCO_3^-$ secretion and duodenal ulcer formation in rats. *Am J Physiol Gastrointest Liver Physiol* **289**, G753-9.

2. **Allen, A. and Flemström, G.** (2005). Gastroduodenal mucus bicarbonate barrier: protection against acid and pepsin. *Am J Physiol Cell Physiol* **288**, C1-C19.

3. **Alvarez, B. V., Vilas, G. L., and Casey, J. R.** (2005). Metabolon disruption: a mechanism that regulates bicarbonate transport. *EMBO J* **24**, 2499-511.

4. **Ando, M.** (1980). Chloride-dependent sodium and water transport in the seawater eel intestine. *J Comp Physiol B Biochem Sys Env Physiol* **138**, 87-91.

5. **Ando, M. and Nagashima, K.** (1996). Intestinal $Na^+$ and $Cl^-$ levels control drinking behavior in the seawater-adapted eel *Anguilla japonica*. *Journal of Experimental Biology* **199**, 711-6.

6. **Ando, M. and Takei, Y.** (2015). Guanylin activates $Cl^-$ secretion into the lumen of seawater eel intestine via apical $Cl^-$ channel under simulated in vivo conditions. *Am J Physiol Regul Integr Comp Physiol* **308**, R400-R410.

7. **Ando, M., Wong, M. K., and Takei, Y.** (2014). Mechanisms of guanylin action on water and ion absorption at different regions of seawater eel intestine. *Am J Physiol Regul Integr Comp Physiol* **307**, R653-63.

8. **Arnaud-Batista, F. J., Peruchetti, D. B., Abreu, T. P., do Nascimento, N. R., Malnic, G., Fonteles, M. C., and Caruso-Neves, C.** (2016). Uroguanylin modulates ($Na^{++}$ $K^+$) ATPase in a proximal tubule cell line: Interactions among the cGMP/protein kinase G, cAMP/protein kinase A, and mTOR pathways. *Biochem Biophys Acta* **1860**, 1431-1438.

9. **Arshad, N. and Visweswariah, S. S.** (2012). The multiple and enigmatic roles of guanylyl cyclase C in intestinal homeostasis. *FEBS Lett* **586**, 2835-40.

10. **Arshad, N. and Visweswariah, S. S.** (2013). Cyclic nucleotide signaling in intestinal epithelia: getting to the gut of the matter. *Wiley Interdiscip Rev Syst Biol Med* **5**, 409-24.

11. **Bakker, R., Dekker, K., De Jonge, H. R., and Groot, J. A.** (1993). VIP, serotonin, and epinephrine modulate the ion selectivity of tight junctions of goldfish intestine. *Am J Physiol Regul Integr Comp Physiol* **264**, R362-8.

12. **Bakker, R. and Groot, J. A.** (1989). Further evidence for the regulation of the tight junction ion selectivity by cAMP in goldfish intestinal mucosa. *J Memb Biol* **111**, 25-35.

13. **Bengtsson, M. W., Jedstedt, G., and Flemstrom, G.** (2007). Duodenal bicarbonate secretion in rats: stimulation by intra-arterial and luminal guanylin and uroguanylin. *Acta Physiol (Oxf)* **191**, 309-17.

14. **Bodinier, C., Boulo, V., Lorin-Nebel, C., and Charmantier, G.** (2009a). Influence of salinity on the localization and expression of the CFTR chloride channel in the ionocytes of *Dicentrarchus labrax* during ontogeny. *J Anat* **214**, 318-329.

15. **Bodinier, C., Lorin-Nebel, C., Charmantier, G., and Boulo, V.** (2009b). Influence of salinity on the localization and expression of the CFTR chloride channel in the ionocytes of juvenile *Dicentrarchus labrax* exposed to seawater and freshwater. *Comp Biochem Physiol A Mol Integr Physiol* **153**, 345-51.

16. **Bosse, Y.** (2014). Endocrine regulation of airway contractility is overlooked. *Journal of Endocrinology* **222**, R61-73.

17. **Bowcutt, R., Forman, R., Glymenaki, M., Carding, S. R., Else, K. J., and Cruickshank, S. M.** (2014). Heterogeneity across the murine small and large intestine. *World J Gastroenterol* **20**, 15216-32.

18. **Bradley, T. J.** (2009). Animal osmoregulation: Oxford University Press.

19. **Carrithers, S. L., Jackson, B. A., Cai, W. Y., Greenberg, R. N., and Ott, C. E.** (2002). Site-specific effects of dietary salt intake on guanylin and uroguanylin mRNA expression in rat intestine. *Regul Pept* **107**, 87-95.

20. **Carvalho, E. S., Gregorio, S. F., Power, D. M., Canario, A. V., and Fuentes, J.** (2012). Water absorption and bicarbonate secretion in the intestine of the sea bream are regulated by transmembrane and soluble adenylyl cyclase stimulation. *J Comp Physiol B Biochem Sys Env Physiol* **182**, 1069-80.

21. **Cats, A., Devries, E., Mulder, N., and Kleibeuker, J.** (1996). Regional differences of physiological functions and cancer susceptibility in the human large intestine. *Int J Oncol* **9**, 1055-69.

22. **Chao, A. C., de Sauvage, F. J., Dong, Y. J., Wagner, J. A., Goeddel, D. V., and Gardner, P.** (1994). Activation of intestinal CFTR $Cl^-$ channel by heat-stable enterotoxin and guanylin via cAMP-dependent protein kinase. *EMBO J* **13**, 1065-72.

23. **Comrie, M. M., Cutler, C. P., and Cramb, G.** (2001a). Cloning and Expression of Guanylin from the European eel (Anguilla anguilla). *Biochem Biophys Res Commun* **281**, 1078-85.

24. **Comrie, M. M., Cutler, C. P., and Cramb, G.** (2001b). Cloning and expression of two isoforms of guanylate cyclase C (GC-C) from the European eel (*Anguilla anguilla*). *Comp Biochem Physiol B Biochem Mol Biol* **129**, 575-86.

25. **Cramb, G., Martinez, A. S., McWilliam, I. S., and Wilson, G. D.** (2005). Cloning and expression of guanylin-like peptides in teleost fish. *Ann N Y Acad Sci* **1040**, 277-80.

26. **Currie, M. G., Fok, K. F., Kato, J., Moore, R. J., Hamra, F. K., Duffin, K. L., and Smith, C. E.** (1992). Guanylin: an endogenous activator of intestinal guanylate cyclase. *Proc Natl Acad Sci* **89**, 947-51.

27. **Cuthbert, A. W., Hickman, M. E., Macvinish, L. J., Evans, M. J., Colledge, W. H., Ratcliff, R., Seale, P. W., and Humphrey, P. P. A.** (1994). Chloride secretion in response to guanylin in colonic epithelia from normal and transgenic cystic-fibrosis mice. *British Journal of Pharmacology* **112**, 31-36.

28. **Cutler, C. P. and Cramb, G.** (2002). Two isoforms of the $Na^+/K^+/2Cl^-$ cotransporter are expressed in the European eel (*Anguilla anguilla*). *Biochim Biophys Acta* **1566**, 92-103.

29. **da Silva Lima, V., Crajoinas, R. O., Carraro-Lacroix, L. R., Godinho, A. N., Dias, J. L., Dariolli, R., Girardi, A. C., Fonteles, M. C., Malnic, G., and Lessa, L. M.** (2014). Uroguanylin inhibits H-ATPase activity and surface expression in renal distal tubules by a PKG-dependent pathway. *Am J Physiol Cell Physiol* **307**, C532-41.

30. **de Sauvage, F. J., Keshav, S., Kuang, W. J., Gillett, N., Henzel, W., and Goeddel, D. V.** (1992). Precursor structure, expression, and tissue distribution of human guanylin. *Proc Natl Acad Sci* **89**, 9089-93.

31. **Diaz, M., Lorenzo, A., Badia, P., and Gomez, T.** (1988). The role of aldosterone in water and electrolyte transport across the colonic epithelium of the lizard, *Gallotia galloti*. *Comp Biochem Physiol A Comp Physiol* **91**, 71-7.

32. **Esbaugh, A. J. and Grosell, M.** (2014). Esophageal desalination is mediated by $Na^+$, $H^+$ exchanger-2 in the gulf toadfish (Opsanus beta). *Comp Biochem Physiol A Mol Integr Physiol* **171**, 57-63.

33. **Esbaugh, A. J., Heuer, R., and Grosell, M.** (2012). Impacts of ocean acidification on respiratory gas exchange and acid-base balance in a marine teleost, *Opsanus beta*. *J Comp Physiol B Biochem Sys Env Physiol* **182**, 921-34.

34. **Evans, D. H., Piermarini, P. M., and Choe, K. P.** (2005). The multifunctional fish gill: dominant site of gas exchange, osmoregulation, acid-base regulation, and excretion of nitrogenous waste. *Physiol Rev* **85**, 97-177.

35. **Forte, L. R.** (1999). Guanylin regulatory peptides: structures, biological activities mediated by cyclic GMP and pathobiology. *Regul Pept* **81**, 25-39.

36. **Forte, L. R.** (2003). A novel role for uroguanylin in the regulation of sodium balance. *J Clin Invest* **112**, 1138-41.

37. **Forte, L. R. and Hamra, F. K.** (1996). Guanylin and uroguanylin: Intestinal peptide hormones that regulate epithelial transport. *News in Physiological Sciences* **11**, 17-24.

38. **Frizzell, R. A., Smith, P. L., Vosburgh, E., and Field, M.** (1979). Coupled sodium-chloride influx across brush border of flounder intestine. *J Membr Biol* **46**, 27-39.

39. **Genz, J. and Grosell, M.** (2011). *Fundulus heteroclitu*s acutely transferred from seawater to high salinity require few adjustments to intestinal transport associated with osmoregulation. *Comp Biochem Physiol A Mol Integr Physiol* **160**, 156-165.

40. **Genz, J., McDonald, M. D., and Grosell, M.** (2011). Concentration of $MgSO_4$ in the intestinal lumen of *Opsanus beta* limits osmoregulation in response to acute hypersalinity stress. *Am J Physiol Regul Integr Comp Physiol* **300**, R895-R909.

41. **Genz, J., Taylor, J. R., and Grosell, M.** (2008). Effects of salinity on intestinal bicarbonate secretion and compensatory regulation of acid–base balance in *Opsanus beta*. *Journal of Experimental Biology* **211**, 2327-2335.

42. **Gilmour, K. M. and Perry, S. F.** (2009). Carbonic anhydrase and acid-base regulation in fish. *Journal of Experimental Biology* **212**, 1647-1661.

43. **Golin-Bisello, F., Bradbury, N., and Ameen, N.** (2005). STa and cGMP stimulate CFTR translocation to the surface of villus enterocytes in rat jejunum and is regulated by protein kinase G. *Am J Physiol Cell Physiol* **289**, C708-16.

44. **Greenberg, R. N., Hill, M., Crytzer, J., Krause, W. J., Eber, S. L., Hamra, F. K., and Forte, L. R.** (1997). Comparison of effects of uroguanylin, guanylin, and *Escherichia coli* heat-stable enterotoxin STa in mouse intestine and kidney: Evidence that uroguanylin is an intestinal natriuretic hormone. *J Inv Med* **45**, 276-283.

45. **Gregorio, S. F., Carvalho, E. S., Encarnacao, S., Wilson, J. M., Power, D. M., Canario, A. V., and Fuentes, J.** (2013). Adaptation to different salinities exposes functional specialization in the intestine of the sea bream (*Sparus aurata* L.). *Journal of Experimental Biology* **216**, 470-9.

46. **Grosell, M.** (2006). Intestinal anion exchange in marine fish osmoregulation. *Journal of Experimental Biology* **209**, 2813-27.

47. **Grosell, M.** (2010). The role of the gastrointestinal tract in salt and water balance. In *Fish Physiology*, vol. 30, pp. 135-164.

48. **Grosell, M.** (2011). Intestinal anion exchange in marine teleosts is involved in osmoregulation and contributes to the oceanic inorganic carbon cycle. *Acta Physiol (Oxf)* **202**, 421-34.

49. **Grosell, M. and Genz, J.** (2006). Ouabain-sensitive bicarbonate secretion and acid absorption by the marine teleost fish intestine play a role in osmoregulation. *Am J Physiol Regul Integr Comp Physiol* **291**, R1145-56.

50. **Grosell, M., Genz, J., Taylor, J. R., Perry, S. F., and Gilmour, K. M.** (2009a). The involvement of $H^+$-ATPase and carbonic anhydrase in intestinal $HCO_3^-$ secretion in seawater-acclimated rainbow trout. *Journal of Experimental Biology* **212**, 1940-8.

51. **Grosell, M., Laliberte, C., Wood, S., Jensen, F. B., and Wood, C.** (2001). Intestinal $HCO_3^-$ secretion in marine teleost fish: evidence for an apical rather than a basolateral $Cl^-/HCO_3^-$ exchanger. *Fish Physiology and Biochemistry* **24**, 81-95.

52. **Grosell, M., Mager, E., Williams, C., and Taylor, J.** (2009b). High rates of $HCO_3^-$ secretion and $Cl^-$ absorption against adverse gradients in the marine teleost intestine: the involvement of an electrogenic anion exchanger and $H^+$-pump metabolon? *Journal of Experimental Biology* **212**, 1684-1696.

53. **Grosell, M. and Taylor, J. R.** (2007). Intestinal anion exchange in teleost water balance. *Comp Biochem Physiol A Mol Integr Physiol* **148**, 14-22.

54. **Grosell, M., Wood, C. M., Wilson, R. W., Bury, N. R., Hogstrand, C., Rankin, C., and Jensen, F. B.** (2005). Bicarbonate secretion plays a role in chloride and water absorption of the European flounder intestine. *Am J Physiol Regul Integr Comp Physiol* **288**, R936-46.

55. **Guba, M., Kuhn, M., Forssmann, W. G., Classen, M., Gregor, M., and Seidler, U.** (1996). Guanylin strongly stimulates rat duodenal $HCO_3^-$ secretion: proposed mechanism and comparison with other secretagogues. *Gastroenterology* **111**, 1558-68.

56. **Guffey, S., Esbaugh, A., and Grosell, M.** (2011). Regulation of apical $H^+$-ATPase activity and intestinal $HCO_3^-$ secretion in marine fish osmoregulation. *Am J Physiol Regul Integr Comp Physiol* **301**, R1682-R1691.

57. **Hallback, D. A., Jodal, M., Mannischeff, M., and Lundgren, O.** (1991). Tissue osmolality in intestinal villi of four mammals in vivo and in vitro. *Acta Physiol Scand* **143**, 271-7.

58. **Halm, D., Krasny, E., and Frizzell, R.** (1985). Electrophysiology of flounder intestinal mucosa. II. Relation of the electrical potential profile to coupled NaCl absorption. *J Gen Physiol* **85**, 865-883.

59. **Hamra, F. K., Eber, S. L., Chin, D. T., Currie, M. G., and Forte, L. R.** (1997). Regulation of intestinal uroguanylin/guanylin receptor-mediated responses by mucosal acidity. *Proc Natl Acad Sci* **94**, 2705-2710.

60. **Hamra, F. K., Forte, L. R., Eber, S. L., Pidhorodeckyj, N. V., Krause, W. J., Freeman, R. H., Chin, D. T., Tompkins, J. A., Fok, K. F., and Smith, C. E.** (1993).

Uroguanylin: structure and activity of a second endogenous peptide that stimulates intestinal guanylate cyclase. *Proc Natl Acad Sci* **90**, 10464-10468.

61. **Hiroi, J., Yasumasu, S., McCormick, S. D., Hwang, P. P., and Kaneko, T.** (2008). Evidence for an apical Na-Cl cotransporter involved in ion uptake in a teleost fish. *Journal of Experimental Biology* **211**, 2584-99.

62. **Iio, K., Nakauchi, M., Yamagami, S., Tsutsumi, M., Hori, H., Naruse, K., Mitani, H., Shima, A., and Suzuki, N.** (2005). A novel membrane guanylyl cyclase expressed in medaka (*Oryzias latipes*) intestine. *Comp Biochem Physiol B Biochem Mol Biol* **140**, 569-578.

63. **Ishiguro, H., Steward, M. C., Naruse, S., Ko, S. B., Goto, H., Case, R. M., Kondo, T., and Yamamoto, A.** (2009). CFTR functions as a bicarbonate channel in pancreatic duct cells. *J Gen Physiol* **133**, 315-326.

64. **Joo, N. S., London, R. M., Kim, H. D., Forte, L. R., and Clarke, L. L.** (1998). Regulation of intestinal $Cl^-$ and secretion by uroguanylin. *Am J Physiol Regul Integr Comp Physiol* **274**, G633-G644.

65. **Kalujnaia, S., Wilson, G. D., Feilen, A. L., and Cramb, G.** (2009). Guanylin-like peptides, guanylate cyclase and osmoregulation in the European eel (*Anguilla anguilla*). *Gen Comp Endocrinol* **161**, 103-14.

66. **Kim, Y. K., Ideuchi, H., Watanabe, S., Park, S. I., Huh, M., and Kaneko, T.** (2008). Rectal water absorption in seawater-adapted Japanese eel *Anguilla japonica*. *Comp Biochem Physiol A Mol Integr Physiol* **151**, 533-541.

67. **Kita, T., Kitamura, K., Sakata, J., and Eto, T.** (1999). Marked increase of guanylin secretion in response to salt loading in the rat small intestine. *Am J Physiol Regul Integr Comp Physiol* **277**, G960-G966.

68. **Ko, S. B., Shcheynikov, N., Choi, J. Y., Luo, X., Ishibashi, K., Thomas, P. J., Kim, J. Y., Kim, K. H., Lee, M. G., and Naruse, S.** (2002). A molecular mechanism for aberrant CFTR-dependent $HCO_3^-$ transport in cystic fibrosis. *The EMBO journal* **21**, 5662-5672.

69. **Kopeikin, Z., Sohma, Y., Li, M., and Hwang, T. C.** (2010). On the mechanism of CFTR inhibition by a thiazolidinone derivative. *J Gen Physiol* **136**, 659-671.

70. **Kuhn, M., Adermann, K., Jahne, J., Forssmann, W. G., and Rechkemmer, G.** (1994). Segmental differences in the effects of guanylin and *Escherichia coli* heat-stable enterotoxin on $Cl^-$ secretion in human gut. *J Physiol* **479**, 433-440.

71. **Kurita, Y., Nakada, T., Kato, A., Doi, H., Mistry, A. C., Chang, M.-H., Romero, M. F., and Hirose, S.** (2008). Identification of intestinal bicarbonate

transporters involved in formation of carbonate precipitates to stimulate water absorption in marine teleost fish. *Am J Physiol Regul Integr Comp Physiol* **294**, R1402-R1412.

72. **Kusakabe, T. and Suzuki, N.** (2000). The guanylyl cyclase family in medaka fish *Oryzias latipes*. *Zoological Sci* **17**, 131-140.

73. **Lan, D., Niu, J., Miao, J., Dong, X., Wang, H., Yang, G., Wang, K., and Miao, Y.** (2016). Expression of guanylate cyclase-C, guanylin, and uroguanylin is downregulated proportionally to the ulcerative colitis disease activity index. *Scientific Reports* **6**.

74. **Li, Z., Knowles, J. W., Goyeau, D., Prabhakar, S., Short, D. B., Perkins, A. G., and Goy, M. F.** (1996). Low salt intake down-regulates the guanylin signaling pathway in rat distal colon. *Gastroenterology* **111**, 1714-21.

75. **Li, Z., Lui, E. Y., Wilson, J. M., Ip, Y. K., Lin, Q., Lam, T. J., and Lam, S. H.** (2014). Expression of Key Ion Transporters in the Gill and Esophageal-Gastrointestinal Tract of Euryhaline Mozambique Tilapia *Oreochromis mossambicus* Acclimated to Fresh Water, Seawater and Hypersaline Water. *PLoS ONE* **9**, e87591.

76. **Marshall, W. and Grosell, M.** (2006). Ion transport, osmoregulation, and acid-base balance. In *The physiology of fishes*, vol. 3, pp. 177-230.

77. **Marshall, W. S., Howard, J. A., Cozzi, R. R., and Lynch, E. M.** (2002). NaCl and fluid secretion by the intestine of the teleost *Fundulus heteroclitus*: involvement of CFTR. *Journal of Experimental Biology* **205**, 745-58.

78. **Martos-Sitcha, J. A., Campinho, M. A., Mancera, J. M., Martinez-Rodriguez, G., and Fuentes, J.** (2015). Vasotocin and isotocin regulate aquaporin 1 function in the sea bream. *Journal of Experimental Biology* **218**, jeb. 114546.

79. **Martos-Sitcha, J. A., Gregório, S. F., Carvalho, E. S. M., Canario, A. V. M., Power, D. M., Mancera, J. M., Martínez-Rodríguez, G., and Fuentes, J.** (2013). AVT is involved in the regulation of ion transport in the intestine of the sea bream (*Sparus aurata*). *Gen Comp Endocrinol* **193**, 221-228.

80. **McDonald, M. D. and Grosell, M.** (2006). Maintaining osmotic balance with an aglomerular kidney. *Comp Biochem Physiol A Mol Integr Physiol* **143**, 447-458.

81. **McDonald, M. D., Grosell, M., Wood, C. M., and Walsh, P. J.** (2003). Branchial and renal handling of urea in the Gulf toadfish, *Opsanus beta*: the effect of exogenous urea loading. *Comp Biochem Physiol A Mol Integr Physiol* **134**, 763-776.

82. **Menard, D.** (2004). Functional development of the human gastrointestinal tract: hormone- and growth factor-mediated regulatory mechanisms. *Can J Gastroenterol* **18**, 39-44.

83. **Müller, T. and Dieplinger, B.** (2012). The guanylin peptide family and the proposed gastrointestinal–renal natriuretic signaling axis. *Kidney Int* **82**, 1253-1255.

84. **Musch, M. W., Orellana, S. A., Kimberg, L. S., Field, M., Halm, D. R., Krasny, E. J., Jr., and Frizzell, R. A.** (1982). $Na^+$-$K^+$-$Cl^-$ co-transport in the intestine of a marine teleost. *Nature* **300**, 351-3.

85. **O'Grady S, M.** (1989). Cyclic nucleotide-mediated effects of ANF and VIP on flounder intestinal ion transport. *Am J Physiol Regul Integr Comp Physiol* **256**, C142-6.

86. **O'Grady, S. M., DeJonge, H. R., Vaandrager, A. B., and Field, M.** (1988). Cyclic nucleotide-dependent protein kinase inhibition by H-8: effects on ion transport. *Am J Physiol Regul Integr Comp Physiol* **254**, C115-21.

87. **O'Grady, S. M., Field, M., Nash, N. T., and Rao, M. C.** (1985). Atrial natriuretic factor inhibits Na-K-Cl cotransport in teleost intestine. *Am J Physiol Regul Integr Comp Physiol* **249**, C531-4.

88. **O'Grady, S. M. and Wolters, P. J.** (1990). Evidence for chloride secretion in the intestine of the winter flounder. *Am J Physiol Regul Integr Comp Physiol* **258**, C243-7.

89. **Ochiai, T., Chijiiwa, Y., Motomura, Y., Iwakiri, Y., and Nawata, H.** (1997). Direct inhibitory effect of adrenomedullin and guanylin on isolated caecal circular smooth muscle cells of guinea pig. *Life Sci* **61**, 1479-85.

90. **Ohbayashi, H., Yamaki, K., Suzuki, R., and Takagi, K.** (1998). Effects of uroguanylin and guanylin against antigen-induced bronchoconstriction and airway microvascular leakage in sensitized guinea-pigs. *Life Sci* **62**, 1833-44.

91. **Pfaffl, M. W.** (2001). A new mathematical model for relative quantification in real-time RT-PCR. *Nucleic Acids Res* **29**, e45.

92. **Rao, M. C. and Nash, N. T.** (1988). 8-BrcAMP does not affect Na-K-2Cl cotransport in winter flounder intestine. *Am J Physiol Cell Physiol* **255**, C246-C251.

93. **Rao, M. C., Nash, N. T., and Field, M.** (1984). Differing effects of cGMP and cAMP on ion transport across flounder intestine. *Am J Physiol Regul Integr Comp Physiol* **246**, C167-71.

94. **Rodriguez, A., Gomez-Ambrosi, J., Catalan, V., Ezquerro, S., Mendez-Gimenez, L., Becerril, S., Ibanez, P., Vila, N., Margall, M. A., Moncada, R. *et al.*** (2016). Guanylin and uroguanylin stimulate lipolysis in human visceral adipocytes. *Int J Obes*.

95. **Rohde, K.** (2002). Ecology and biogeography of marine parasites. *Adv Mar Biol* **43**, 1-86.

96. **Rozenfeld, J., Tal, O., Kladnitsky, O., Adler, L., Efrati, E., Carrithers, S. L., Alper, S. L., and Zelikovic, I.** (2012). The pendrin anion exchanger gene is transcriptionally regulated by uroguanylin: a novel enterorenal link. *Am J Physiol Renal Physiol*
**302**, F614-F624.

97. **Ruhr, I. M., Bodinier, C., Mager, E. M., Esbaugh, A. J., Williams, C., Takei, Y., and Grosell, M.** (2014). Guanylin peptides regulate electrolyte and fluid transport in the Gulf toadfish (*Opsanus bet*a) posterior intestine. *Am J Physiol Regul Integr Comp Physiol* **307**, R1167-79.

98. **Ruhr, I. M., Mager, E. M., Takei, Y., and Grosell, M.** (2015). The differential role of renoguanylin in osmoregulation and apical $Cl^-/HCO_3^-$ exchange activity in the posterior intestine of the Gulf toadfish (*Opsanus beta*). *Am J Physiol Regul Integr Comp Physiol* **309**, R399-R409.

99. **Sabbatini, M. E., Gorelick, F., and Glaser, S.** (2014). Adenylyl cyclases in the digestive system. *Cell Signal* **26**, 1173-81.

100. **Sattin, G., Mager, E. M., Beltramini, M., and Grosell, M.** (2010). Cytosolic carbonic anhydrase in the Gulf toadfish is important for tolerance to hypersalinity. *Comp Biochem Physiol A Mol Integr Physiol* **156**, 169-75.

101. **Schulz, S., Chrisman, T., and Garbers, D.** (1992). Cloning and expression of guanylin. Its existence in various mammalian tissues. *J Biol Chem* **267**, 16019-16021.

102. **Schulz, S., Green, C. K., Yuen, P. S., and Garbers, D. L.** (1990). Guanylyl cyclase is a heat-stable enterotoxin receptor. *Cell* **63**, 941-948.

103. **Schulze, K. S.** (2015). The imaging and modelling of the physical processes involved in digestion and absorption. *Acta Physiol (Oxf)* **213**, 394-405.

104. **Seidler, U., Blumenstein, I., Kretz, A., Viellard-Baron, D., Rossmann, H., Colledge, W., Evans, M., Ratcliff, R., and Gregor, M.** (1997). A functional CFTR protein is required for mouse intestinal cAMP-, cGMP- and $Ca^{2+}$-dependent $HCO_3^-$ secretion. *J Physiol* **505**, 411-423.

105. **Singer, T. D., Tucker, S. J., Marshall, W. S., and Higgins, C. F.** (1998). A divergent CFTR homologue: highly regulated salt transport in the euryhaline teleost *F. heteroclitus*. *Am J Physiol Regul Integr Comp Physiol* **274**, C715-C723.

106. **Skadhauge, E.** (1969). The mechanism of salt and water absorption in the intestine of the eel (*Anguilla anguilla*) adapted to waters of various salinities. *J Physiol* **204**, 135-158.

107. **Skadhauge, E.** (1974). Coupling of transmural flows of NaCl and water in the intestine of the eel (*Anguilla anguilla*). *Journal of Experimental Biology* **60**, 535-546.

108. **Smith, H. W.** (1930). The absorption and excretion of water and salts by marine teleosts. *Am J Physiol Legacy Content* **93**, 480-505.

109. **Sousa, C. M., Havt, A., Santos, C. F., Arnaud-Batista, F., Cunha, K., Cerqueira, J. B. G., Fonteles, M. C., and Nascimento, N. R.** (2010). The relaxation induced by uroguanylin and the expression of natriuretic peptide receptors in human corpora cavernosa. *J Sex Med* **7**, 3610-3619.

110. **Spiegel, S., Phillipper, M., Rossmann, H., Riederer, B., Gregor, M., and Seidler, U.** (2003). Independence of apical $Cl^-/HCO_3^-$ exchange and anion conductance in duodenal $HCO_3^-$ secretion. *Am J Physiol Gastrointest Liver Physiol* **285**, G887-G897.

111. **Takei, Y.** (2008). Exploring novel hormones essential for seawater adaptation in teleost fish. *Gen Comp Endocrinol* **157**, 3-13.

112. **Takei, Y., Hiroi, J., Takahashi, H., and Sakamoto, T.** (2014). Diverse mechanisms for body fluid regulation in teleost fishes. *Am J Physiol Regul Integr Comp Physiol* **307**, R778-92.

113. **Takei, Y., Kawakoshi, A., Tsukada, T., Yuge, S., Ogoshi, M., Inoue, K., Hyodo, S., Bannai, H., and Miyano, S.** (2006). Contribution of comparative fish studies to general endocrinology: structure and function of some osmoregulatory hormones. *J Exp Zool A Comp Exp Biol* **305**, 787-98.

114. **Takei, Y. and Yuge, S.** (2007). The intestinal guanylin system and seawater adaptation in eels. *Gen Comp Endocrinol* **152**, 339-51.

115. **Tanday, S.** (2014). Guanylin hormone loss could trigger colon cancer. *The Lancet Oncology* **15**, e537.

116. **Taylor, J., Mager, E., and Grosell, M.** (2010). Basolateral NBCe1 plays a rate-limiting role in transepithelial intestinal $HCO_3^-$ secretion, contributing to marine fish osmoregulation. *Journal of Experimental Biology* **213**, 459-468.

117. **Toriano, R., Ozu, M., Politi, M. T., Dorr, R. A., Curto, M. A., and Capurro, C.** (2011). Uroguanylin regulates net fluid secretion via the NHE2 isoform of the $Na^+/H^+$ exchanger in an intestinal cellular model. *Cell Physiol Biochem* **28**, 733-742.

118. **Tresguerres, M., Levin, L. R., Buck, J., and Grosell, M.** (2010). Modulation of NaCl absorption by $[HCO_3^-]$ in the marine teleost intestine is mediated by soluble adenylyl cyclase. *Am J Physiol Regul Integr Comp Physiol* **299**, R62-R71.

119. **Wang, Y., Soyombo, A. A., Shcheynikov, N., Zeng, W., Dorwart, M., Marino, C. R., Thomas, P. J., and Muallem, S.** (2006). Slc26a6 regulates CFTR activity *in vivo* to determine pancreatic duct $HCO_3^-$ secretion: relevance to cystic fibrosis. *EMBO J* **25**, 5049-57.

120. **Weems, W. A.** (1981). The intestine as a fluid propelling system. *Ann Rev Physiol* **43**, 9-19.

121. **Wilson, J. and Castro, L.** (2010). Morphological diversity of the gastrointestinal tract in fishes. *Fish Physiology* **30**, 1-55.

122. **Wilson, R., Millero, F., Taylor, J., Walsh, P., Christensen, V., Jennings, S., and Grosell, M.** (2009). Contribution of fish to the marine inorganic carbon cycle. *Science* **323**, 359-362.

123. **Wilson, R. W. and Grosell, M.** (2003). Intestinal bicarbonate secretion in marine teleost fish – source of bicarbonate, pH sensitivity, and consequences for whole animal acid-base and calcium homeostasis. *Biochim Biophys Acta* **1618**, 163-174.

124. **Wilson, R. W., Wilson, J. M., and Grosell, M.** (2002). Intestinal bicarbonate secretion by marine teleost fish – why and how? *Biochim Biophys Acta* **1566**, 182-193.

125. **Wood, C. M. and Grosell, M.** (2012). Independence of net water flux from paracellular permeability in the intestine of *Fundulus heteroclitus*, a euryhaline teleost. *Journal of Experimental Biology* **215**, 508-517.

126. **Yuge, S., Inoue, K., Hyodo, S., and Takei, Y.** (2003). A novel guanylin family (guanylin, uroguanylin, and renoguanylin) in eels: possible osmoregulatory hormones in intestine and kidney. *J Biol Chem* **278**, 22726-33.

127. **Yuge, S. and Takei, Y.** (2007). Regulation of ion transport in eel intestine by the homologous guanylin family of peptides. *Zoolog Sci* **24**, 1222-30.

128. **Yuge, S., Yamagami, S., Inoue, K., Suzuki, N., and Takei, Y.** (2006). Identification of two functional guanylin receptors in eel: multiple hormone-receptor system for osmoregulation in fish intestine and kidney. *Gen Comp Endocrinol* **149**, 10-20.